ON THE CONTROL OF AIRPORT DEPARTURE OPERATIONS

A Thesis
Presented to
The Academic Faculty

by

Pierrick Burgain

In Partial Fulfillment
of the Requirements for the Degree
Doctor of Philosophy in the
School of Electrical and Computer Engineering

Georgia Institute of Technology
December 2010

ON THE CONTROL OF AIRPORT DEPARTURE OPERATIONS

Approved by:

Professor Jeff Shamma,
Committee Chair
School of Electrical and Computer Engineering
Georgia Institute of Technology

Professor John-Paul Clarke
School of Aerospace Engineering
Georgia Institute of Technology

Professor Eric Feron, Advisor
School of Aerospace Engineering
Georgia Institute of Technology

Professor Karen Feigh
School of Aerospace Engineering
Georgia Institute of Technology

Professor Stephen MacLaughlin
School of Electrical and Computer Engineering
Georgia Institute of Technology

Professor George Riley
School of Electrical and Computer Engineering
Georgia Institute of Technology

Date Approved: November 2010

TABLE OF CONTENTS

LIST OF TABLES

LIST OF FIGURES

CHAPTER I

INTRODUCTION

This thesis is focused on airport departure operations; its objective is to assign a value to surface surveillance information within a collaborative framework. The research develops a cooperative concept that improves the control of departure operations at busy airports and evaluates its merit using a classical and widely accepted airport departure model. The research then assumes departure operations are collaboratively controlled and develops a stochastic model of taxi operations on the airport surface. Finally, this study investigates the effect of feeding back different levels of surface surveillance information to the departure control process. More specifically, it examines the environmental and operational impact of aircraft surface location information on the taxi clearance process. Benefits are evaluated by measuring and comparing engine emissions for given runway utilization rates.

1.1 Airport operations concepts

Airport operations have attracted considerable attention during the past 30 years. As environmental regulations develop and the demand for air traffic increases, air traffic operations in the National Airspace System need to become more efficient and scalable. New airport Collaborative Decision Making (CDM) concepts and Common Situational Awareness (CSA) enabled by new surveillance technologies form the basis of these operational enhancements.

1.1.1 Collaborative Decision Making

Collaborative Decision Making is defined as a "joint government/industry initiative aimed at improving air traffic management through increased information exchange

among the various parties in the aviation community" [9]. Generally, CDM enables the collaboration and cooperation of air traffic stake-holders. For instance, in Air Traffic Management, Ground Delay Programs (GDP) match arrival demand and arrival capacity at an airport. These GDPs are combined with a CDM system called Flight Schedule Monitor, which helps airline share partial schedule information and collaboratively reorganize their flights, through exchanges and cancelations of arrival slots.

At the airport level, CDM allows air traffic stakeholders to overcome the deleterious effects of the competitive nature of arrival and departure operations. Airport CDM provides stakeholders with the means to share information and, incidently, pool some of their resources to efficiently manage the complexity and variability of airport operations. Consequently, CDM favors the development of novel and more efficient departure control policies.

1.1.2 Common Situational Awareness

In related efforts [39, 36], new surveillance technologies such as Surface Management System or Advanced Surface Movement Guidance and Control System provide access to more information, called airport Common Situational Awareness (CSA); CSA is the sharing of information related to aircraft identification and ground position between all interested parties. It improves the quality of surface surveillance information that is fed back to the departure control process. Consequently, CSA can be leveraged to improve the control and fine-tuning of airport operations, and lower emissions within a collaborative framework.

1.2 Research approach

First a concept to collaboratively improve the control of taxi clearances is developed, then the impact of improved surface surveillance information on the control of taxi clearances is evaluated in terms of emission reduction.

1.2.1 Collaborative control of pushbacks

The Collaborative Virtual Queue (CVQ) is a mechanism that enables collaborative decision making at the airport level. The CVQ manages aircraft in the vicinity of the terminal; following airline requests, it establishes pushback or taxi clearance slots, and stacks the slots in a queue. As airport resources become available and aircraft are allowed to taxi, slots are transformed into issued pushback or taxi clearances. Slots are assigned to airlines. Each airline can assign arbitrary flights to the slots it owns. This approach, based on virtual queuing, contributes to fine-tuning departure operations without necessarily removing the laissez-faire environment valued by airlines. The initial results on the CVQ indicate that virtual queuing yields significant additional control to airlines for last-minute flight reordering. At the same time, it reduces emissions and airline operating costs.

1.2.2 Feeding back surface surveillance information

Second, stochastic models of taxi departure operations are developed for airport configurations with one, two, and three ramp areas, assuming departure operations are collaboratively controlled according to the rules defined above. The departure control process is fed back with different levels of information. For each of these information levels, and for several runway utilization rates, the average number of taxiing aircraft is measured. These results, expressed in average number of aircraft, can be easily translated in terms of ground emissions. The fewer aircraft at a given utilization rate, the fewer emissions. For instance, this research shows that at Seattle airport, controlling taxi clearances optimally using surface surveillance reduces emissions by 6% when the airport functions near capacity, compared with a threshold policy which limits the number of taxiing aircraft. The contribution of this investigation is twofold. First, the results provides insight into the value of surface surveillance information

within a collaborative framework such as the CVQ. Second, it helps determine the impact of partial surface information in cases where an intelligent system, knowledgeable of the stochastic behavior of surface operations, is in control.

1.2.3 Outline

The thesis is organized as follows. The introduction summarizes the main airport operations concepts and the research approach. It also presents the origins and history of airport ground operations, and it details past research on how to improve them. The second chapter develops a cooperative departure control process for airport operations, and it outlines its potential benefits. Finally, the third chapter proposes a novel approach to the problem of assigning a value to surface surveillance information within the collaborative framework discussed in Chapter two. This approach considers different levels of information, and quantifies their impact on departure operations. The value of surface surveillance information value for New-York LaGuardia and Seattle-Tacoma International Airport are estimated in terms of emissions, for several runway utilization rates.

1.3 Background

Prior work on the origins and history of airport ground operations is reviewed to explain the motivation behind this research. As air traffic demand keeps growing, airport ground operations face environmental and operational challenges. Recent air traffic initiatives have been undertaken to mitigate the environmental impact of airport surface operations and improve ground operations efficiency. Prior research has detailed the stochastic and queuing nature of departure operations, and proposed improvements and optimization methods. In addition, prior work has outlined the importance of collaboratively controlling departure operations to provide ground controllers with more control authority. Finally, technological improvements have provided more accurate surface surveillance information. Empirical studies on improved

surface surveillance information have shown that it may significantly help improve departure operations.

1.3.1 Air traffic growth and airport congestion

The U.S. National Airspace System (NAS) is expected to grow around 2.4% per year over the next 20 years and accommodate around 1.6 times today's traffic level by 2028 [38, 49, 54, 16], as illustrated in Fig. 1. The anticipated growth in air traffic is expected to bring additional concerns to an already congested system [48, 65].

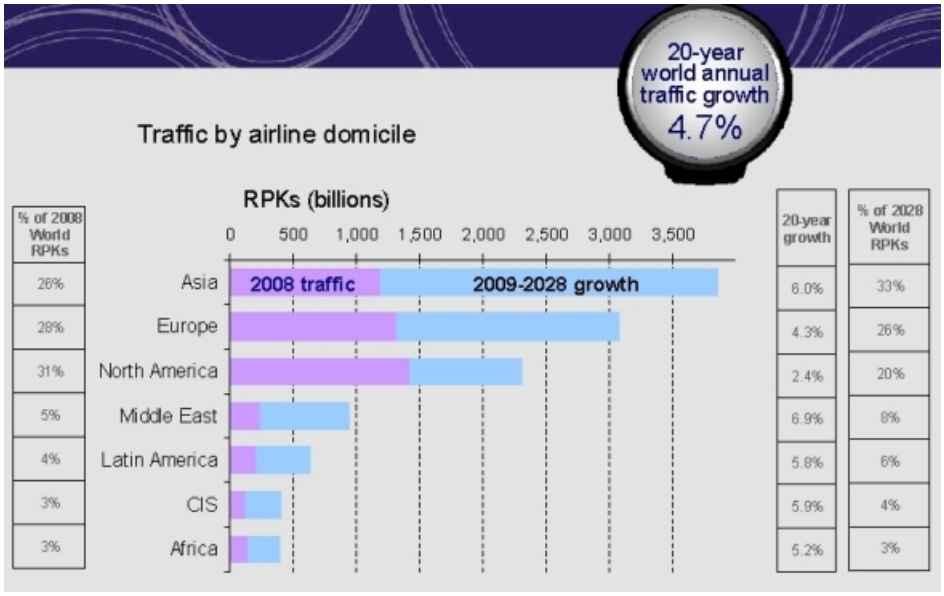

Figure 1: Worldwide air traffic growth projections [38]

Along with physical increases of airport capacities, the future generations of the air transportation system will require new concepts of operations to handle the growth. Even though the development of smaller regional airports is expected, it is predicted that major airports will always run at full capacity [49]. In some cases, airports will not be able to expand their capacity sufficiently to meet the increasing demand. Airports like New-York LaGuardia will be physically restrained by the lack of space for new runways or ramps. Such airports are bound to become and remain air traffic bottlenecks.

1.3.2 Environmental aspect

The contribution of aviation to CO_2 and NOx emissions around airports is expected to increase significantly by 2025 and beyond [67, 46]. Hence, environmental impacts are expected to be the fundamental constraint on air transportation growth [69]. Indeed, concerns over pollution have forced governmental, environmental, and regulatory agencies to start implementing emissions abatement procedures at certain airports, such as La Guardia [1]. Starting in 2012, in the European Union, CO_2 emissions will be capped at the average 2004/2006 levels. This will concern all flights arriving at, and departing from, European airports. In the United States, Section 231 of the Clean Air Act gives the Environmental Protection Agency (EPA) the authority to regulate aircraft emissions, and to adopt emissions standards for U.S.-flagged aircraft [66]. Additionally, many efforts are being conducted towards emissions-reduction technologies and concepts, such as electric taxi, with new operational procedures expected to provide the greatest near-term benefits [69].

Aircraft engines produce more hydrocarbon (HC), carbon monoxide (CO), and oxides of nitrogen (NOx) relative to the total consumption of fuel, when they are idle than during take-off or climb conditions [47].

1.3.3 Current initiatives for improving departure operations

To tackle this environmental, structural, technological, and organizational issue, the NextGen concept of operations [49] encourages research in surface traffic operations aimed at lowering emissions and improving surface traffic planning (Table 1), while concurrently reducing the need for government intervention and control of resources [49, Lines 1709–1726]. Experiments aimed at improving surface operations have been conducted in 2010 at Logan airport, they focused on managing surface queues to reduce emissions [18].

Table 1: NextGen research and policies issues

Ref	**Line Reference**	**Issue**
R-46	At times of peak demand, major airports conduct Super-Density Operations in which capacity-enhancing arrival and surface procedures are implemented to maximize runway throughput.	How will we design and implement systems to be resilient to failures and robust to operator error?
R-135	Advanced capability to integrate and balance noise, emissions, fuel burn, land use, efficiency, and costs effects of alternative measures and alternatives allow selection of optimum operational modes, mitigation strategies, and surface planning procedures.	Identify improvements to surface planning procedures to reduce emissions.

According to [6], EUROCONTROL is currently fine-tuning the Airport Collaborative Decision Making Departure Manager (CDM DMAN) concept of operations and is preparing the necessary implementation guidelines. DMAN is a centralized concept for surface traffic management. Though DMAN is not comparable to the US decentralized and laissez-faire environment, it incorporates Collaborative Decision-Making (CDM) as a tool for managing departure operations. DMAN "keeps the number of aircraft on the taxiway at an optimal level" and "keeps the taxiways open for other traffic without blocking stands for arrivals, reduces controller workload, improves punctuality and predictability, facilitates co-operation between aerodrome ATC, airlines and airport operators, enhances CFMU [i.e. Central Flow Management Unit slot-revisions] and slot compliance, and exploits the departure capacity of the respective runway" [6]. Recently, in Charles de Gaulle, one such CDM project started, aimed at improving the use of available capacity under normal and adverse conditions [4]. The primary focus of this project is on information sharing and departure slot shifting, for airport operations under nominal conditions. Reportedly, the ability for airlines to swap aircraft within a virtual queue was critical to their acceptance of the new departure procedures. Under adverse condition, the focus is on collaborative strategies that will help deal with off nominal procedures. For example, such strategies involve a better control of aircraft on the surface to increase the efficiency of the de-icing process, using "new communication systems between the tower and the de-icing command center to better coordinate aircraft movements" [4].

1.3.4 Queuing Models of Departure Operations

Prior works have emphasized the stochastic nature of airport departure operations and the complexity of interacting queues. In this respect, significant work has been conducted on modeling operations using queuing models and developing methods that tackle the stochastic aspect of departure operations to reduce surface inefficiencies

and more particularly improve taxi operations [34, 59, 25, 44]. In particular, Feron et al. [34] discussed how gate holding could provide a means to effectively reduce the average runway queuing time, decrease operating costs incurred by airlines on the surface, and reduce emissions. Pujet et al. [59] developed a queuing model of airport departure operations and demonstrated that, with only a simple gate holding policy relying solely on the number of taxiing aircraft, operating costs and emissions could be significantly reduced. Later, Carr et al. [25] describe an approach for modeling and controlling queueing dynamic under severe flow restrictions and Idris et al. [44] develop a queueing model for taxi-out time estimations. These studies, by describing operations as queuing processes, focus on the stochastic nature of ground operations, and emphasize the difficulty of fine tuning surface operations in congested situations.

1.3.5 Collaborative Control of Surface Operations

Most studies of airport operations agree on the importance of collaboratively controlling gate-holding along with pushback sequencing and include optimization methods to increase airport throughput and reduce surface inefficiencies. For example, Anagnostakis et al. [14] focused on flight sequencing and scheduling; Capozzi [23, 24] on surface automated traffic control, and Balakrishnan and Jung [17] and later Rathinam et al. [60] on aircraft taxi scheduling optimization. Kim [53] studied how gate assignments and pushback schedule could lower physical conflicts at the ramp. A past study [17] has demonstrated that optimizing the scheduling of taxiway operations can result in reduced taxi-times, and shorter queues on the airport surface. Simaiakis and Balakrishnan [62] also showed that implementing queue management strategies on the aircraft departure process could lead to taxi time reductions, which could then yield reductions in fuel burn and emissions. They considered gate-to-runway traffic states, and studied how surface queues could be managed to reduce taxi-out times.

Furthermore, optimizing operations, especially in congested situations, can be complicated by competition between airlines, which prefer to maintain control over their operations. The development of collaborative departure processes can help improve the control of ground operations.

1.3.6 Surface Surveillance Information

Concurrently with CDM, airport surface surveillance technologies are under development and accurate aircraft ground position information becomes more easily available [5, 2, 19, 31]. Several studies examine the safety enhancements that improved surface surveillance can provide by reducing runway incursion incidents and conflicts [71, 63, 61]. Another study focuses on using surface surveillance to precisely control taxiing aircraft and increase the efficiency of active runway crossings [29].

Previous experiments in a collaborative environment show that the operational improvement achieved by airport surface surveillance technologies is directly related to the information being provided to the end-user. Howell et al. [41], for example, directly measure the impact of surveillance data sharing on surface operations at Memphis International Airport and at Metropolitan Wayne County Airport. They show that surface surveillance data made available to ground controllers directly lead to shorter taxi times. At the Memphis airport, it reduces average taxi time during Visual Approach conditions (visibility greater than five miles and ceiling greater than 5000 feet) by 6.6 percent, and during Instrument Approach conditions by 17.5 percent. In another field study, [42] Howell et al. take advantage of a surface surveillance outage to examine its impact on airline operations. They measure changes in taxi-out times, queue lengths, and departure rates before, during, and after the outage. They find that, for similar levels of airport surface queues, surface surveillance decreases taxi-out times. Furthermore, recent work investigates the practical integration of surface surveillance for aircraft arrivals in a collaborative environment [15, 50, 43]. However,

there has been little academic research on measuring and quantifying improvements directly related to feeding back surface surveillance information to the departure process that controls aircraft in the vicinity of the terminal.

CHAPTER II

COLLABORATIVE CONTROL OF PUSHBACK CLEARANCES

This chapter studies and estimates the potential benefits of using a Collaborative Decision Making (CDM) concept that improves the last-minute control of pushbacks and preserves the decentralized laissez-faire environment of US airports: The Collaborative Virtual Queue (CVQ). The CVQ uses virtual queueing to enable last-minute flight swapping and hold aircraft away from runway queues. The additional control of pushback clearances, enabling last-minute intra-airline pushback reordering actions, is evaluated in terms of passenger waiting time reduction.

2.1 Airport departure congestion

The anticipated growth in air traffic is expected to bring additional concerns to an already congested system [48, 65]. At major airports, airlines and air traffic service providers strategically optimize their operations to operate at full capacity during activity peaks, under the assumption of favorable conditions. Moreover, airlines sometime over-schedule flights, regardless of available airport resources. In other words, when the departure and arrival schedules are created, it is assumed that the available arrival and departure rates are not limited for any reason other than nominal runway capacity and safety constraints. In addition to tight planning, the stochastic nature of surface operations implies that there are enough aircraft taxiing out to ensure a constant, near maximum runway service rate [25]. Consequently major airports are very sensitive to unexpected events such as bad weather, which can disrupt throughput and result in congestion. At busy airports, such as Atlanta Hartsfield International

Airport, it is not uncommon to have queues of 30 or 45 aircraft waiting to take off at the active runways.

To cope with congestion, the air traffic service provider, airports, and airlines have several options:

1. They can try to reduce congestion by:
   (a) Increasing capacity by building more runways, or by reducing aircraft separation using new technologies such as microwave radars to monitor wake vortices.
   (b) Forcing restrictions on departure planning through methods such as departure slots.
2. They can also optimize operations by:
   (a) Centralizing operations around airport authorities to ease information sharing, optimize throughput, and lower inefficiencies.
   (b) Using collaborative decision making to improve operations, while respecting the competitive environment.

Solution 1-(a), increasing airport capacity, is not always easily applicable; finding enough space to add runways can be problematic. Solution 1-(b), using slot restrictions, can reduce schedule overloading [52]. This method has merit in certain cases. Currently, there are 4 federally slot-controlled airports (New York LaGuardia, New York JFK, Reagan Washington National, and Chicago O'Hare). Slot restrictions prevent highly congested situations that can impact the whole National Airspace System. However slot restricted airports still need strategies to deal with degraded departure conditions. In other words, slot restrictions cannot always protect from unplanned throughput disruptions. These disruptions can be triggered by events such as frequent

changes in wind direction, forcing airport control towers to switch runway configurations several times during a short period, Ground Delay Programs, or simply first fix (first waypoint after take-off) closures due to bad weather. Centralizing operations provides greater control to airport authorities and air traffic services providers, reduces the set of private airline responsibilities, and suppresses the laissez-faire environment. This solution is far from the usual operations conducted at US airports, which have highly decentralized operations. Airlines control their ramp operations at least until aircraft are ready to push back; in some cases they also control pushbacks and part of the taxiways within their ramp areas. The control towers gives airlines clearances to push back or exit their ramp areas on a first-come first-serve (FCFS) basis. Consequently, attempts to take control of pushback sequences and ground resources faces high resistance from airlines.

Collaborative Decision Making (CDM), solution 2-(b), can help airports to reach an intermediate solution that does not centralize operations. This chapter studies the potential benefits of CDM applied to ground operations during congested situations. CDM has already proven its effectiveness in flow management with the Flight Schedule Monitor (FSM) [37]. Indeed, FSM is a system whose main role is to implement Ground Delay Programs at originating airports for flights destined to an airport where the arrival demand is expected to exceed the estimated arrival capacity for an upcoming time period. FSM enables airlines to collaboratively reschedule their flights to match the arrival demand with the reduced arrival capacity at the destination airport, as is described below.

The competitive environment, in which airlines operate under tight margins, plays an important role. At most airports, airlines compete to ensure on-time performance and for access to airport resources. Therefore, in the absence of regulating policies, airlines react to a limited throughput capacity by trying to push back earlier to get their aircraft in the queue as early as possible [56] . Once aircraft are in queue on

the taxiway system, airlines lose optimization capabilities. Indeed, by "racing to the runway", they lose the option to swap their own flights and reorganize their actual departure sequences.

To manage congestion, any optimization scheme for decentralized operations first needs to find a solution that provides airlines incentives for not stacking their aircraft in a saturated runway queue. This can be achieved by motivating airlines to keep aircraft at the gate or use parking spots to hold aircraft while the departure system is saturated. The direct benefits of gate holding, such as lower operating costs and reduced ground emissions, are explored in depth in [59]. Observations of a freight company operating at night as the sole operator at its US hub airport confirmed that holding aircraft is the cornerstone of optimizing congested departure operations. Holding aircraft, along with controlling runway queue lengths, allows the freight company to swap its own flights with respect to their priority level. This real-time re-ordering is especially useful when the departure rate is reduced, since it allows the most valuable aircraft to take off with less delay. Future congestion is a certainty; however CDM concepts can increase flexibility of the departure flight sequence, yielding significant operational improvements.

2.2 Departure operations concept: the Collaborative Virtual Queue

The Collaborative Virtual Queue (CVQ) is a queue management method, whereby pushback or spot taxi clearance requests are stacked in a virtual queue, and aircraft are held at the gate or at tarmac spots before taxiing to the runway. The queue is continuously serviced by clearances from the air traffic service providers, who decide if the departure system can handle additional traffic, without sacrificing safety or performance. Airlines keep control of their flight prioritizations and requests for pushback or taxi clearances; therefore the CVQ is transparent to airline operations. In other words, the CVQ provides a collaborative system which keeps decisions decentralized

and regulates the flow of aircraft on the taxiway.

Fig. 2 illustrates the CVQ concept. The Collaborative Virtual Queue allows airlines to hold aircraft away from taxiway and runway saturated queues. By doing so, the CVQ creates last-minute flight swapping opportunities, that airlines can exploit to improve their real-time departure operations. This method can also increase the accuracy of predicting taxi times, since it reduces the number of aircraft on the taxiway. As a result, when ground operations are restricted due to demand/capacity imbalances, a CVQ can control the level of taxiway congestion, while endowing airlines with their fair share of departure capacity and the flexibility to sequence flights.

The following paragraphs describe how the Collaborative Virtual Queue can be integrated within departure operations.

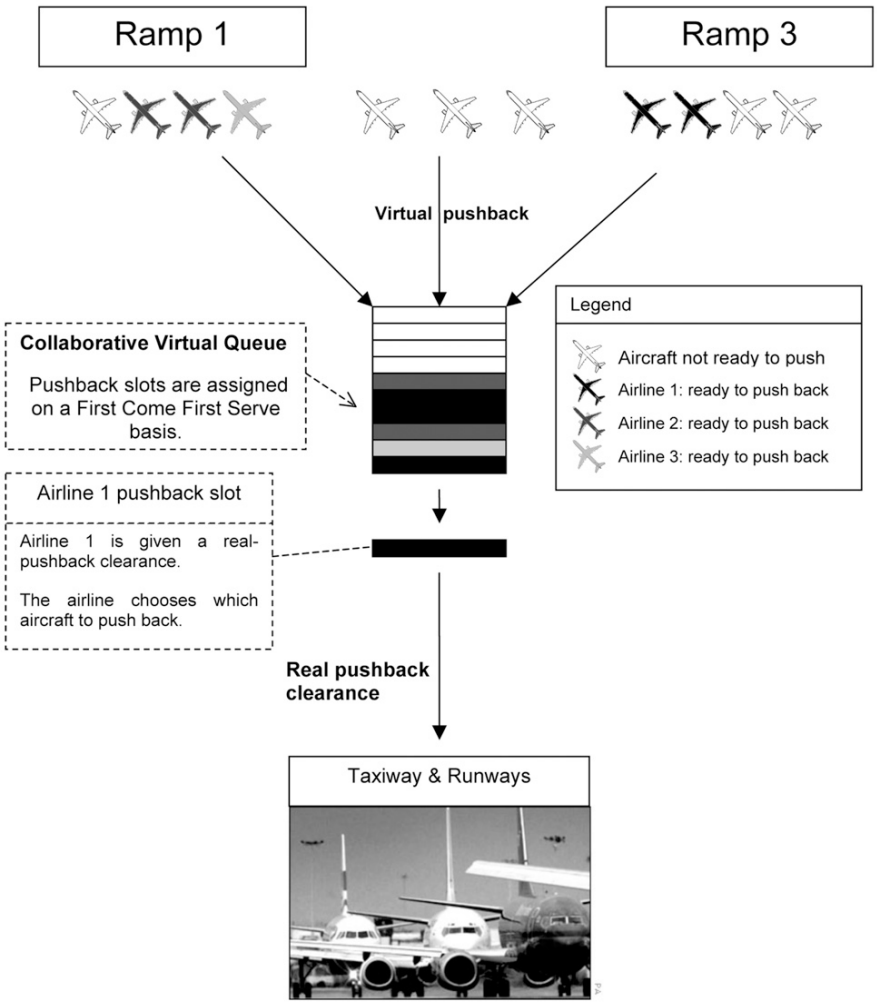

Figure 2: Collaborative Virtual Queue

2.2.1 Time frame

The Collaborative Virtual Queue can be used to manage aircraft at the ramp or in the ramp area between the ready-to-taxi time and the actual pushback time or ramp exit time.

Uncertainties in turn-around times are an issue for any departure optimization process that requires precise forecasting of an aircraft's ready-to-push-back time. Carr and Theis [26] describe limitations of pushback forecasting as the limit of turn-around time predictability for future operations. They conclude that future Air Traffic Management processes must be designed with robust mechanisms for coping with push-back time variations. Supporting their study, Mohleji and Tene [56] also observe that the uncertainties in ready-to-push-back times and in taxi-out times motivate airlines to use time buffers in their pushback forecasts when they file their flight plans. As a consequence of these uncertainties, aircraft are allowed to participate in the Collaborative Virtual Queue only after there is little or no uncertainty about their ready time, e.g., when the pilot asks for pushback clearance or when the doors are closed.

2.2.2 Sequence of operations

The CVQ sequence of operations to manage pushback clearances is now described in detail, (see Fig. 2).

- When an aircraft on the ramp asks for a pushback clearance or a ramp exit taxi clearance, the aircraft either stays at the gate or at the exit spot, if the taxiway system is saturated. If the gate or spot is needed for an arrival, it moves to an alternative parking spot, such as a "penalty box". A matching clearance slot is created. This is a virtual taxi clearance.

- A clearance slot is a floating pushback or taxi clearance that identifies the aircraft's airline. It contains the virtual clearance time. It may include any other

aircraft information that is directed to the airline regarding the optimization of flight sequencing.

- The virtual queue administrator stacks the clearance slot in the CVQ.
- Once the controller of the movement area requests an aircraft, the airline with the slot at the head of the virtual queue is given a pushback or taxi clearance. This aircraft request may be indexed on a gate-holding threshold policy or a more complex policy. The airline may assign a real clearance to any of its aircraft that have already entered the Collaborative Virtual Queue. This virtual queue respects the competitive environment currently generated by the FCFS policy applied by air traffic control towers at most U.S. airports. Notice that this procedure does not interfere with other departure processes occurring before the ready time or after the clearance process. It merely provides flexibility for the airline to swap its own flights when they have different priorities.
- If the departure system has enough capacity to accept all aircraft asking for pushback or ramp-exit without saturating the system, the CVQ has no influence on the departure operations.

By definition, any aircraft corresponding to a virtual slot must be ready to push back or exit the ramp when asked to. Therefore any flight affected by a ground delay program must be removed from the queue until it can be released according to the GDP. As of 2010, this technique appears to be used at Charles-de-Gaulle (CDG), the ability for airlines to swap aircraft within a virtual queue was critical to their acceptance of the new departure procedures in the context of CDM at CDG [4].

2.2.3 Decisions and support

This section addresses the possible roles of the three main agents involved in the CVQ concept of operations: the air traffic services provider, the airlines involved, and the

airport of interest. These roles may vary since not all airports run their operations identically.

2.2.3.1 Air traffic services provider

From the airport control tower, the controllers manage the runway clearances and portions of the taxiways leading to these runways. Within the CVQ concept of operations, the controllers still regulate clearances, taking into account restrictions such as miles-in-trail and departure first fix saturations. In addition, the controllers assess the saturation state of the taxiway system. When the taxiway system is not saturated, they tell ramp controllers how many additional aircraft can be released before reaching saturation. These communications are sent by radio or possibly through an information system that is part of the CVQ system, linking the tower directly to the ramp. In case of a GDP, the controller clears the corresponding virtual slot from the virtual queue, until the aircraft is able to push back, at which point it is added to the CVQ.

2.2.3.2 Airlines

The airlines perform the following actions.

Pushback pre-clearances and clearances: Ramp controllers receive pushback requests and issue clearances. Within the CVQ context, ramp controllers first receive a message from the airport tower controllers, who work for the air traffic services provider, specifying the maximum number of aircraft to push back or clear for ramp exit. Then, looking at the virtual queue, ramp controllers select the next slot in the queue. In case the ramp controllers do not work directly for the airline, they contact the corresponding airline, and give a pre-clearance by asking which of their ready-to-go aircraft is to push back or clear for taxi. For instance, at Atlanta Hartsfield International Airport some of the ramp operations are managed by an independent

company. It is possible that the chosen aircraft cannot physically push back or is prevented from taxiing due to external constraints outside the airline's responsibilities. The ramp controller then asks the airline either to send another aircraft or to wait until the chosen aircraft is ready. In most other cases, ramp controllers work directly for an airline. In this case, they have control over an airline's fleet within a limited ramp area. In order to implement collaborative operations such as CVQ, these ramp controllers need to collaborate with other airport ramp controllers to respect the CVQ order.

Requesting a virtual slot in the CVQ: Airline pilots request clearances from ramp or air traffic service provider controllers once the aircraft is ready to go. Within the CVQ context, pilots request a virtual slot once there is little doubt left on their ability to push back or taxi.

Selecting aircraft to push back: Once the tower asks for an aircraft, a virtual slot is selected and the corresponding airline must assign an aircraft for pushback or for ramp exit. In order to provide additional flexibility to ramp controllers, airlines may supply them with a second choice. Indeed, if their first choice is not physically realizable, the controller can still accommodate the airline slot by releasing a secondary aircraft.

Ensuring aircraft are cleared: Airlines are responsible for their virtual slot. For instance, if the holding time is very long, the airline may require additional lead-time for the aircraft to push back, and should plan accordingly by looking at their position in the virtual queue.

2.2.4 Airport throughput management

A threshold policy is used to evaluate the benefits of virtual queuing. This policy has been used in previous gate-holding studies [59]. It limits the number of taxiing aircraft in the movement area. The limitation of the number of taxiing aircraft must not constrain the airport throughput. We used the method described by Pujet et al. in [59] to set an optimal holding threshold. Pujet showed how the limit on the number of aircraft taxiing out can be computed by observing the average throughput as a function of the number of taxiing aircraft.

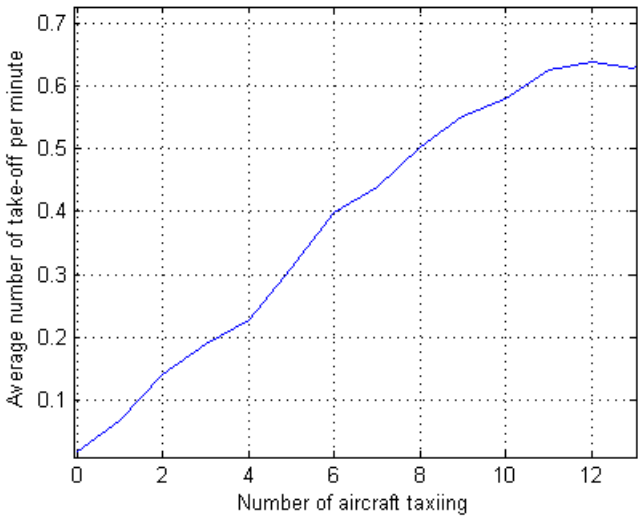

Figure 3: Average throughput as a function of the number of taxiing aircraft, for Logan Airport.

Thus, this limit implicitly includes time variations depending on gate and runway location from pushback to wheels-off time. Using ASPM data for the Boston Airport in cases where only runway 9 was opened for departures, it was determined that the number of aircraft taxiing out needed to be equal to or greater than 11 to saturate the taxiway system and reach the highest departure rate, as illustrated in Fig. 3. Therefore, for the threshold policy, the maximum number of planes taxiing out is set to 11 in order to not limit the airport throughput.

The biggest challenge faced by threshold policies, or any other policy limiting

the number of taxiing aircraft, is space availability requirements for new arrivals (at the gate or on the taxiway). In most airports, gate occupation and parking space requirements are cyclical; every day there is a time when the arrival rate is lower than the departure rate. This frees gate and parking capacity that can be exploited to hold aircraft. Pujet et al. quantitatively addressed the gate availability issue at Boston Logan Airport. They showed that gate holding rarely required the use of an additional gate/parking space ([59], page 15). Should this happen nevertheless, aircraft can wait for their turn in a parking area, possibly using current "penalty boxes" designed for flow management.

An actual threshold policy was observed at the US hub airport of a freight company. During a visit to this airport, we conducted interviews and observed operations. At night, most of the airport ramps are controlled by a single airline. As a result, this airline limits the number of aircraft taxiing out to 8 aircraft per runway. This allows them to increase take-off time predictability and re-order their flight sequence in real time. Therefore, the conditions are close to the conditions simulated for a Collaborative Virtual Queue (CVQ) at Boston Airport, which limits to 11 the number of aircraft taxiing out for departures on runway 9. The CVQ's purpose is to control the number of taxiing aircraft in competitive situations, and allow multiple airlines to benefit from last-minute flight swapping capabilities.

2.3 Model of airport departure ground operations

In order to evaluate the Collaborative Virtual Queue concept of operations proposed in this section, we modeled the Boston Logan Airport operations configured for departures on runway 9 alone. Airlines hand control of their aircraft over to the Air Traffic Control Tower immediately following pushback [59, 25], therefore the CVQ is directly managing the pushback clearances. This model evaluates the flexibility enabled by last-minute flight swapping and gate holding, especially during high levels

of congestion on taxiways at times of high departure rates.

2.3.1 Departure system

This section briefly describes the model architecture, departure schedule, virtual queue, taxiways, and runways. Several studies [59, 25, 45] have demonstrated that the degree of complexity and the number of unpredictable factors affecting ground operations are such that ground operations are best modeled by stochastic queuing models. The departure model (Fig. 5), from the ramp to the runway, is based on the queuing model and calibration method developed by Pujet and Carr [59, 25] for the Boston Logan Airport, which diagram is shown in Fig. 4. It is calibrated using recent ASPM historic data, from January 2006 to September 2006 at Boston Logan Airport, under the runway configuration with departures on runway 9. The model is calibrated to reproduce the light traffic taxi time distribution, runway queuing time distributions, and takeoff rate as a function of the number of taxiing aircraft [59, 25]. In addition, the model emulates the collaborative virtual queue and airline pushback decisions by sweeping through different pushback policies which are detailed below.

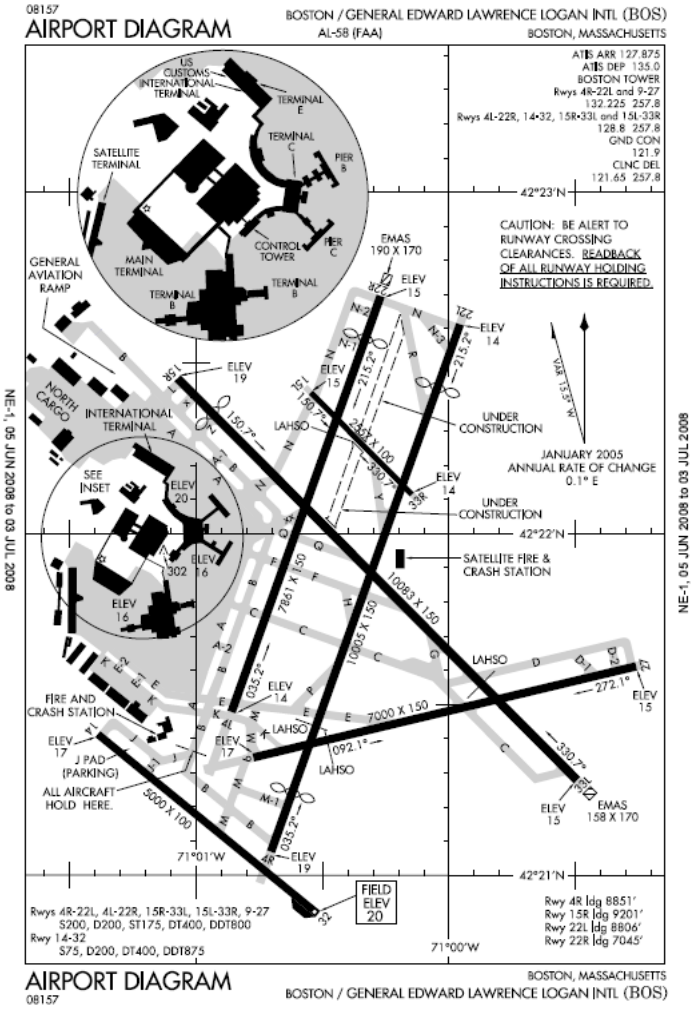

Figure 4: Airport Diagram of Logan International

2.3.1.1 Architecture

Fig. 5 illustrates the process flow of the model. The Collaborative Virtual Queue keeps track of ready aircraft at the ramps before they push back on the taxiway. A runway queue links the taxiway system and departure runway 9. The congestion level is estimated by counting the number of aircraft out on the taxiway and in the runway queue.

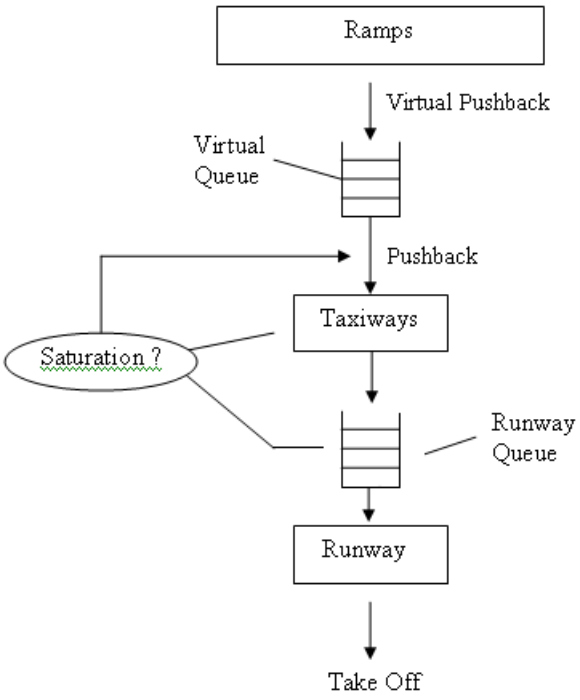

Figure 5: Schematic representation of departure operations

2.3.1.2 Departure Schedule

Aircraft appear at the ramps; their pushback schedules and weight categories are determined from historic data.

2.3.1.3 Virtual queue modeling

When an aircraft is ready, a pushback slot is created and enters the virtual queue. If the departure system is not saturated, the airline with the next pushback slot is

allowed to push back the aircraft of its choice.

2.3.1.4 Taxiways

The taxiway is modeled stochastically [59]. The time an aircraft spends taxiing follows a gaussian distribution. The gaussian distribution is selected to match a light traffic taxi-out distribution derived from the ASPM database.

2.3.1.5 Runways and takeoffs

When aircraft reach runway 9, they enter the departure runway queue as illustrated in Fig. 5. The runway itself is modeled as a server whose service rate is generated by the sum of 2 Bernoulli variables; the use of 2 Bernoulli variables allows adjustment of the variance for a given departure service rate. These variables are calibrated to fit the mean and standard deviation of the take-off rate when the number of taxiing aircraft is higher than 12 (derived from the ASPM database and [59]). Therefore, the miles-in-trail restrictions enforced by the control tower are included within the stochastic description of the runway system.

2.3.2 Airline push-back policies

The Collaborative Virtual Queue allows airlines to adjust their departure operations by choosing which aircraft to push back when a slot becomes "mature". Their push-back policy could trade-off between (i) decreasing the average time their passengers have waited before takeoff or (ii) minimizing the waiting times among their aircraft. This can led to two extreme pushback policies:

- Airlines can choose not to swap flights, that is, they apply a First-Come-First-Served (FCFS) policy, and clear the aircraft which was ready to go first. In this case they minimize the expected differences in waiting times between their aircraft.

- Alternatively, airlines can choose to minimize the average time their passengers spend in the aircraft between ready time and wheels-off time. To do so, among the aircraft waiting for pushback in the CVQ, airlines would always push back the aircraft with the largest number of passengers first. This policy is denoted by "Heaviest Aircraft First" policy.

2.3.2.1 Passengers and aircraft mix

The number of passengers per aircraft is derived from the aircraft weight category and the average number of seats per aircraft of this category (Table 2). In the cost function defined below, the variable $NumberOfPassengersInAC$ denotes the number of passengers per aircraft.

Table 2: Aircraft departure mix

Plane Type	Percentage	Average Seats
Heavy	16.73	214
Large	77.21	97
Small	6.06	4

2.3.2.2 Cost functions

A cost function attributes the costs to holding aircraft. When an airline pushes back one of its available aircraft, it chooses the aircraft whose holding cost is the highest according to its policy.

The FCFS policy can be implemented using any strictly increasing function of the holding time at the gate, as it orders the aircraft by time spent at the gate. Let $TimeSinceReady$ be the time an aircraft is held at the gate from when it has declared that it is ready to push back. One cost function C_1 which corresponds to the FCFS policy is:

$$C_1 = TimeSinceReady$$

The Heaviest Aircraft First (HAF) policy can be implemented using any cost function C_2 that respects the classification of aircraft sizes. One cost function which corresponds to the Heaviest Aircraft First (HAF) policy is:

$$C_2 = NumberOfPassengersInAC$$

A multi-objective cost function, combining C_1 and C_2, was developed to gradually switch from a FCFS policy to a Heaviest Aircraft First policy, as a parameter α was swept from 0 to 1. More specifically, α is the weight factor determining the tradeoff between policies. By sweeping α from 0 to 1, the push back policy gradually switches from the FCFS policy (C_1) to the Heaviest Aircraft First policy (C_2).

The w_1 and w_2 parameters are the normalizing factors of C_1 (FCFS) and C_2 (HAF) in the total cost function $C(\alpha)$. The values of w_1 and w_2 were chosen empirically to control the separation of intermediate policies between the FCFS policy and the HAF policy. $w_1 = 2$ is in dollars per minute, and $w_2 = 1$ is in dollars per passenger.

For each value of α, 64 days of operations were simulated using $C(\alpha)$ as the cost function for every aircraft.

$$C(\alpha) = w_1 \cdot C_1 \cdot (1 - \alpha) + w_2 \cdot C_2 \cdot \alpha$$

2.3.3 Results

These results are obtained using the model described in section 2.3, which simulates the Boston Logan departure operations from January 2006 to September 2006 with departures on runway 9 based on ASPM historical data. We define active aircraft as aircraft that are ready to be cleared to taxi from the ramp, or that are already taxiing.

2.3.3.1 Real-time Intra-Airline Last-minute Switching Benefits

This section studies potential benefits created by the possibility of modifying the pushback sequence at the last minute. The Collaborative Virtual Queue enables gate holding and flight swapping in the pushback sequence. The maximum number of aircraft taxiing out is set to 11 in order to maximize the airport throughput, as illustrated in Fig. 3; this respects the condition discussed previously under the airport throughput management and gate holding strategy.

***Trade-off and flexibility*:** The flight swapping capabilities of the CVQ provide airline with more operational freedom. This freedom can be illustrated by the airline ability to set a tradeoff level between minimizing waiting times for passengers, and minimizing inequity among departing aircraft (i.e. minimizing the standard deviation of aircraft waiting times). To do so, we simulate departure operations for a range of trade-offs parameterized by α. The cost function $C(\alpha)$ determines the cost of each aircraft at the ramp when α varies from 0 to 1, as discussed previously. The two extreme cost functions $C(0)$ and $C(1)$ correspond to the extreme pushback policies as follow:

- $\alpha = 0$ corresponds to a FCFS push-back policy, minimizing differences between aircraft waiting times.
- $\alpha = 1$ corresponds to a Heaviest Plane First policy, minimizing passenger waiting times.

For every intermediate trade-off policy, 64 days of operations are simulated, i.e. for every $C(\alpha)$, α was varied from 0 to 1 by increments of 0.05. The simulation period was set to 72 hours. The departure operations are first simulated assuming they are shared by 3 independent airlines (at Boston Logan Airport, 3 airlines out of 68 represented 30% of the departure operations from January to September 2006). In

the next section, we study the influence of distributions of airline departure operations on the CVQ in more detail.

On average, small aircraft carry 4 passengers, medium aircraft carry 97 passengers, and heavy aircraft carry 214 passengers. Fig. 6 illustrates the average passenger waiting time [1], for $\alpha = 0$, 0.5, and 1 (see section 2.3.2). The top curve, $\alpha = 0$, shows the average passenger waiting time in the FCFS case, i.e. when there is no optimization. The bottom curve, $\alpha = 1$, shows the average passenger waiting time in the Heaviest Plane First case. The curve $\alpha = 0.5$ represents an intermediate policy, where heavy aircraft have an advantage but are not systematically more important than small planes which have been waiting longer at the gate for push-back clearance. There is no difference between the curves if the number of active planes [2] is below 11, i.e. below the gate-holding threshold, because the Collaborative Virtual Queue has no influence on operations. However, when the number of active planes saturates the airport departure capacity, the Collaborative Virtual Queue gives airlines the option to shorten the average passenger waiting times. This is why at 20 active planes out, the average passenger waiting time for the "Heaviest Plane First"policy ($\alpha = 1$) is 7.5 minutes lower than the average passenger waiting time for the FCFS policy ($\alpha = 0$).

Fig. 7, 8, and 9 illustrate the trade-off between minimizing passenger waiting times, and minimizing inequities between aircraft of the same airline; the inequity is measured by the standard deviation of intra-airline aircraft waiting times. Lines represent fitted curves and points represent simulation results. One can notice the exponential relationship between standard deviation of aircraft waiting times and passenger waiting time benefits. Indeed, the sum of 2 exponential functions of order

[1] The average passenger waiting time is defined as the weighted average of plane waiting times, using the number of passengers per plane as the weights. The plane waiting time is the time between ready-to-push-back and wheels-off.

[2] The number of active planes is the number of planes whose state is between ready-to-push-back and wheels-off.

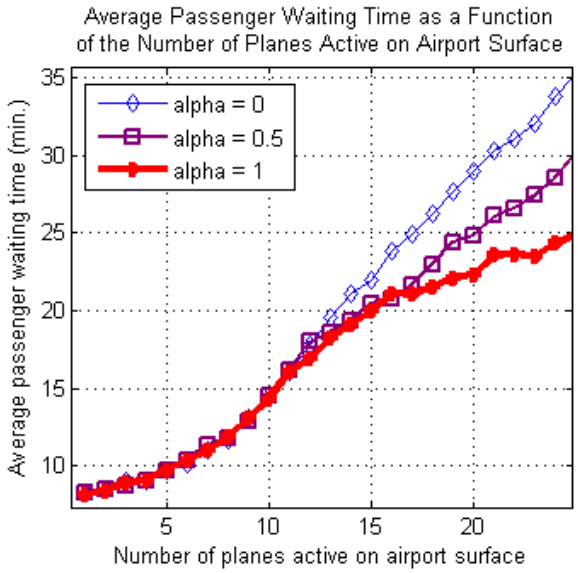

Figure 6: Impact of the number of active planes on the average passenger waiting time. The number of active planes is the number of planes whose state is between ready-to-push-back and wheels-off.

1 and 2 is found to closely reproduce the experimental results. Consequently, the 3 distributions were fitted using functions of the type: $f = A{\cdot}\exp(\beta \cdot x^2){+}B{\cdot}\exp(\delta \cdot x)$, where A, B, β, δ are fitting parameters and x is the passenger waiting time benefits in (%).

Fig. 7 shows the standard deviation of aircraft waiting time as a function of the benefits in terms of passenger waiting times. The average inequity in waiting times between aircraft is illustrated by the standard deviation of aircraft waiting times; it is minimum when there is no last-minute flight swapping and $\alpha = 0$, and maximum for $\alpha = 1$, for the Heaviest Plane First policy. The passenger waiting time benefits is defined as the reduction in passengers waiting times, when compared with a FCFS policy, expressed in percent. It is estimated by comparing the average passenger waiting time for a specific α, with the average passenger waiting time in the case $\alpha = 0$. Fig. 7 shows that airlines increase the standard deviation of their aircraft waiting times by 2.5 minutes (in Fig. 7, the difference between the curve at 10% and at 0% is : 8.0 - 5.5 = 2.5 minutes), to reduce by 10% the average waiting time,

compared with the FCFS case.

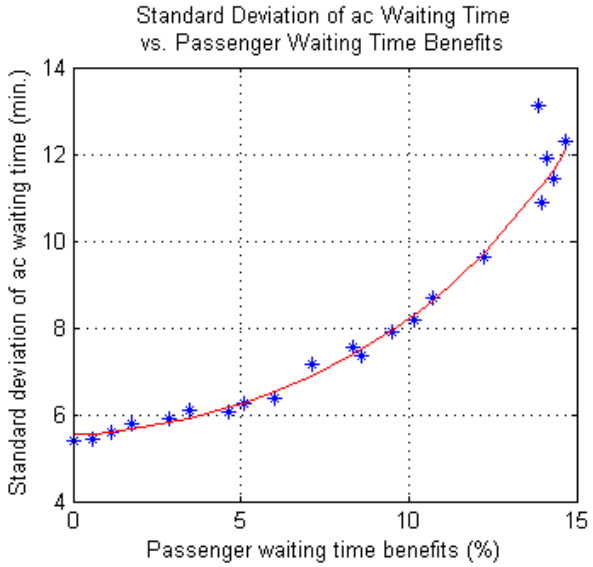

Figure 7: Standard deviation of average aircraft waiting time as a function of the reduction in passenger waiting time. The continuous line is the exponential fit.

Fig. 8 details how the trade-off affects every type of plane. This figure displays the evolution of the aircraft waiting time, for each aircraft type, as a function of the passenger waiting time benefits in percent. The percent change in the aircraft waiting time is estimated by comparing the average waiting time of same-type aircraft with the average waiting time of all aircraft [3]. For instance, Fig. 8 illustrates a policy which yields a 40% increase in average waiting times for small planes, a quasi status-quo for medium planes, and a 27% decrease for heavy planes. This policy results in a 10% decrease in the average passenger waiting time. This policy corresponds to $\alpha = 0.65$.

Fig. 9 is similar to Fig. 7, but it emphasizes the *standard deviation* of plane waiting times by airplane category: small, medium , or heavy. For high values of α, it decreases the standard deviation of waiting time for heavy planes, while it

[3]The expected average waiting time of all aircraft is not affected by changes of policy. Indeed, when a company decides to push back an aircraft before another one, the company departure rate remains the same, it transfers the delay from one aircraft to another. The simulation confirmed that the average aircraft waiting time was constant.

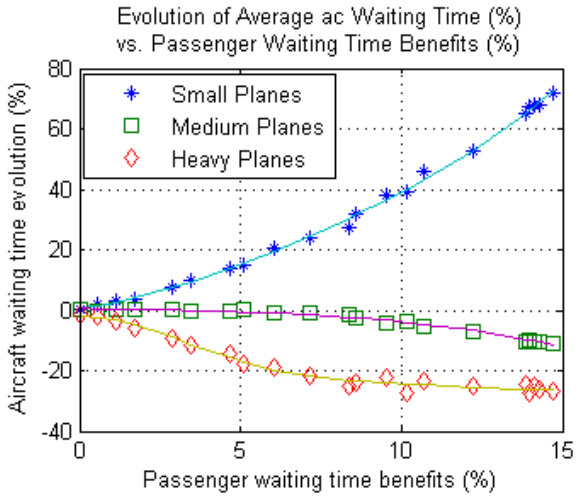

Figure 8: Evolution in percent of the aircraft waiting time, for each aircraft type, as a function of the passenger waiting time benefits in percent. Each point represents a value of α between 0 and 1, on the graph α rises from left to right.

dramatically increases it for small aircraft. For instance, a policy, which yields a 10% decrease in the average passenger waiting time, induces a 20 second decrease in the standard deviation of waiting times for heavy aircraft. In the mean time, this policy increases the standard deviation of waiting times by 30 seconds for medium aircraft, and by 3 minutes for small aircraft. Considering that small aircraft have on average 10 times fewer passengers than medium aircraft and 20 times fewer passengers than heavy aircraft, this policy could represent a plausible airline choice.

***Influence of Airline Departure Distributions*:** The market share of airline departure operations influences optimization options. A decrease in an airline's local market share diminishes the airline probability of having two aircraft in the CVQ, hence smaller airlines are less likely to benefit from flight swapping opportunities. Therefore, when airlines have fewer operations at the airport, there is a smaller difference between a FCFS policy ($\alpha = 0$) and a "Heaviest Aircraft First" policy ($\alpha = 1$). To analyze the impact of departure distributions, operations are simulated using multiple distributions of airline departure operations. Fig. 10 illustrates the 3 departure distributions studied. The first distribution corresponds to a monopoly where one

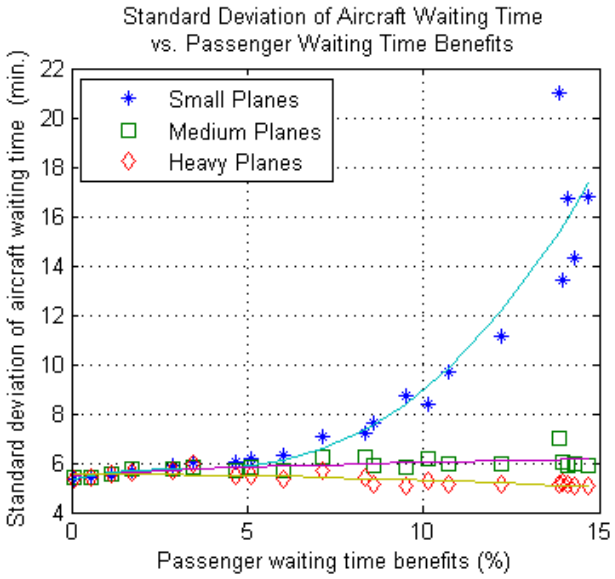

Figure 9: Standard deviation of the average aircraft waiting time, classified per type, as a function of the passenger waiting time benefits

airline, or a group of allied airlines, dominates all operations, the second corresponds to five airlines, or five group of allied airlines, sharing all departure resources, and the last distribution corresponds to ten airlines, or ten group of allied airlines, sharing all departure resources. The monopoly was simulated by assigning the same airline to every departure. The other two airline distributions with five and ten different airlines are obtained by selecting the five or ten first airlines (airline ranks and departure shares are given in Table 3) and assigning the departures to these airlines.

Table 3: Airlines departure mix

Airline Grade	Flag	Percentage of Departures
AA	USA	10.60%
AB	USA	9.27%
AC	USA	9.04%
AD	USA	8.95%
AE	USA	8.14%
AF	USA	6.77%
AG	USA	5.93%
AH	USA	5.87%
AI	USA	5.87%
AJ	USA	3.73%

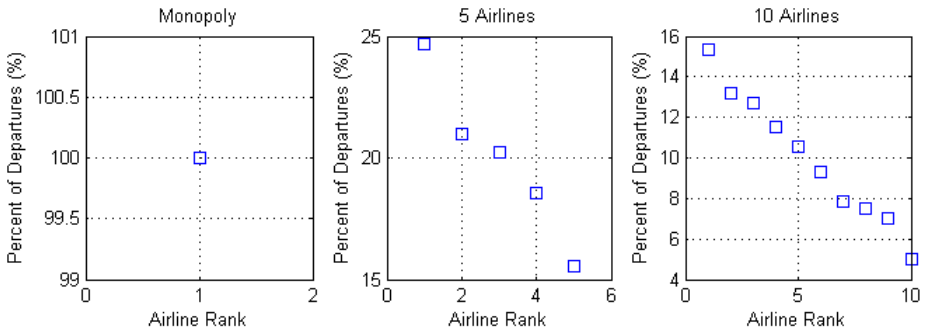

Figure 10: Airlines' share of departure operations

The case where ten airlines share departure operations is a good approximation of actual airline departure operations at Boston Logan Airport. Indeed, the first 10 airlines account for 74% of the total departure operations at Logan Airport, while each of the other 58 airlines which departed during the same period represent less than 3.5% each, totaling 26% of departure operations.

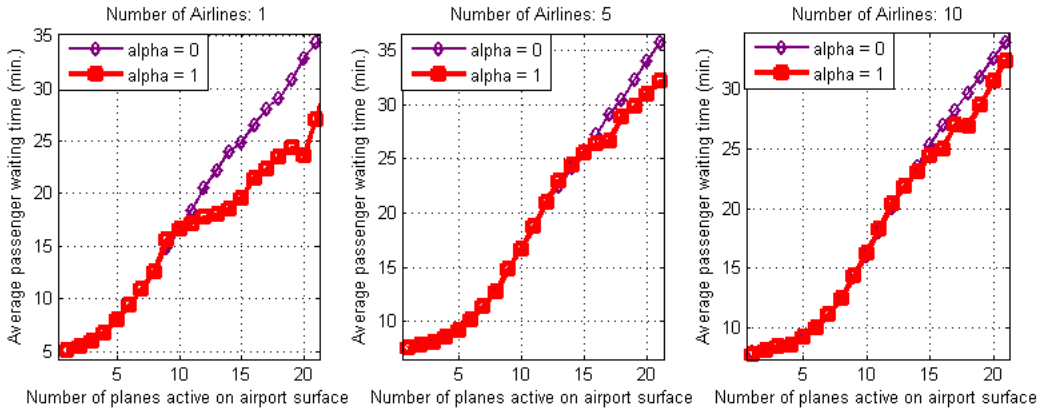

Figure 11: Impact of the number of active planes on the average passenger waiting time for three airline distributions

Fig. 11 shows that the average passenger waiting time can still be significantly reduced when departure operations are dominated by 10 airlines. Thus, during congested departure operations, a Heaviest Plane First policy ($\alpha = 1$) can reduce the expected passenger waiting time by 3%, while not affecting airport departure capacity.

2.3.3.2 Benefits Summary

This research shows that the implementation of a Collaborative Virtual Queue can shorten the average of departure taxi time, inducing a decrease in departure operating costs such as fuel usage. It also benefits the local environment since it reduces emissions on the ground. In addition, it can provide flexibility for the airlines to reorder their pushbacks according to their last-minute priorities while reducing the need for government intervention. Airlines can, for instance, shorten the average waiting time per passenger, or lower the wheels-off time unpredictability for heavy aircraft at the expense of small aircraft. The CVQ also helps the scalability in traffic load and demand, by controlling the number of planes taxiing out. Note that the Collaborative Virtual Queue concept does not intend to dictate a specific optimization scheme and will let airlines decide what is best for their business model; this Collaborative Decision Making concept merely provides new degrees of freedom for operators and enables a better control of the departure process.

CHAPTER III

ESTIMATING THE VALUE OF SURFACE SURVEILLANCE INFORMATION WITHIN A COLLABORATIVE FRAMEWORK

Nowadays, new technologies pertaining to Collaborative Decision Making (CDM) have appeared and have begun facilitating the centralization of information and the collaboration among the different air traffic stakeholders. Previous experiments [41, 42] have shown that the operational improvement achieved by these technologies is directly related to the information being provided to the end-user controlling ground operations. More particularly, airport surface surveillance technologies enable airport Common Situational Awareness (CSA), where accurate information related to aircraft identification and ground position is made more widely available to all interested parties. The two most common surveillance systems for airport surface operations, are the Surface Management System (SMS) and the Advanced Surface Movement Guidance and Control System (A-SMGCS) [39, 36]. However, there is no clear unified methodology to analyze how surface surveillance information may benefit ground operations optimization.

The objective of this chapter is thus to estimate, how surface surveillance information will affect departure operations, and to quantify potential ground emission reductions.

The previous chapter argues that the currently implemented First-Come-First-Serve system motivates aircraft to push-back as soon as they are ready, resulting in excessive build-up of queues on the taxiway system, growing congestion, potential

gridlocks, and safety concerns. One of the priorities of the Joint Planning and Development Office (JPDO) is to reduce airport congestion [11, 49, 10]. To do so, it is important to improve the control of operations at the ramp, [59, 22]; this control is a corner stone of surface operations. In case of congestion, a cooperative concept, such as the Collaborative Virtual Queue developed in the previous chapter, may transform this push system, where aircraft are sent by airlines toward the runway queue as soon as they are ready, into a pull system, where demand from the ground controllers drives the pushbacks. For this chapter, it is assumed that future cooperative systems will provide more control over the timing of clearances issued to aircraft at the ramp, especially during congested situations. These clearances will have the capability to be optimized, to efficiently balance the use of airport resources and the number of taxiing aircraft, with the help of new advanced technologies.

To clarify the impact of surface information, we study operational improvements that occur when more information is fed back to the departure control process. More precisely, this study defines surface information in terms of aircraft ground position, ramp access to the taxiway system, and runway queue length. We aim at evaluating the potential of surface surveillance technologies in the case where Collaborative Decision Making enables the centralization and fine-tuning of the control of taxi clearances for aircraft at the border of the movement area; the movement area is the part of the airport controlled by the FAA and used by aircraft for landing, takeoff and taxiing. It does not include the airport ramp.

A stochastic model of taxi departure operations is developed. The analytical decision process controlling taxi clearances at the ramp is represented using Markov Decision Processes (MDP) and Partially Observable Markov Decision Processes (POMDPs), while the taxiway system is modeled as a Markov Process. The latter is calibrated to simulate departure operations at LaGuardia Airport and Seattle-Tacoma Airport.

Surface surveillance information is fed back to an intelligent agent controlling operations. To estimate the value of this information, the performance obtained when the agent has access to full information is compared with the performance obtained when the agent has access to a low level of information. The first section details the calculation of the Markov Process transition probabilities, the calibration process, and the valuation method, for a single ramp area model. The second and third sections simulate more complex taxiway systems composed of multiple ramp areas. These more complex models closely simulate busy ground operations at LaGuardia Airport and Seattle-Tacoma Airport. They are validated against historical data. The ramp area locations are chosen based on the topology of LaGuardia Airport and Seattle-Tacoma Airport. The impact of surveillance information is stronger for the multiple ramp models, therefore several levels of partial information are defined and evaluated. Finally, the last section summarizes the research and findings.

3.1 Single Ramp Area Connected To a Single Runway: LaGuardia Airport

The information valuation method is detailed and applied to estimate the impact of surveillance information in the case when aircraft are cleared from a single ramp area at LaGuardia. Operations are modeled as a Markov Decision Process and the model is calibrated using LaGuardia Airport historical data. The impact of surveillance information for a single ramp area airport is assessed and discussed.

3.1.1 Stochastic Modeling of Surface Departure Operations

The proposed stochastic model emulates departure surface operations where:

- Exact aircraft positions are available
- Aircraft trajectories are unpredictable and follow a stochastic distribution

This model respects the queueing nature and unpredictability of departure operations. The operations are described in an aggregate fashion, therefore specific ground operations such as deicing operations are not explicitly modeled. The data used in the development of the model, as well as the model calibration and validation, are described in the following section.

3.1.1.1 Data

The model is calibrated using Aviation System Performance Metrics (ASPM) data covering the period January 2006 - September 2006. ASPM data were filtered to select LaGuardia Airport operations under runway configuration (22-13), with arrivals operations on runway 22 and departures operations on runway 13, as shown in Fig. 12. This configuration is the most used configuration at LaGuardia and represents 29.4% of all departure operations.

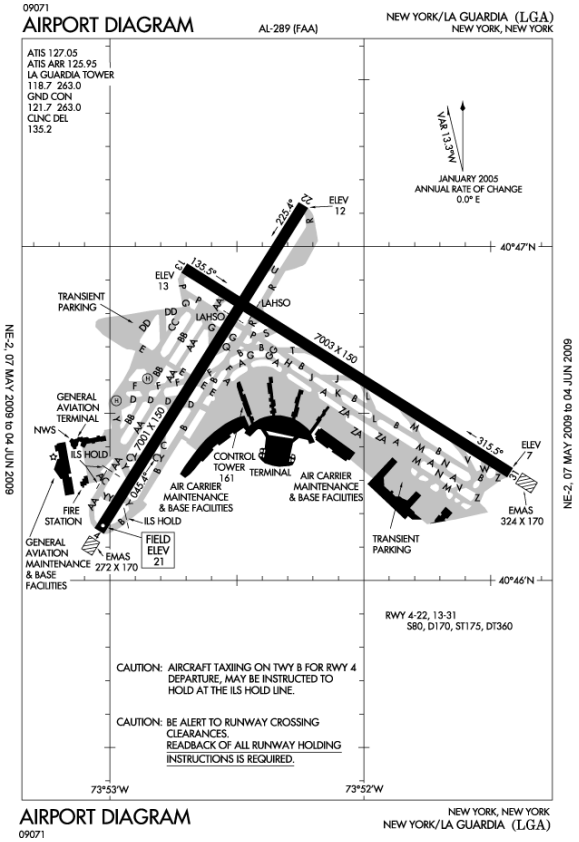

Figure 12: Map of LaGuardia Airport [35]

3.1.1.2 Departure Operations Modeling

Operations at New York LaGuardia Airport are modeled as a Markov Decision Process. The model is discrete-state and discrete-time. Aircraft locations can take a finite number of positions, defined by a spatial sampling of the taxiway system. At each time step aircraft have the opportunity of moving to the next available spatial sample.

Markov Decision Process: The model assumes that each surface state (i.e. the set of aircraft positions on airport surface) determines the transition probability to the next surface state, given the next taxi clearance decision. It also implies that the surface state represents the highest level of position information available to ground controllers, when clearing an aircraft for taxiing.

Model Description: The model emulates the queueing nature of runway operations, and the stochastic nature of aircraft taxi trajectories, to simulate how ground controllers may use taxi position information to give a push-back or taxi clearance. When a clearance is issued by ground controllers, an aircraft enters the movement area at a single entry point. The movement area of the taxiway-system is modeled, in this section, as a single taxiway. The next state of the system is unknown because, at each time-step, aircraft have a constant probability of either moving forward or stopping. In other words, one can not surely predict where a taxiing aircraft will be the next minute. However, knowledge of the current aircraft position provides information regarding the probability of every possible future position. For example, Fig. 13 represents a taxiway that can hold two aircraft on adjacent spatial samples. The current state corresponds to a taxiway with one aircraft in the first spatial sample. This aircraft has a probability m of moving forward unencumbered and a probability

$1 - m$ of stopping.

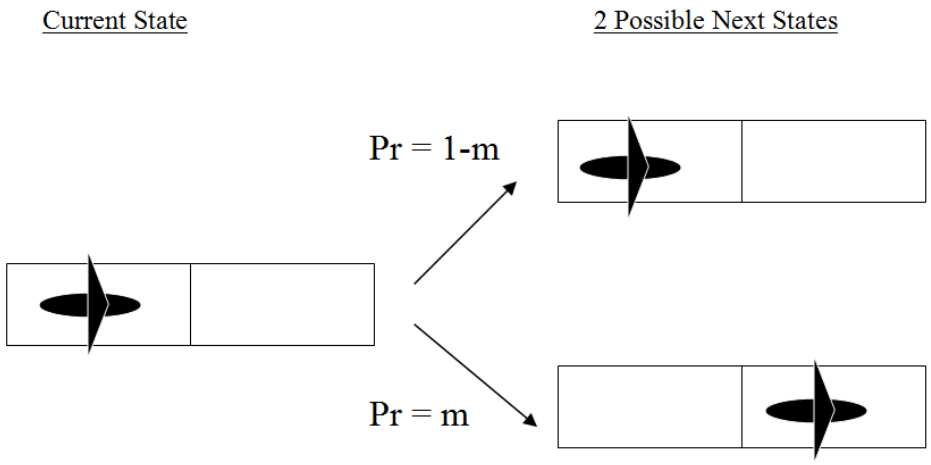

Figure 13: State transition: aircraft motion

When aircraft arrive at the runway threshold, they enter a limited capacity buffer directly servicing the runway, and the aircraft order is maintained on the taxiway system. For example, if the taxiway is made of one spatial sample, and the current state represents no aircraft in the runway buffer and one aircraft on the taxiway, the probabilities for the two possible next states are given by Fig. 14.

The take-off clearance process is simulated as a steady state stochastic process using the sum of two Bernoulli variables. This sum provides the means to calibrate, not only the average, but also the standard deviation of the take-off rate. The uncertainty related to the take-off time illustrates the limited prediction capabilities that agents issuing ground clearances have regarding the exact take-off clearance time.

Surface States Coding: Each state is represented as a binary vector composed of three parts: the control point, the taxiway, and the runway queue, as illustrated in Fig. 15. The control point represents the entry point of the taxiway. When a taxi clearance is issued, the control point is switched from 0 to 1 to indicate that an aircraft was cleared to taxi toward the runway. The second part is the taxiway, which

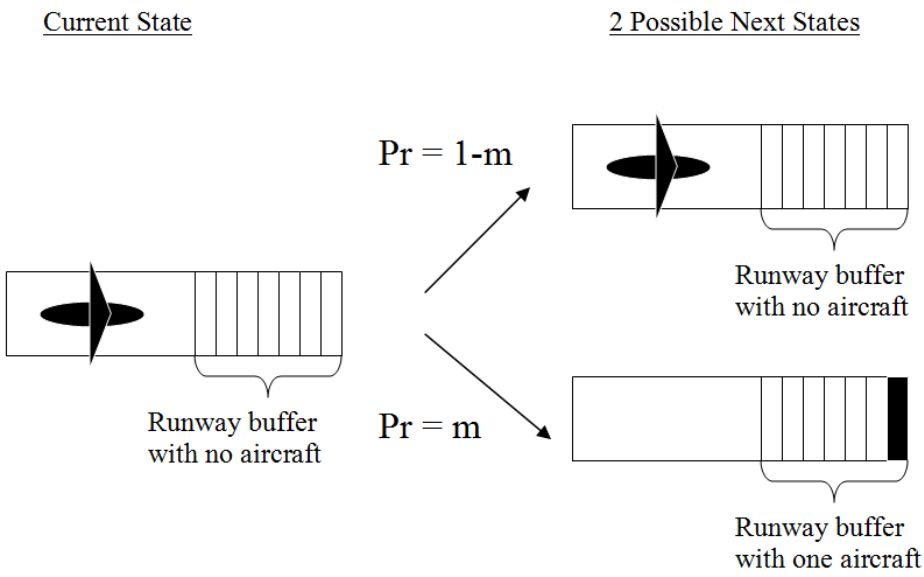

Figure 14: State transition: aircraft arriving at runway threshold

is directly connected to the control point. The taxiway is spatially sampled, with only one aircraft allowed per spatial sample. The vector's elements are set to one when the corresponding spatial s ample is occupied by an aircraft, and zero otherwise. The runway threshold queue state, illustrated in Fig. 15, is expressed as a binary number representing the number of queueing aircraft. This vector is then appended to the binary vector representing the state of the surface. For instance, if there are 3 aircraft queueing at the runway threshold, the binary vector 011 is appended at the end of the state vector. Finally, the overall binary vector is expressed as a decimal number, which will be its state identification number. For instance, in Fig. 15 , the vector 001001101011 is state 619, and corresponds to 3 aircraft on the taxiway and 3 aircraft in the runway queue.

Indices and Notations: The state space and the state index space are linked by a bijective index function. In the rest of this thesis, the notation i refers to the index of a state vector. The notation $i[s]$ refers the s^{th} component of the state vector $i \in S$.

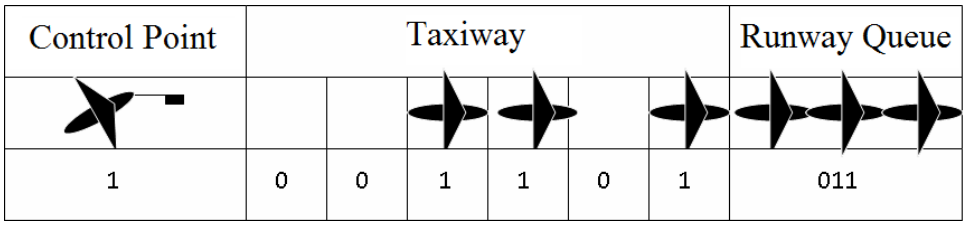

Figure 15: State space model

Parameters: The system is entirely specified by the following parameters:

- L_s : The taxiway length represented by one spatial sample
- T_s : The sampling time
- N: The number of spatial samples
- m: The probability of moving forward at the next time step
- c_1 and c_2: The probability of receiving a take-off clearance for an aircraft at the runway threshold is determined by two Bernoulli variables with parameters c_1 and c_2
- B: The maximum capacity of the runway threshold aircraft buffer

The model of departure operations is a Markov Decision Process. Thus, it is entirely defined by the probabilities to transition from a state i to another state j, knowing that the decision to send an aircraft on the taxiway is k (with $k = 1$ corresponding to the decision of sending the next aircraft, and $k = 0$ corresponding to the decision of not sending an aircraft). These probabilities are the model transition probabilities, and are noted $P_{j|ik}$. These probabilities were evaluated from the parameters described above. The model accounts for a little bit more than 220,000 non-zero transition probabilities.

3.1.1.3 Markov Decision Process: States and Transition Probabilities

The transition probabilities are generated by enumerating through all possible simultaneous sub-transitions that lead to a feasible state. Sub-transitions are defined as atomic transitions that happen during the same time step. In this section, the process, sets, and functions which have been developed to generate the transition probabilities are described in detail.

Fundamental Functions: Let S be the state space, and K the decision space. $S = \{0,1\}^{N+B}$ and $K = \{0,1\}$. In other words, S is the set of all binary vector of size $N+B$ and K is the set formed by a single binary variable.

Let T be the transition space, T is the set of all triplets $(i,j,k) \in S \times S \times K$.

Let P be a function from the space T to the probability value space $[0\ \ 1]$ such that for all $tr = (i,j,k) \in T, P_{j|ik} = P(tr)$. The transition space needs to be generated and the function P must be defined for every transition $tr = (i,j,k) \in T$.

Let T_f be the set of feasible transitions, defined by $T_f = \{tr \in T \mid P(tr) > 0\}$. Only feasible state transitions must be evaluated to find the function P. All feasible state transitions $tr = (i,j,k) \in T_f$ are the result of the succession of the sub-transitions which happened during the previous time step, starting in state i.

Let $Next$ be the set-valued function from S to the set of subsets of $S \times K \times [0\ \ 1]$, which takes any state $i \in S$ as argument and generates the set of triplets $(j,k,P_{j|ik}) \in S \times K \times [0\ \ 1]$ which are comprised of the feasible next states, the feasible decisions, and the value of the transition probability.

Then, the complete set of feasible transitions and corresponding transition probabilities is given by Eq. (1),

$$\{(tr, P(tr)), \forall tr \in T_f\} = \{(i,j,k,P_{j|ik}) \in T \times [0\ \ 1] \mid (j,k,P_{j|ik}) \in Next(i)\}. \quad (1)$$

The function $Next$ is composed of the succession of several atomic sub-transitions. Let Sub be the sub-transition function from $S \times K \times [0..1] \times \{1, \ldots, N_{sub}\}$ to $S \times K \times [0\ \ 1]$. Then $Next(i)$ is defined for all i in S by the equations (2),

$$Next(i) = S_{N_{sub}}(i), \tag{2}$$

where $S_{N_{sub}}(i)$ is generated by the succession of sub-transitions defined in equations (3), $\forall (i, n) \in S \times \{0, .., N_{sub} - 1\}$, $S_n(i) \in S \times K \times [0..1]$,

$$\begin{aligned} S_0(i) &= (i, 0, 1), \\ S_{n+1}(i) &= Sub(S_n(i), n + 1). \end{aligned} \tag{3}$$

Each sub-transition function $Sub(., n)$ is a function from $S \times K \times [0..1]$ to $S \times K \times [0..1]$ corresponding to one atomic state transition. This function generates the next intermediate states and decisions, and assigns the corresponding transition probabilities to them. To develop $Sub(., n)$, first a feasibility function is defined, then a mapping from sub-transitions to event probabilities is described, and finally the atomic transformation functions are introduced.

Let Fs_n be the graph of the sub-transformation n from S to $\{0, 1\}$, that is, $\forall i \in S$, $Fs_n(i) = 1$ if the sub-transition n is applicable to state i and 0 otherwise.

Let pr_n be a list of probabilities in $[0..1]$, pr assigns a unique atomic sub-transition probability to each specific transition n and this value is the probability that the sub-transition happens, knowing it is feasible, i.e. $Fs_n(i) = 1$.

Let at_n be the atomic transformation n from $S \times K$ to $S \times K$. at_n takes a state-decision couple (i, k) and applies the transformation number n to the state vector i, if feasible, i.e. if $Fs_n(i) = 1$. In case this sub-transformation corresponds to a decision, it updates k.

The function $Sub(., n)$ is defined by Eq. (4), $\forall (i, k, p, n) \in S \times K \times [0..1] \times \{1..N_{sub}\}$,

$$Sub(i,k,p,n) = \begin{cases} \{(i,k,p)\} & \text{if } Fs_n(i) = 0, \\ \left\{ \begin{array}{lcl} ((i,k) & , & p \cdot (1 - pr_n)) \\ (at_n(i,k) & , & p \cdot pr_n) \end{array} \right\} & \text{if } Fs_n(i) = 1. \end{cases} \quad (4)$$

From the Model Parameters to the Sub-transitions: To transition from one time step to another, a state i undergoes several sub-transitions, e.g. a take-off and an aircraft motion. The set of feasible next states, the corresponding decisions, and probabilities, are given by $Next(i)$ which is defined by the succession of the N_{sub} sub-transition functions, as defined in Eq.(2) and Eq. (4). Each sub-transition function $Sub(.,n)$ is defined by the n^{th} atomic transition function at_n, its corresponding probability function pr_n, and its graph function Fs_n, for n in $\{1..N_{sub}\}$, as shown in Eq. (4).

Sub-transitions may be classified into three classes: take-offs, aircraft moves, and taxi clearances. The sub-transitions are evaluated in the following order: First take-offs, then clearances, and finally aircraft moves. N is the number of bits assigned to the taxiway and B is the number of bits assigned to the runway queue, therefore the state $i \in S$ is a $N + B$ bit vector. $i[n]$ designates the n^{th} bit of the state vector i. Let $bin2dec$ be the function which converts binary numbers into decimal numbers and $bin2dec$ its inverse. This section describes how at_n, pr_n, and Fs_n are set by the parameters described in section 3.1.1.2, for all n in $\{1..N_{sub}\}$.

Take-offs

Fs_1 tests if one aircraft is ready to take-off,

$Fs_1(i) = (1 \leq bin2dec(i[N+1:N+B]) \leq 2)$.

Knowing there is one aircraft ready to take-off, the probability of the aircraft

to take off is:

$pr_1 = 1 - c_1 \cdot c_2$,

the transformation at_1 creates a state vector with one aircraft removed from the runway queue, $i[N : N + B - 1] = bin2dec(dec2bin(i[N + 1 : N + B]) - 1)$.

Fs_2 tests if there are enough aircraft for two take-off,

$Fs_2(i) = bin2dec(i[N + 1 : N + B]) \geq 2$.

Knowing there are two aircraft ready to take-off, the probability of having two take-offs is: $pr_{2_1} = 1 - c_1 \cdot c_2$,

the transformation $at_{2_1}(i)$ creates a state vector where one aircraft is removed from the runway queue, $i[N : N+B-1] = bin2dec(dec2bin(i[N : N+B-1])-2)$.

Knowing there is two aircraft ready to take-off, the probability of having only one take-off is: $pr_{2_2} = c_1 \cdot (1 - c_2) + c_2 \cdot (1 - c_1)$,

the transformation at_{2_2} creates a state vector with two aircraft removed from the runway queue, $i[N : N + B - 1] = bin2dec(dec2bin(i[N : N + B - 1]) - 2)$.

Taxi clearances

Fs_3 tests if the ramp access is free of aircraft,

$Fs_3(i) = (i[1] = 0)$.

Since this taxi clearance is a decision which leads to an outcome with a probability of one: $pr_3 = 1$,

the transformation $at_3(i, k) = ([1\ i[2 : N + B]], 1)$ sets the decision to 1, and adds a plane in the first spatial sample, $i[1] = 1$.

Aircraft move

The sequence of the move sub-transitions is such that the aircraft closest to the runway queue moves first.

Fs_4 tests if an aircraft can enter the runway queue,

$Fs_4(i) = ((i[N] = 1)\&((i[N+1:N+B]) < 2^B - 1))$.

Knowing there is an aircraft ready to move, and that it can enter the queue, the probability is given: $pr_4 = m$,

the transformation at_4 moves an aircraft from spatial sample N to the queue $i[N] = 0$ and $i[N+1:N+B] = dec2bin(bin2dec(i[N:N+B-1]) + 1)$.

$Fs_{13-s}(i) = move(i, s)$, for $s \in 1, .., 8$, tests if an aircraft can move from sample s to the next $s+1$,

$move(i, s) = ((i[s] = 1)\&(i[s+1] = 0))$.

Knowing there is an aircraft ready to move, and that it can move, the probability is given: $pr_{13-s} = m$,

the transformation at_{13-s} moves an aircraft from spatial sample s to spatial sample $s+1$, $i[s+1] = 1$ and $i[s] = 0$.

3.1.1.4 Model Calibration

This section describes how the parameters determining the behavior of the model were set. The calibration of the model is based on the analysis of the selected ASPM data, as well as direct observations of airport satellite pictures. The following quantities are defined: L_s corresponds to observations of physical distances between taxiing aircraft. T_s is defined as the shortest characteristic time of the different phenomena captured by the model. The variables N, the number of spatial samples of the taxiway, and m, the probability of moving forward when unencumbered, are calibrated using taxi statistics derived from ASPM data. Finally, c_1, c_2, which define the take-off probabilities, and B, the runway buffer size, are calibrated using take-off statistics coupled with estimates of the number of taxiing aircraft.

Sampling Time: The temporal resolution of the ASPM data is one minute. Our model sampling frequency was set to match the sampling rate of the data against which it is calibrated and T_s is set to one minute.

Departure Capacity: Heavy traffic surface operations were identified using a simple input-output model to evaluate the departure capacity and calibrate the take-off clearance variables c_1 and c_2. Such a model counts the number of push-backs, and subtracts the number of take-offs to obtain the number of taxiing aircraft. Heavy traffic corresponds to the number of aircraft for which the average number of take-off per minute saturates. In the case of LaGuardia Airport, heavy traffic is achieved when 14 or more aircraft are taxiing toward the runway. In particular, data show that the airport throughput rate has a mean of 0.605 aircraft per minute and a standard deviation of 0.578 aircraft per minute when the taxiway system is saturated. The take-off clearances are modeled using the sum of two Bernoulli variables c_1 and c_2 of parameter 0.5140, and 0.0929, respectively (variables following a Bernoulli distribution of parameter p equal to 1 with success probability p and 0 with failure probability $1-p$). The sum of the two random variables is evaluated at every minute and determines how many aircraft take off. The value of these two parameters was determined by solving the following system of equations:

$$\text{Average} = c_1 + c_2 = 0.605 \tag{5}$$

$$\text{Std Deviation} = \sqrt{c_1 \cdot (1 - c_1) + c_2 \cdot (1 - c_2)} = 0.578 \tag{6}$$

Taxiway: Once the departure rate variables are calibrated, the taxiway variables N and m are calibrated to reproduce light-traffic unimpeded taxi-time average, and standard deviation, for aircraft pushing back from the busiest ramp area. The standard deviation and average of light-traffic taxi times were evaluated using the ASPM database. The taxi-out time is defined as the time between push-back and wheels-off

and includes pushback, taxi, and waiting for take-off clearance times. In addition, ASPM data provide unimpeded taxi out times, i.e. times it takes for aircraft to transit from pushback to take-off when the taxiway system is empty and aircraft can travel directly to the runway threshold. The unimpeded taxi-out times are defined by the FAA as "the estimated Taxi Out Time for an aircraft by carrier under optimal operating conditions (when congestion, weather, or other delay factors are not significant). This number is estimated by calendar year and season for each carrier and airport reporting ASQP and ARINC data" [8]. These times depend on the ramp area from which aircraft have pushed back. They are computed by the FAA as follow: "first, the unimpeded taxi-out time is redefined in terms of available data as the taxi-out time when the departure queue is equal to one and the arrival queue is equal to zero. Then, a linear regression of the observed taxi-out times with the observed departure and arrival queues is conducted, and the unimpeded taxi-out time is estimated from this equation by setting the departure queue equal to 1 and arrival queue equal to 0" [62].

First, light density surface operation periods were selected using a simple input-output model to find the approximate number of taxiing aircraft. Light traffic is defined as fewer than 5 aircraft taxiing on the surface. The input-output method consists of adding the number of push-backs and subtracting the number of take-offs for each minute of ASPM data.

Second, the ramp area was identified using the unimpeded taxi-out times. Aircraft pushing back from the same or nearby ramp areas are very likely to have the same unimpeded taxi-out time. According to ASPM data for flights departing from LaGuardia Airport, the most common unimpeded taxi-out time for all departure operations was 12.9 minutes. Thus, to select aircraft pushing back from the busiest area, departures with 12.9 minutes unimpeded taxi-out time were chosen.

Third, the taxi-out times were filtered to remove unrealistically short taxi-out

times corresponding to errors in ASPM data. The ASPM data shows that the minimal *unimpeded* nominal taxi-out time for Laguardia is 6.7 minutes. As explained earlier, these unimpeded taxi-times are evaluated independently from the taxi-out times that are recorded during operations. Therefore taxi-out times shorter than 6.7 minutes were filtered out. Fourth, taxi times were filtered to remove times including significant queuing, when taxi-times exceeded the maximal unimpeded nominal taxi-out time of 16.4 minutes.

Finally, the average and the standard deviation of the light traffic taxi-out time distribution at LaGuardia for aircraft pushing back from the busiest ramp area were identified: The average is 13.56 minutes and the standard deviation is 2.00 minutes. This taxi-out time includes the taxi time, the time spent at the runway threshold waiting for clearance, and the push-back time:

$$t_{taxi-out} = t_{pushback} + t_{taxi} + t_{takeoff-clearance} \tag{7}$$

Assuming that the time to push-back, the taxi time, and the waiting time for a take-off clearance are independent, the standard deviation for the taxi time is then given by the following formula:

$$Std(t_{taxi}) =$$

$$\sqrt{Std(t_{taxi-out})^2 - Std(t_{pushback})^2 - Std(t_{TO-clear.})^2} \tag{8}$$

Fig. 16 shows the distribution of light-traffic taxi-out times for departures with 12.9 minute unimpeded taxi-out time at LaGuardia.

- Pushbacks: Average duration of pushback was evaluated by Delcaire and Feron [30] at 2 minutes. Based on the data collected in their report, it is fair to estimate the standard deviation of pushback duration at 80 seconds, or 1.33 minutes.

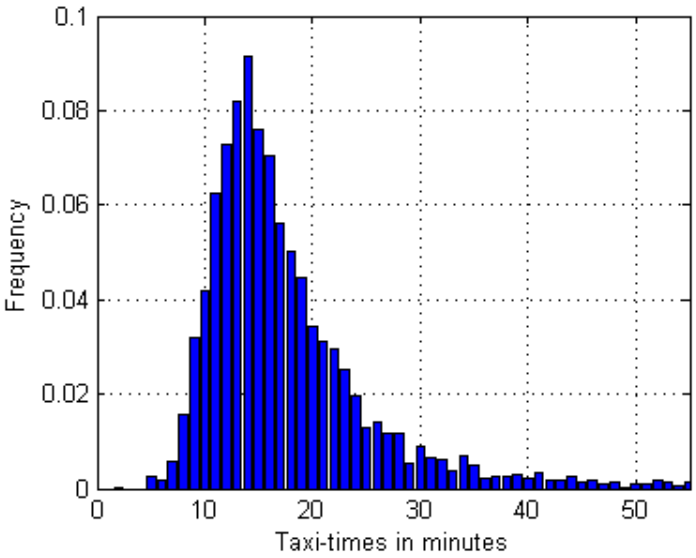

Figure 16: Light traffic taxi-times distribution

- Take-off clearance: Taxi-out times include waiting times for take-off clearance at the runway threshold. However, the model calibration should not include the variation caused by this waiting time. In this model, the average waiting time for one aircraft at the runway threshold before clearance is $1/0.605 = 1.65$ minutes, and the standard deviation 1.04 minutes.

- Taxi time: According to (7) and (8), the taxi time has a standard deviation of $\sqrt{2.00^2 - 1.04^2 - 1.33^2} = 1.07$ minutes and an average of $13.56 - 1.65 - 2 = 9.91$ minutes.

  The probability m of moving forward, and the number of steps N, were calibrated to match the average and standard deviation of taxi times in light traffic under nominal conditions. N and m solve the following system of equations.

$$\text{Average} = \frac{N}{m} \cdot T_s = 9.91 \text{ minutes} \tag{9}$$

$$\text{Standard Deviation} =$$

$$\frac{N}{m} \cdot \sqrt{\frac{1-m}{N}} \cdot T_s = 1.07 \text{ minutes} \tag{10}$$

Which gives,

$$N = 8.88 \approx 9 \text{ steps}$$

$$m = 0.90 \approx \frac{9}{\text{Average}} = 0.9084$$

- Calibrating B: The aircraft buffer at the runway threshold simulates aircraft that queue closely to each other in order to ensure a high utilization rate. The buffer capacity needs to be large enough to allow ground controllers to absorb uncertainties in take-off clearance time and taxi time. The standard deviation yielded by the sum of these two times for a single aircraft is $\sqrt{1.07^2 + 1.04^2} = 1.49$ minutes.

  The buffer was calibrated to be able, when fully loaded, to supply aircraft for a time close to 3 times this standard deviation, i.e. 4.47 minutes. Thus, the buffer size was approximated to provide enough aircraft to cover at least 4.47 minutes, which is $4.47/0.605 = 7.39 \approx 7$ take-ff clearances. The capacity was set to 7 aircraft and the buffer was coded using 3 bits, as illustrated in Fig. 15.

- Calibrating L_s: A 200-meter separation between taxiing aircraft was suggested in previous work on taxi operations [17, 68]. Hence, L_s was set to 200 meters.

The calibration values for the system parameters are summarized in Table 4.

Table 4: Calibration values

Calibration Variables	**Values**
L_s	200 meters
T_s	60 seconds
N	9
m	0.9084
c_1	0.5140
c_2	0.0929
B	7

3.1.1.5 Model Validation

Using ASPM data, LaGuardia's average throughput rate is expressed as a function of the number of taxiing aircraft. The graph provided in Fig. 17 shows the throughput as a function of the number of taxiing aircraft, and yields the average take-off rate. Fig. 17 also shows the throughput as a function of the number of taxiing aircraft for the stochastic model identified above. The model behaves similarly to the airport, and faithfully reproduces the queueing and stochastic nature of departure operations. When the number of taxiing aircraft reaches 11, the model saturates, and yields a maximum take-off rate distribution averaging 0.605 aircraft per minute, with a standard deviation of 0.578 aircraft per minute. These are identical to the average (0.605) and the standard deviation (0.578) of the take-off rate at LaGuardia, when the taxiway is saturated by departing aircraft. The saturation level of the take-off rate for the model is reached at a lower number of taxiing aircraft than for LaGuardia because the model emulates taxiing aircraft starting only at the control point of one ramp area, on one major taxiway, whereas ASPM data accounts for all departure ground operations beginning at pushback. In section two and three, more complex models are used, based on multiple ramp areas. We show that these more complex models better simulate departure operations at LaGuardia Airport and Seattle-Tacoma Airport.

3.1.2 Impact of aircraft position information

To understand and valuate the impact of aircraft position information on departure operations, an approach based on the optimization of Markov Decision Processes (MDP) and Partially Observable Markov Decision Processes (POMDP) was developed. This approach is applied to two distinct levels of surface information and one benchmark policy:

- a high level of surface information, named "full state feedback",
- a low level of aircraft surface position information, named "estimated state

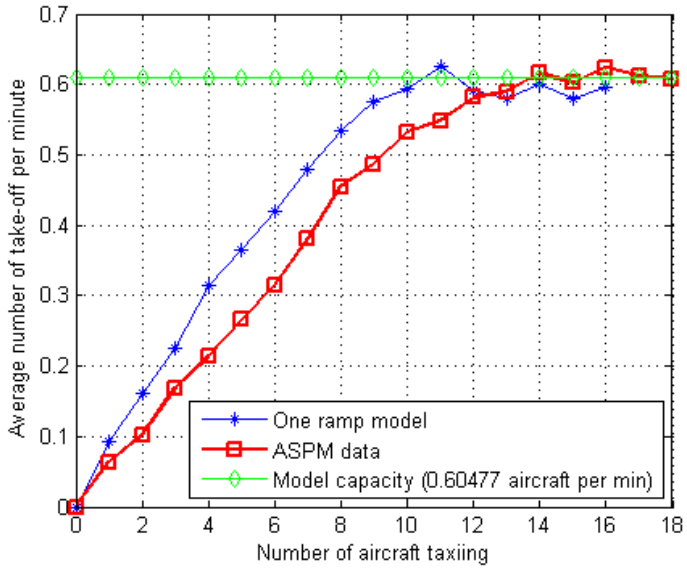

Figure 17: LaGuardia throughput as a function of the number of taxiing aircraft, from the one ramp model and ASPM data. The ASPM data reflects all departure operations on the ground starting at pushback.

feedback",

- a basic benchmark policy relying solely on the number of aircraft, named "threshold policy" [59, 34].

3.1.2.1 Approach

The objective of this approach is to evaluate how the level of information available on aircraft position affects potential taxi-time reductions, for a given rate of runway utilization, and within a collaborative framework enabling the fine tuning of taxi clearances, when aircraft exit the ramp area.

Assumptions: Ground controllers operate as optimally as allowed by existing technology: they know the behavior of the system, and given the level of information available, they understand what the best policy is. Their goal is to maximize the departure runway utilization rate, while controlling aircraft to minimize taxi times.

It is assumed that there is enough departure demand for FAA ground controllers to always have an aircraft waiting to be cleared for taxi, since this corresponds to peak demand times. The aircraft is either cleared for push-back, if it pushes directly on the movement area, or cleared for taxi, if it has already pushed back on the ramp area, and is waiting at a control point to enter the movement area.

Optimal clearance policy: Departure operations were modeled as a discrete Markov Decision Process, i.e. a finite set of states with steady transition probabilities from any state to any other, given a decision. Each state has a cost, an optimal clearance policy is the set of decisions that minimizes the expected averaged cost over an infinite time horizon.

Trade-offs and cost structure: Each state i is given a cost C_i. This cost is the sum of the number of taxiing aircraft $N_{ac}(i)$ and a cost attributed to the non-utilization of the runway $\delta_r(i)$ multiplied by a constant β. The variable $\delta_r(i)$ is equal to 1 if there is no aircraft in the runway buffer and to 0 if there is at least 1 aircraft. For every state i, the cost C_i attributed to that state is given by Equation 11,

$$C_i = N_{ac}(i) + \beta \cdot \delta_r(i). \tag{11}$$

As β increases, the optimal policy favors maximizing the runway utilization rate over minimizing the number of taxiing aircraft. β and C_i are expressed in number of aircraft per minute. β is the ratio of the cost of non-utilization of the runway for one minute over the cost of having one aircraft on the taxiway for one minute.
Each optimal policy is Pareto optimal and captures the trade-off between minimizing taxi time and maximizing runway utilization rate.

Valuation: The metrics used to value information are runway utilization and number of taxiing aircraft. Runway utilization is the percentage of time the runway

buffer had at least one aircraft, number of taxiing aircraft is the average number of aircraft present on the surface. There is a direct trade-off between maximizing runway utilization and minimizing the number of taxiing aircraft.

For every trade-off, optimal policies are evaluated under two levels of information: full state feedback, where the controller has access to each aircraft position on the taxiway, and estimated state feedback, where the controller only has access to the number of taxiing aircraft on the taxiway, and knows if the control point is occupied. The latter situation typically corresponds to cases where visibility is poor and there is no surface surveillance system to provide the missing aircraft position information. In addition, performance is as well evaluated for a basic threshold policy which serves as a benchmark.

3.1.2.2 Full information: Full State Feedback and optimal policies

Under full state feedback, the agent controlling the clearances can fully observe the surface state. The optimal decision k is a function of the state i, which is itself fully determined by the observation o:
$k = \Pi(i) = \Pi(f(o))$ where f is a bijective function from the observation space to state space and Π is the decision policy, a surjective function from the state space to the decision space.

Each value of Beta represents a trade-off level between maximizing runway utilization and minimizing taxi times, β is fixed, and each state cost is defined by (11). Using linear optimization techniques, it is possible to find the optimal decision policy Π that minimizes the expected cost per time step [40]. If $i(t)$ is the state at time t, then

$$\text{Expected Cost} = \lim_{n\to\infty} E\left(\frac{1}{n}\cdot\sum_{t=0}^{n} C_{i(t)}\right). \tag{12}$$

Notations:

- Let ι be the state at time n.

- Let η be the state at time n+1.
- Let κ be the decision variable value at time n.
- Let $y_{ik} = P(\iota = i, \kappa = k)$ be the probability of being in state i and taking decision k. The optimal decision k is given by the optimal policy: $k = \Pi(i)$.
- Let $p_{j|ik} = P(\eta = j|\iota = i, \kappa = k)$ be the probability of having the next state j knowing the current state is i and the decision chosen is k.

For a steady state process with $M + 1$ states and K decisions, the expected cost per time step is [40]

$$\lim_{n\to\infty} E(\frac{1}{n} \cdot \sum_{t=0}^{n} C_{i(t)}) = \sum_{i=0}^{M} \sum_{k=1}^{K} C_{ik} \cdot y_{ik}. \tag{13}$$

Consequently, the cost function for this linear optimization is

$$\text{Minimize } Z = \sum_{i=0}^{M} \sum_{k=1}^{K} C_{ik} \cdot y_{ik}. \tag{14}$$

Subject to:

1. Constraints on state-decision probability variables:

$$\sum_{i=0}^{M} \sum_{k=1}^{K} y_{ik} = 1 \tag{15}$$

$$y_{ik} \geq 0, \text{for } i = 0..M; k = 1..K \tag{16}$$

2. Constraints governing state transitions:

$$\sum_{k=1}^{K} y_{jk} - \sum_{i=0}^{M} \sum_{k=1}^{K} y_{ik} \cdot p_{j|ik} = 0, \tag{17}$$

for $j = 0..M;\ k = 1..K$

Once the optimal set of steady state probabilities of being in state i and taking decision k, y_{ik}, is evaluated and the corresponding optimal pushback policy is given by

$$\text{if } y_{ik} > 0 \text{ then } \Pi_i = 1 \text{ else if } y_{ik} = 0 \text{ then } \Pi_i = 0 \tag{18}$$

3.1.2.3 Partial information: Estimated State Feedback

In this scenario, the agent has access to the number of taxiing aircraft, and he knows whether or not it is physically possible to clear an aircraft (there may be another aircraft in the way). In real-life situations, this partial information is always available because ramp controllers keep track of the number of aircraft that have pushed back, and the number of aircraft that have taken-off. In addition, communication technologies ensure simple Input-Ouput information is easily available. For instance, Aircraft Communications Addressing and Reporting System (ACARS) is a digital datalink system for transmission of short relatively simple messages between aircraft and ground stations via radio or satellite and provides aircraft take-off times. Under limited aircraft position information, the system becomes a Partially Observable Decision Process (POMDP). There exists several methods to solve POMDPs optimally [28, 27, 64, 51]. These methods are computationally very demanding for a finite time horizon, and not appropriate for an infinite time horizon. Indeed, finite-horizon POMDPs are PSPACE-complete [58] and infinite-horizon POMDPs are undecidable [57].

Most Likely State: For these reasons, methods applicable to an infinite time horizon and computationally more tractable were considered [28]. The Markov process that is modeled for LaGuardia includes more than 220,000 transitions with non-zero probabilities. Heuristic methods are computationally faster, and better suited to determine effective control laws for this POMDP. Among these, the Most Likely State

(MLS) algorithm was selected because it is applicable to an infinite time horizon and compares favorably with other effective heuristic algorithms [28]. Moreover, its steps resemble the behavior of a decision maker under uncertainty. Indeed, this heuristic control strategy consists of estimating the most likely current state, and choosing the corresponding optimal decision, using the optimal decision policy evaluated in the full state feedback case. Fig. 18 illustrates the information available to the decision maker.

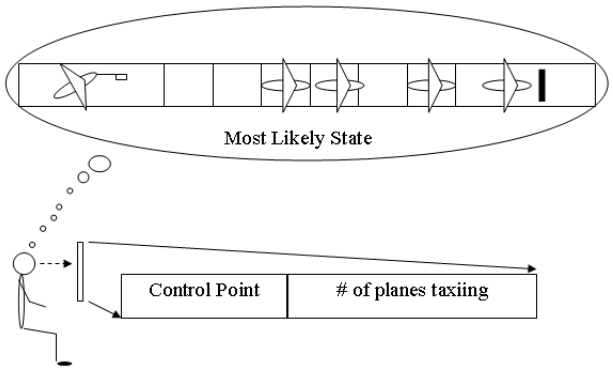

Figure 18: Estimation of the taxiway system state by a decision maker

The variables used in the MLS algorithm are defined as follow:

- Let Θ designate the index of the current observation. The current observation is the number of taxiing aircraft and wether or not it is physically possible to clear an additional aircraft for pushback or taxi.

- Let b_i be the probability of being in state i for all states i of the state space. b is the belief state vector.

- Let $p_{o|j} = P(\Theta = o|\eta = j)$ be the probability of observing o, knowing the current state is j, for all observations o in the observation space, and for all states j in the state space.

The updater function takes the previous belief state b, the current observation o, the

previous decision k, and returns the current belief state vector b'.

The following equation is derived from Bayes' rules [55]:

$$b'_j = \frac{p_{o|j} \sum_{i=0}^{M} p_{j|ik} \cdot b_i}{\sum_{j=0}^{M} p_{o|j} \sum_{i=0}^{M} p_{j|ik} \cdot b_i}. \tag{19}$$

Fig. 19 details the heuristic control of taxi clearance decisions based on partial observations.

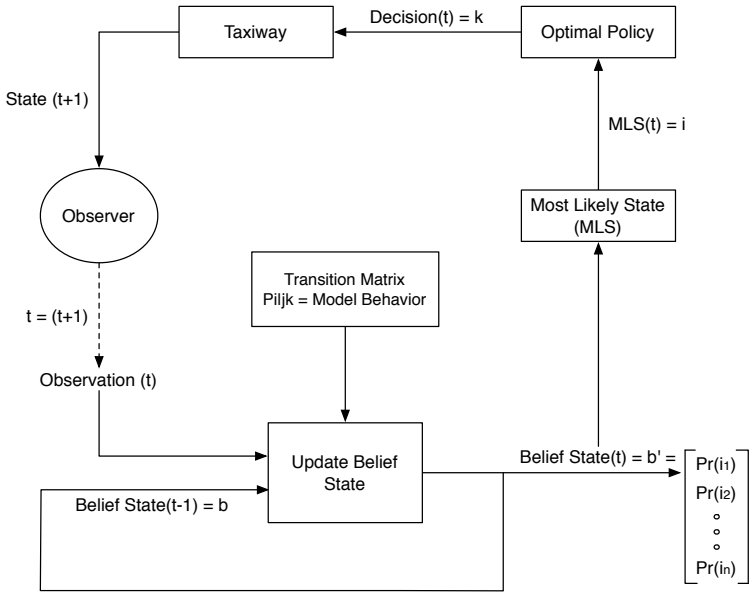

Figure 19: Heuristic control of taxi clearance decisions based on partial observation

Observation probability matrix: This paragraph details how observations are defined and how the probability matrix $p_{o|j}$ is evaluated. The information contained in an observation is given by the probability matrix $p_{o|j}$. This probability is key to evaluate the probability of having every state j given a specific observation o and previous belief b. Eq. (19) explains how observations of the surface are incorporated into the decision process during the update of the belief state.

Let O be the observation space and c be the total number of components, or piece of information, included in each observation $o \in O$. Then O is a subset of $\Re^c$. In this

scenario there are two pieces of information, $c = 2$, the number of taxiing aircraft N_{ac}, and whether or not it is physically possible to clear an aircraft using ($RampFree$), a binary variable. An observation is a vector defined by

$$o = \begin{bmatrix} N_{ac} & RampFree \end{bmatrix}. \tag{20}$$

The algorithm generating the observation probability matrix uses an injective function, which attributes a unique observation index $n(o)$ to every observation o. The injective function converts the observation vector with 2 components into a binary vector of $[roundup(log2(max(Nm_{ac}))) + roundup(log2(max(RampFree)))]$ bits to then reconvert it back to its decimal value, as illustrated in Eq. (21).

$$n(o) = bin2dec(\begin{bmatrix} dec2bin(N_{ac}) & dec2bin(RampFree) \end{bmatrix}) \tag{21}$$

For any state j, there exists only one information that can be observed $o(j)$, consequently for a system with N possible observations and M states, observation probabilities are zeros and ones, i.e. $\forall(o_n, j) \in \{1..N\} \times \{1..M\}$, $p_{o_n|j} \in 0, 1$. Eq. (22) shows how the $p_{o|j}$ matrix is evaluated.

$$p_{o_n|j} = \begin{cases} 1 \text{ if } o_n = n(o(j)), \\ 0 \text{ if } o_n \neq n(o(j)). \end{cases} \tag{22}$$

3.1.2.4 Benchmark: the threshold policy

A threshold policy is a pushback control law, which relies solely on the current number of taxiing aircraft to make a push-back decision. This simple control law computes the number of taxiing aircraft $N(i)$ for state i and compares it to a given threshold value Th [59]. If the number of aircraft is greater than the threshold, no pushback clearance is issued, and $k = 0$. On the other hand, if that number is smaller than

the threshold, a pushback clearance is issued, and $k = 1$. This is summarized by the following Eq. (23),

$$k = \begin{cases} 1 \text{ if } N(i) > Th, \\ 0 \text{ if } N(i) \leq Th. \end{cases} \tag{23}$$

3.1.3 Results and discussion

This section presents the results yielded by the taxi-clearance policies when surface information is available, partially available, and when the benchmark threshold policy is used.

3.1.3.1 Optimal policies

As discussed above, each policy corresponds to a trade-off between maximizing runway utilization, and minimizing the number of taxiing aircraft for two different levels of information. The full state feedback policy is exactly optimal, the estimated state feedback is a heuristic algorithm that controls aircraft taxi clearances by estimating the most likely aircraft positions based on partial observation, and finally the threshold benchmark policy which issues a taxi clearance when the number of taxiing aircraft is below the threshold.

The multiple curves in Fig. 20 correspond to the full state feedback case and illustrates every optimal policy, for several values of the trade-off parameter beta. Every curve displays the pushback frequency as a function of the number of taxiing aircraft when the pushback decision is taken.

As the value of the trade-off parameter β increases, the policy becomes simpler and converges toward a threshold policy. At the highest level of runway priority, represented by the bottom right curve on Fig. 20, aircraft are continuously pushed back as fast as possible.

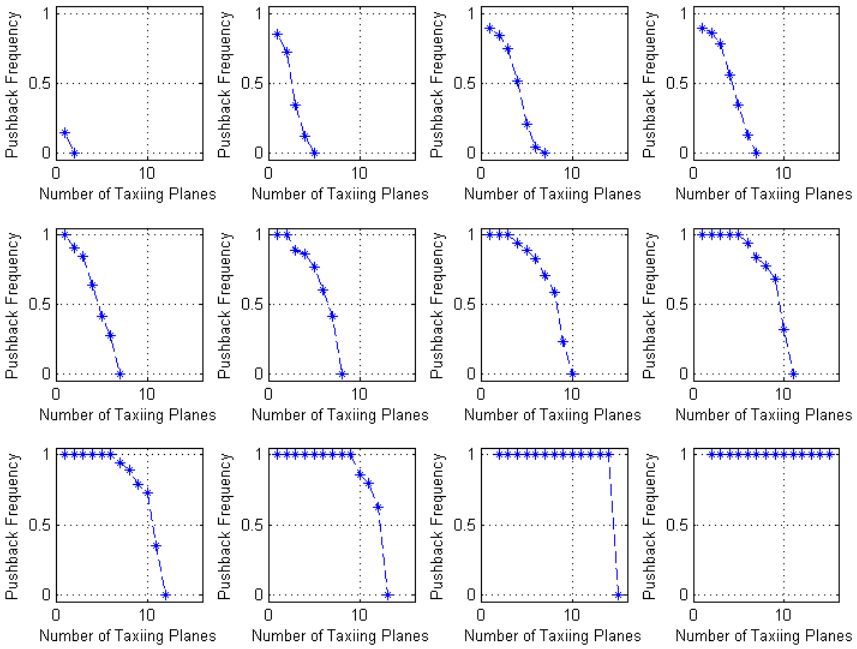

Figure 20: Push-back frequency as a function of the number of taxiing aircraft, for each trade-off value β in $\{6, 7, 8.6, 9.3, 10, 15, 25, 40, 60, 100, 1000, 10^4\}$. The upper left figure corresponds to $\beta = 6$ and the bottom right to $\beta = 10^4$.

3.1.3.2 Optimal policies validation

Motivation: This section validates the optimal pushback policies found by the optimization software CPLEX used to solve the linear program described in section 3.1.2.2. It verifies that these policies actually perform as well as the optimization software suggests. Indeed, the performance of these policies can be derived directly from the CPLEX output variables y_{ik}, since these variables are the steady state probabilities for all pairs (i, k) of state i and decision k. However there is a risk that actually replaying the optimal policies will not perform as predicted. Indeed, computers have a limited precision and can perform operations on a limited number of significant digits. CPLEX uses double-precision arithmetic in its computations [7]. Similarly, Matlab computations are limited to the double-precision arithmetic [12]. This is a binary format that occupies 64 bits (8 bytes) and its significand

has a precision of 53 bits. Therefore the maximum number of significant digits is $log_{10}(2^{53}) = 15.95$. Consequently, if the number of significant digits needed to express the transition probabilities exceeds 16, or if CPLEX's intermediate computations yield results with more than 15 significant digits, there will be accuracy issues. Potential problems may also arise when the data provided to the optimization software is not accurate enough, as this can happen during the evaluation and the writing of the transition probabilities into the '.lp' files, which are the files used to feed the problem to the optimization software. This latter accuracy problem can be easily identified and corrected by looking directly into the '.lp' files.

Therefore, solutions yielded by an optimization software should not be trusted without proper validation.

Validation: The results yielded by simulating operations and controlling pushbacks using the optimal policies are compared with the results which are directly derived from the CPLEX output variables.

Fig. 21 illustrates the runway utilization rates of the optimal policies as a function of their average number of taxiing aircraft. Each point corresponds to a Pareto-optimal policy, which was evaluated for a value of the trade-off parameter β. Two curves, the one marked with stars and the plain curve, represent the set of performances of the optimal policies under full state feedback (i.e. the decision-maker knows the aircraft exact positions on the taxiway, and finds the best time to issue a taxi clearance). The curve marked with stars is the CPLEX output curve: each of its points is directly derived from the CPLEX output variables y_{ik}. The plain curve is the simulation curve: each of its points is obtained by simulating operations over 3.5 days and controlling the pushbacks according to the corresponding optimal policy.

The both curves are almost identical, hence validating the equivalence between the CPLEX output and the corresponding simulation of the optimal policy derived

in Eq. (18). Fig. 22 quantifies the difference in percent between the average number of taxiing aircraft yielded by the CPLEX output and the average number of taxiing aircraft yielded by the simulation, as a function of the utilization rate. The optimal solution is reliable and comparable to the simulation, for most utilization rates up to 0.94. There is a small divergence of performance for one point with a utilization rate above 0.95; the CPLEX output indicates an average number of taxiing aircraft that is 2.5 percent lower than the average reached when the optimal policy is simulated. This small difference is created by the rounding errors discussed above and some noise from for the simulation. However all other policies perform within 1 percent of what is predicted, and 9 out of 12 policies perform at 0.5 percent and closer of predictions, as illustrated in Fig. 22.

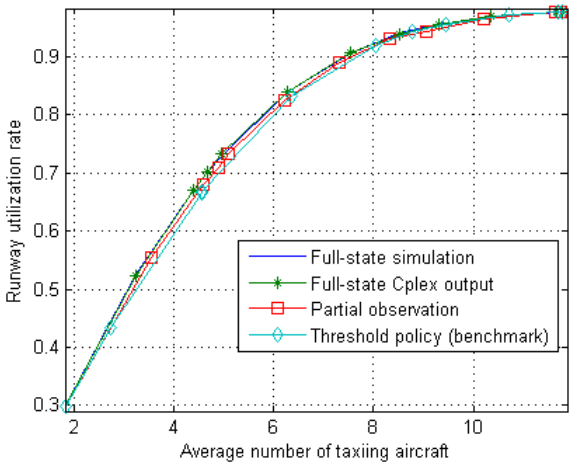

Figure 21: Runway utilization rate as a function of the average number of taxiing aircraft

3.1.3.3 Analysis

The two remaining curves (with squares and diamond) in Fig. 21 show results for the estimated state feedback and the benchmark threshold policies. The curve identified by squares represents the performance of optimal policies under partial information or estimated state feedback (the decision-maker only knows the number $N(i)$ of taxiing

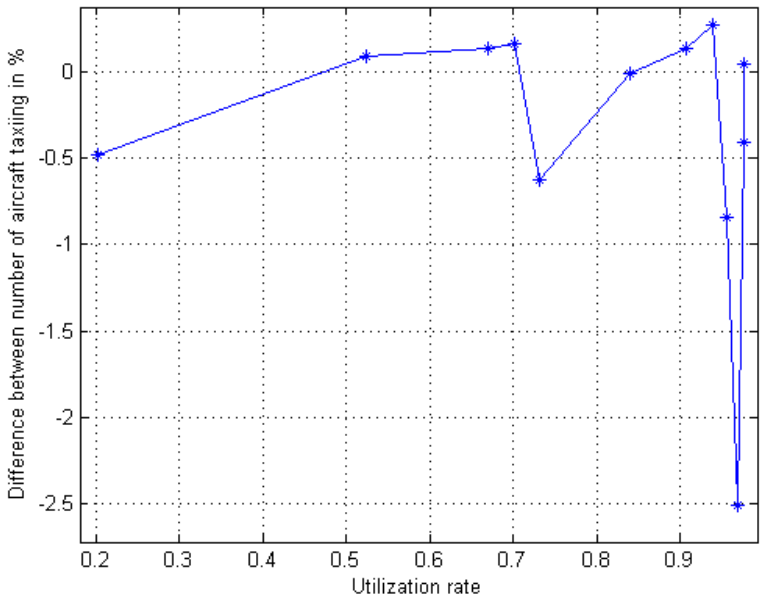

Figure 22: Difference in percent between number of taxiing aircraft yielded by the CPLEX output and number of taxiing aircraft yielded by the simulation, as a function of the utilization rate

aircraft, the previous belief state b, and estimates the most likely set of aircraft positions before making a decision). The curve identified by diamonds represents the benchmark threshold policy.

Fig. 23 and 24 are obtained based on the information displayed in Fig. 21. In particular, Fig. 23 outlines improvements in utilization rate provided by the two levels of information, full and partial. It compares utilization rates yielded by the different scenarios with the utilization rate yielded by the threshold policy. These improvements are then drawn against the corresponding average number of taxiing aircraft . Fig. 24 outlines improvements in traffic load, and therefore reductions of emissions. It compares, for different utilization rates, the average number of taxiing aircraft yielded by the different levels of information with those yielded by the benchmark threshold policy.

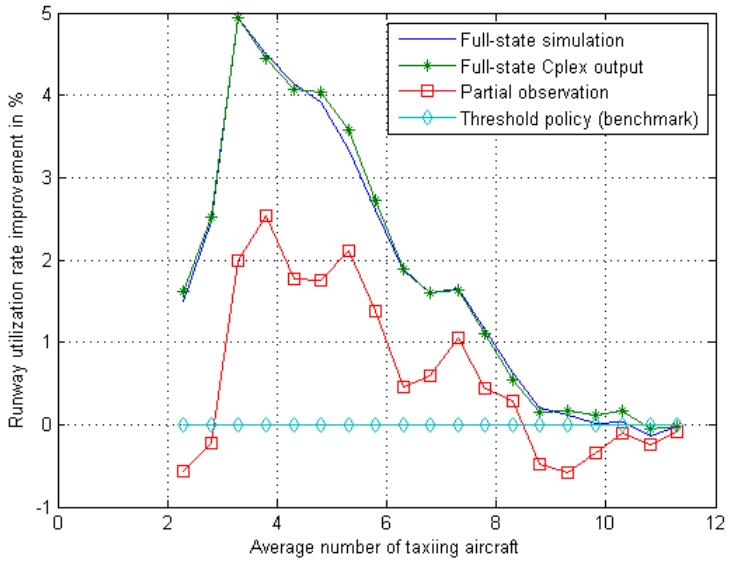

Figure 23: Runway utilization rate improvement as a function of the average number of taxiing aircraft

Runway utilization rate: The availability of surface position information allows operators to control pushback clearances and better utilize runway resources. However, there is no significant improvement when the runway is used above 90%. Compared with the benchmark threshold policy, surface surveillance information helps increase runway utilization by at most 1.5%. That improvement quickly declines to almost zero as the runway utilization rate reaches 95%.

Better results are found for intermediate utilization rates. Typically, these intermediate utilization rates correspond to cases where adverse conditions provide incentives to lower the runway utilization rate. For example, the airport throughput can be limited by downstream restrictions such as take-off queues at first fixes. Bad weather can limit visibility and force controllers to reduce runway utilization for safety reasons. In these cases, where the purpose is not to constantly have an aircraft ready for take off, surface surveillance information yields interesting benefits when used to precisely control pushback clearances on a single taxiway. These improvements result from a better timing of aircraft arrival at the runway threshold, which minimizes the

number of times the runway is idle. Under full state feedback, there is a maximum improvement of 5% in runway utilization, when compared with the threshold policy case, for a policy yielding an average of 3.3 taxiing aircraft on the single taxiway. Under estimated state feedback (partial observation curve in Fig. 24), the maximum increase in runway utilization is 2.5%, when compared with the threshold policy case, for a policy yielding an average of 3.8 taxiing aircraft on the single taxiway.

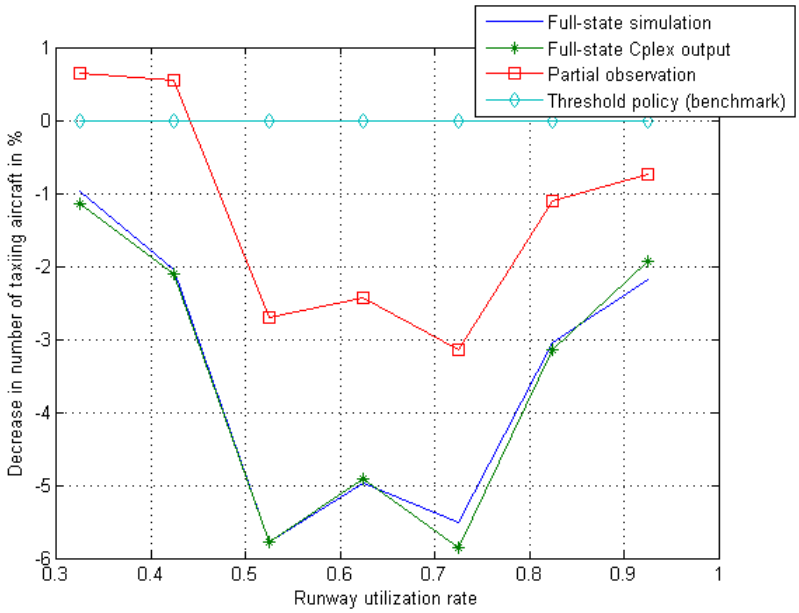

Figure 24: Taxi-load improvement as a function of the runway utilization rate

Taxi-load: Similarly to runway utilization rates, there are few benefits yielded by precisely controlling pushback clearances on a single taxiway using surface surveillance information, when the airport throughput is unconstrained. When the runway utilization rate increases above 90%, the number of taxiing aircraft is decreased by 2% when compared with the threshold policy and by a mere 1% when compared with the estimated state feedback. As the runway utilization increases above 95%, the benefits converge toward zero.

However, there are benefits when the airport operates under adverse conditions,

which limit its throughput and provide incentives to reduce its runway utilization rates. When the runway utilization rate is between 50% and 72%, having access to surface surveillance information helps reduce the average number of aircraft by 5% to 6% when compared with the threshold policy. When only partial information is available and operators try to estimate the position of aircraft on the taxiway, the surface load is decreased by a factor between 2.5% and 3%.

Environmental costs: The present section discusses associated reduction in emissions. It was established in the previous section that there were no significant benefits when the airport works at high levels of runway utilizations, therefore this section focuses on potential benefits at intermediate levels of runway utilization. These levels can be motivated by adverse weather conditions and other stringent downstream flow restrictions.

Table 5 provides engine emissions in grams/minute for aircraft queuing on taxiways. This table was computed using standard thrust setting (percentage of maximum Sea-Level static thrust) for taxi/ground idle (7 percents throttle setting) [70], as well as emission indices as defined by the International Civil Aviation Organization (ICAO) [47]. The last row of this table represents the average emissions per minute per aircraft queuing at LGA airport, and is based on fleet mix operating at this airport (as provided by the ASPM) database). Such table links the previous results on the reduction of the number of taxiing aircraft to potential reductions in emissions.

Table 5: Jet engine aircraft emissions (g/min/aircraft)

Aircraft/Engine	**HC**	**CO**	**NOx**
LJ40 TFE731-2-2B	57.72	168.77	8.12
E145 AE3007A	14.76	102.02	22.52
E135 AE3007A1/3	25.00	137.83	18.27
B712 BR700-715A1-30	2.42	187.43	61.86
B733 CFM56-3-B1	31.19	470.59	53.35
A319-20 CFM56-5-A1	16.98	213.52	48.53
A321 CFM56-5B1	45.07	398.74	64.58
B737 CFM56-7B20	37.20	310.80	51.60
B738 CFM56-7B24	31.39	287.76	57.55
CRJ1 CF34-3A1	23.51	253.56	22.74
CRJ2 CF34-3B	27.52	279.26	21.83
CRJ7 CF34-8C1	0.66	206.34	35.69
E170 CF34-8E5	1.00	139.47	35.40
DC93 V2525-D5	1.61	190.92	72.19
MD82-83 JT8D-209	63.01	220.47	54.73
MD88 JT8D-219	56.13	203.70	58.06
B762 JT9D-7R4D	30.81	217.89	101.06
B763 JT9D-7R4E	29.44	219.32	108.73
B752 RB211-535C	34.56	450.96	82.56
Average for LGA	24.35	194.56	36.79

Fig. 24 shows that a surface surveillance system may improve already optimized taxi operations, and consequently reduces emissions further by at most an additional 3%, without reducing the runway utilization rate. This estimate gives an upper bound for additional savings achievable by providing an agent with surveillance information, the agent being also capable of estimating aircraft positions under partial information. The 3% saving is achieved by reducing the average number of taxiing aircraft while maintaining a runway utilization rate between 50% and 72%.

Fig. 25 more specifically illustrates the actual reduction in NOx emissions yielded by providing surface surveillance information. Compared with a simple threshold policy, emissions can be reduced by up to 11.2 grams per minute. Furthermore, when compared with the case where an operator estimates aircraft positions based on partial information, surface surveillance information can reduce NOx emissions by up to 5.2 grams per minute. This maximum reduction in emissions is achieved for a 72% runway utilization rate. At the same 72% utilization rate, other emissions are also minimized: HC emissions are reduced by 3.4 grams per minute and CO emissions by 27.3 grams per minute.

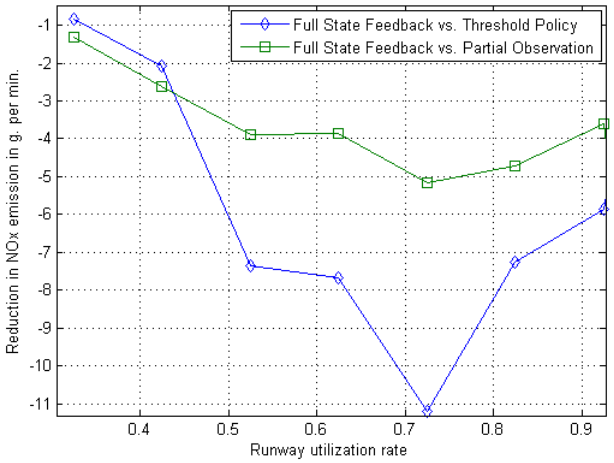

Figure 25: Reduction in NOx emissions (in g/min) as a function of the runway utilization rate

3.1.3.4 Summary

The maximum savings occur for intermediate utilization rates and taxi-loads. As the utilization rate becomes closer to the maximum achievable rate, the optimal policy converges toward simply clearing aircraft for taxi as quickly as possible. Therefore, the gains derived from surface surveillance information decrease as the runway utilization rate increases (Fig. 21). This behavior can be observed in Fig. 20. Using surface surveillance information to precisely control pushback clearances on a single taxiway does not yield any significant benefit when the average number of taxiing aircraft exceeds 8 or the runway utilization rate increases above 90%. Similarly, there is little need for ground surveillance when the level of utilization rate remains below 50% and the average number of taxiing aircraft remains below 3. In both low utilization and high utilization cases, partial input-output information and threshold policies are sufficient to effectively manage surface queues.

It is important to note that this model of departure operations corresponds to a low level of airport modeling complexity, since it only models clearance to taxi on a single taxiway toward a single runway. As the level of complexity of departure operations increases, it is expected that the value of surface surveillance information, in terms of potential emission reduction, will be more significant.

3.1.4 Conclusion

This section presents a stochastic model for airport surface operations, and provides an approach to surface surveillance information valuation. In particular, this research explores the relations between resolution of airport surface surveillance, optimization capabilities, and valuation of surface surveillance systems, in an operational context where these systems are used to precisely control pushback clearances to lower emissions.

The model is developed as a Markov Decision Process and calibrated for La-Guardia Airport operations for the year 2006. It provides observable aircraft position information. Furthermore, it faithfully reproduces the queuing nature of departure operations, and accounts for uncertainties in aircraft trajectories on the taxiway by accounting for their stochastic behavior. The valuation of information is assessed through three distinct scenarios representing two levels of available information and one simple benchmark threshold policy. These scenarios assume that departure operations are optimized within a Collaborative Decision Making framework [22] that enables tactical tuning of push-back or taxi clearances at the entry point of the movement area.

The results have shown that, for a simple taxiway system comprised of a single taxiway leading to one runway, surface surveillance information alone does not significantly improve the performance of optimal clearance control for nominal airport departure operations with runway utilization rates above 90%. Indeed, when compared with the case where an intelligent agent has access to partial information, the exact surface surveillance information yields at most a 1 % decrease in emissions.

This small benefit quickly disappears as the runway utilization rate increases above 95%. However, it is shown that under adverse conditions, when airport throughput is limited by downstream flow restrictions and the runway utilization is lowered to a rate between 50% and 72%, using surface surveillance information to precisely control pushbacks yields a reduction in emissions between 5% and 6%. In this situation, it is estimated that surface surveillance information can improve optimization of departure operations. In particular, it reduces the number of taxiing aircraft by up to 3% when compared with operations where partial information is used to estimate aircraft positions and take an optimal decision.

This section concludes that, for a single taxiway, there is no significant operational

benefits yielded by optimizing pushback clearances using surface surveillance information since a threshold policy will perform practically as well for runway utilization rates above 90%. However surface surveillance systems may bring additional value when used, for example, to precisely control aircraft trajectories on the taxiway, or to optimize more complex surface operations. Additional value is generated from displaying surface surveillance to the controllers who can sort what information is important, and evaluate if the situation requires special attention. It helps ground controllers avoid and manage potential gridlocks, and can increase safety by, for instance, confirming that no aircraft is on the wrong taxiway or runway.

3.2 Two conflicting ramp areas: LaGuardia Airport

The departure operations model, described in section 3.1, which simulates aircraft taxiing from one ramp area to the runway, is used to study the value of surface surveillance for single ramp area airport departure operations. However, the model displays limited simulation capabilities when trying to reproduce all ground departure operations at LaGuardia Airport, as illustrated in Fig. 17. Hence, a two ramp area model is developed. The two ramp area model accurately simulates ground operations at LaGuardia Airport, for runway utilization rates above 30 %. The model assumes traffic is high and there is always an aircraft at both ramp areas, ready to receive a taxi clearance and move toward the runway queue. The model is validated against historical ASPM data.

Additionally, at high utilization rates, for the one ramp area model, the optimal policies rely on long surface queues to maximize the airport throughput. The optimal policies become simpler and similar to a threshold policy, and they perform close to the estimated state feedback policies and threshold policies. For this reason, it is of particular interest to study more complex taxiway systems. The corresponding more

complex departure operations may provide the agent with enough control to both decrease the risk of wasteful queues on the taxiway and at the same time guarantee a high utilization rate. Consequently, the impact of surface surveillance information may increase, especially for high runway utilization rates.

3.2.1 Stochastic modeling of surface departure operations

A model and equations have been developed to optimize departure surface operations at LaGuardia. This model includes a second ramp area connected to the taxiway system and clearance decisions are optimized. The purpose of the second model is to better represent ground operations at LaGuardia and focus on potential interactions between two ramps. These ramp compete for access to the runway, and at the same time cooperate to maintain an appropriate runway utilization rate. One ramp area has a clear topological advantage. More specifically, the second ramp area represents the ramp which is the closest to the runway, as shown in Fig. 26. The topological advantage enables a better control of runway utilization. Two different rules enforcing fairness between ramp areas are studied: a fixed alternating ramp policy and a policy aimed at assuring statistical fairness. Both are described in detail in the following section 3.3.1.1.

3.2.1.1 Decisions

In the first model, the one described in section 3.1, only pushbacks from ramp one were controlled, therefore a simple binary variable was sufficient to represent the taxi clearance decision. However, in this new model, decisions need to be optimized for ramp one and two at the same time. Therefore, the Linear Programm is now optimizing a Markov Decision process based on two decision variables, d_1 and d_2, which are the decisions to clear an aircraft from ramp one and ramp two, respectively. The notations remain the same, i designates the state of the taxiway system and k is the decision in the equations governing the Markov Decision Process. However, to

Figure 26: LaGuardia - two ramp area model

express the pair (d_1, d_2) of decision, k takes values between 0 and 3, such that the binary value of k is a binary pair e.g. $k = (1, 0) = 10_2 = 2 =$ (pushback from ramp 1, no pushback from ramp 2).

3.2.1.2 Calibration

The two-ramp-area model builds upon the model described in section 3.1.1.2. The second ramp area access is modeled based on the topology of the LaGuardia Airport taxiway system. In the previous model, each spatial sample represents 200 meters. It is established in section 3.1.1.4 that traffic coming from ramp one is appropriately modeled using 9 spatial samples, therefore the ramp area modeled corresponds to a taxiway entry point which is located 1800 meters from the runway queue. Ramp one is illustrated in Fig. 26 and corresponds to the US Airways and Delta Airlines terminals. Ramp two is located selecting the ramp area which is the closest to the runway 13. The distance between the second ramp area and the runway is measured directly on the LaGuardia satellite picture, as shown in Fig. 26. The average distance

between the runway queue and the second ramp area is around 600 meters. The ramp connection is best represented by linking the second ramp area to the main taxiway, about 400 meters before the runway queue. Ramp two corresponds to the Central Terminal Building.

In this second model, the taxiway stochastic properties were chosen consistently with the previous calibration of the one ramp area model. More specifically, an aircraft with no obstacle in front of it has a probability m of moving to the next spatial sample, where each spatial sample represents 200 meters of taxiway. Therefore, the entrance of the second ramp area was placed two spatial samples away from the runway queue, and the ramp exit was represented by another spatial sample, totaling three spatial samples between the runway queue and the ramp threshold. Fig. 27 describes the model architecture.

The state vector is represented by a binary vector of dimension twelve. Two bits are used to code the runway queue, which can hold up to three aircraft. Ten bits are used to describe the taxiway system. Among these ten bits, eight bits describe the main taxiway and two bits represent the ramp accesses. Fig. 27 illustrates the architecture of the new model, where each box in the graph may contain at most one aircraft.

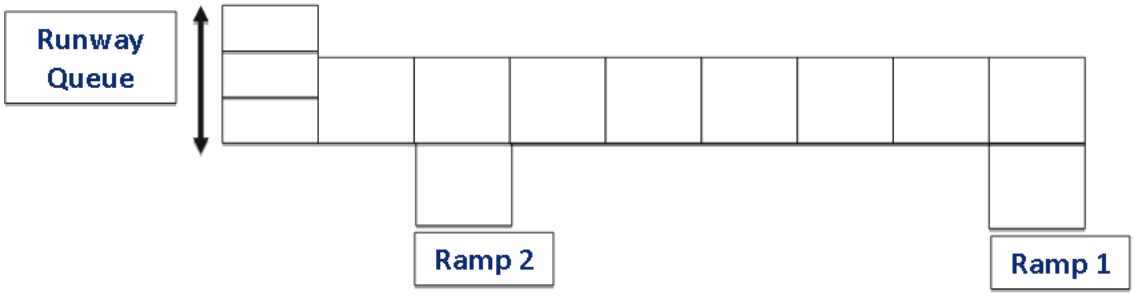

Figure 27: LaGuardia - two ramp area model

The taxi-time from ramp area 2 to the runway queue was estimated using Eq. (7). The model yields a 6.4 unimpeded taxi-out time, which is consistent with the

shortest nominal unimpeded taxi-time at LaGuardia given by the ASPM data , that is, 6.7 minutes.

3.2.1.3 Model Validation

Using ASPM data, LaGuardia airport average throughput rate is expressed as a function of the number of taxiing aircraft. The graph provided in Fig. 28 shows the airport throughput as a function of the number of taxiing aircraft, and yields the average take-off rate. Fig. 28 also shows the throughput as a function of the number of taxiing aircraft for the stochastic model. The model behaves similarly to the airport, and faithfully reproduces the queueing and stochastic nature of departure operations. When the number of taxiing aircraft reaches 11, the model saturates, and yields a maximum take-off rate distribution averaging 0.598 aircraft per minute, with a standard deviation of 0.585 aircraft per minute. These are similar to the average (0.605) and the standard deviation (0.578) of the take-off rate at LaGuardia, when the taxiway is saturated by departing aircraft. The saturation level of the model take-off rate is reached at a lower number of taxiing aircraft than for the ASPM data because the model accounts for operations on the taxiway only from the ramp control points. By contrast, the ASPM data includes all aircraft on the ground starting at pushback. The ASPM data does not provide aircraft position, therefore it is not possible to distinguish aircraft still pushing back at the ramp from aircraft which are at the ramp exit control points. To isolate taxiway operations starting at the control points from the rest of the ramp operations in the ASPM data, the ASPM curve has been shifted to match the saturation level of both curves. For runway utilization rates above 30%, the shift efficiently isolates taxiway operations starting at the control points in the ASPM data, as illustrated in Fig. 29. Note that the two-ramp model performs better than the one-ramp model. The performance curve for the one ramp model (given in Fig 17) was shifted in an attempt to adjust to the

saturation level and match the ASPM curve saturation. However, this attempt failed because the slope of the performance curve of the one-ramp model does not match the slope yielded by the experimental performance curve obtained from the ASPM data.

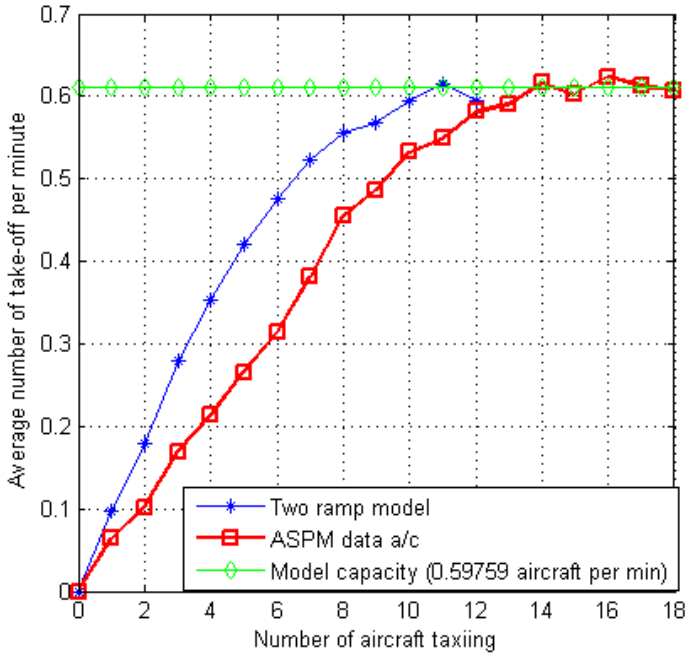

Figure 28: LaGuardia throughput as a function of the number of taxiing aircraft, from the two ramp model and ASPM data. The ASPM data reflects all departure operations on the ground starting at pushback.

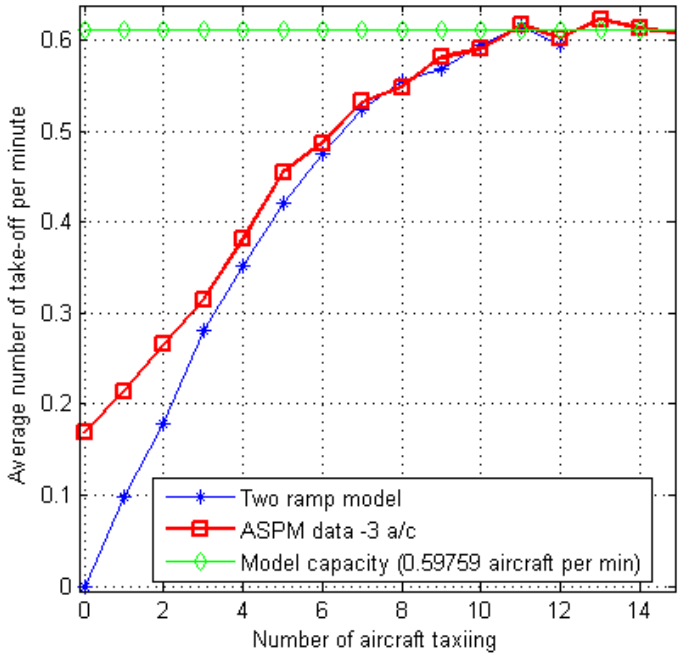

Figure 29: LaGuardia throughput as a function of the number of taxiing aircraft, from the two ramp model and ASPM data. The ASPM curve is shifted by 3 aircraft to isolate taxiway operations starting at ramp exit control points, for utilization rates above 30%.

3.2.1.4 Runway utilization rate and cost function

A constraint is added to set the runway utilization rate to a desired value and the cost function is simplified. On the one hand, adding this constraint shortens the optimization processing time and gives more control over the generation of the optimal policies, on the other hand it allows over-constraining and may result in unfeasible problems. Therefore it is important to find an upper bound for the runway utilization rate feasibility when validating the model, in section 3.2.3.1.

The state-decision transition equations (17) and the stochastic variable boundary equations, equation (15) and Eq. (16), are unchanged. The runway utilization rate r is enforced by adding the additional constraint (24) to the state-decision probabilities. Therefore the runway utilization rate is not a factor used in determining state costs anymore, and the cost function was simplified to reflect only the number of taxiing aircraft, as shown in Eq. (25). However, the objective function to be minimized remains the same as Eq. (14).

For a steady state process with $M + 1$ states and K decisions, the constraint enforcing a runway utilization rate of r is given by

$$\sum_{i|\delta_r(i)=0} \sum_{k=1}^{K} y_{ik} = r, \tag{24}$$

where the variable $\delta_r(i)$ is equal to 1 if there is no aircraft in the runway buffer and to 0 if there is at least 1 aircraft.

The state cost function becomes

$$C_i = N_{ac}(i), \tag{25}$$

where $N_{ac}(i)$ is the number of taxiing aircraft for state i.

3.2.2 Impact of Aircraft Position Information

The fundamental approach to understand and valuate the impact of aircraft position information is the same, as that described in section 3.1.2.1. It is based on the

optimization of Markov Decision Processes (MDP) and Partially Observable Markov Decision Processes (POMDP).

However, the optimization of the two ramp model yields a significantly more complex optimal policies. These policies must solve conflicts between ramps, cooperate to ensure fairness, and anticipate and react to last-minute events. Therefore, to better capture the higher complexity, the methodology presents a few differences when compared with the single ramp area model. First, the notion of fairness between ramp areas is defined and implemented within the control strategies. Second, several levels of partial information are studied to better capture the performance differences for intermediate levels. What follows therefore includes the study of:

- a high level of surface information, named "full state feedback",
- five lower levels of aircraft surface position information, named "estimated state feedback", level one being the lowest information level and level five the highest level, before "full state feedback",
- a basic benchmark policy relying solely on the number of aircraft, named "threshold policy".

3.2.2.1 Fairness rules between ramp areas

The fairness rule ensures pushbacks are fairly split between both ramp areas. The additional ramp area provides a second source of aircraft, which is closer to the runway queue. Therefore it enables last minute tactical opportunities to fix situations when the runway is at risk of being starved and it helps reduce wasteful surface queues. However the runway proximity gives an unfair advantage to ramp area two. Two methods ensuring fairness are studied: a fixed alternating ramp policy and the "statistical fairness" policy.

Fixed alternating ramp policy: This method ensures that the issuance of pushbacks alternates between ramps. Therefore all the pushback decisions are given following the sequence: ramp one, ramp two, ramp one, ramp two, etc ...

First, the state space is extended to include a memory bit mem_i in state i that remembers which ramp has received an extra pushback. This bit is set by the following equation when the succession of states is evaluated.

$$mem_j = \min([\max([mem_i - d_2 + d_1, 0]), 1]), \tag{26}$$

where j is the updated state at $t+1$ after decisions where taken and i is the state at time t. i is the state from which the pair of taxi releases is chosen. $mem_i = 0$ means that the last ramp which received an extra pushback is ramp 1, $mem_i = 1$ means that the last ramp which received an extra pushback is ramp 2.
Second, the transition probabilities are set to the value 0 when only one ramp receives a pushback, i.e. $k = (1, 0) = 2$ or $k = (0, 1) = 1$, and it is not the turn of this ramp to clear an aircraft, as described in Eq. (27).

$$\text{if } (mem_i = 0 \ \& \ k = 1) \text{ or } (mem_i = 1 \ \& \ k = 2) \text{ then } P_{ijk} = 0. \tag{27}$$

Fair benchmark threshold policy: As in the study of the single ramp model, a threshold pushback policy has been used as a benchmark. This fair benchmark threshold policy is alternating between the ramp areas one and two to enforce fairness between the ramp areas. The system of equations (28) below describes how one of the four decision couples k described in section 3.3.1.1 is chosen for a given threshold Th. $N(i)$ designates the number of taxiing aircraft, and mem_i is the memory bit defined in the previous paragraph. If the number of taxiing aircraft is above the threshold Th, the threshold policy will try to send an aircraft, while respecting the fixed ramp alternating policy. First it tests if an aircraft from both ramps can be sent ($k = 3$). If this is not possible, it tests which ramp has been waiting the longest to clear an

aircraft and chooses it ($k = 1$ or $k = 2$). If there is no fair decision available, the policy waits until it can clear an aircraft respecting the alternating rule. For each threshold Th, the decision function K_{Th} is defined for all i in the state space by

$$\begin{cases} \text{if } N(i) > Th, & \begin{cases} \text{if } i[1] = i[2] = 0 \text{ then } k = 3, \\ \text{else if } mem_i = 0 \wedge i[2] = 0 \text{ then } k = 1, \\ \text{else if } mem_i = 1 \wedge i[1] = 0 \text{ then } k = 2, \\ \text{else } k = 0. \end{cases} \\ \text{if } N(i) \leq Th \text{ then } k = 0. \end{cases} \tag{28}$$

The threshold policy alternating between ramp one and ramp two is combined with the state transition probabilities to define a Markov Process, which can be described and solved based on its transition probabilities. The Markov chain probabilities are retrieved from the threshold control control law K_{Th} defined Eq. (28) and the Markov decision process probabilities P_{ijk}. Indeed $P_{i|j}(Th) = P_{i,j,K_{Th}(j)}$. The steady state probabilities of the Markov Process, $\Pi_i(Th)$ defined for all i in the state space, solve Eq. (29) and (30).

$$\Pi_j(Th) - \sum_{i=0}^{M-1} \Pi_i(Th) \cdot p_{j|i} = 0, \text{ for } j = 0..M-1, \tag{29}$$

where M is the total number of states,

$$\sum_{i=0}^{M-1} \Pi_i(Th) = 1. \tag{30}$$

The exact value of the utilization rate u_{Th} for the threshold policy with threshold Th is given by,

$$u_{Th} = \sum_{\forall i \in S | runwayOcc(i)=1} \Pi_i(Th), \tag{31}$$

where $runwayOcc(i) = 1$ when there is at least one aircraft in the runway queue and

0 otherwise. The average number of taxiing aircraft N_{Th} is given by,

$$N_{Th} = \sum_{i=0}^{M-1} N_i \cdot \Pi_i(Th), \tag{32}$$

where N_i is the number of taxiing aircraft of state i.

Statistically fair taxi clearance policy: In this case, the optimal policy does not guarantee that pushback clearances will follow any kind of fixed fair sequence. Instead, it ensures that the average number of pushbacks from each ramp will be the same, on average. The fairness constraint (33) below is added. The constraint ensures that the probability of taking the decision to send only an aircraft from ramp one ($k = 2 = (1, 0)$) is equal to the probability of taking the decision to send only an aircraft from ramp 2 ($k = 1 = (0, 1)$). This constraint is

$$\sum_{i=1}^{M} y_{i1} = \sum_{i=1}^{M} y_{i2}. \tag{33}$$

3.2.2.2 Levels of information

The single ramp area model had only one level of partial information. However, due to its higher complexity, the analysis of the two ramp model benefits from the study of a broader range of results spanning across several levels of information.

This section details the different levels of surface information that were made available to the agent controlling the clearances, by estimating which state has the highest probability of existing, given the surface information. The agent uses the Most Likely State algorithm developed in section 3.1.2.3. Equations (22) and (21) in section 3.1.2.3 explain how different observation vectors may be integrated into the observation probability matrix. Eq. (19) describes how this matrix is used within the heuristic algorithm to update the belief state.

As more information is provided to the agent, the accuracy and efficiency of the

Most Likely State algorithm increases. The progression between the levels of information can be clearly observed below. Their performance converges toward the "full-state feedback" level. These levels are described in this section, along with their respective observation vectors.

Level one, the control points: The first level of information includes the total number of taxiing aircraft. It also indicates if taxi clearances from ramp area one and two are feasible, which is specified by how many aircraft are in each of the spatial samples represented in orange in Fig. 30.

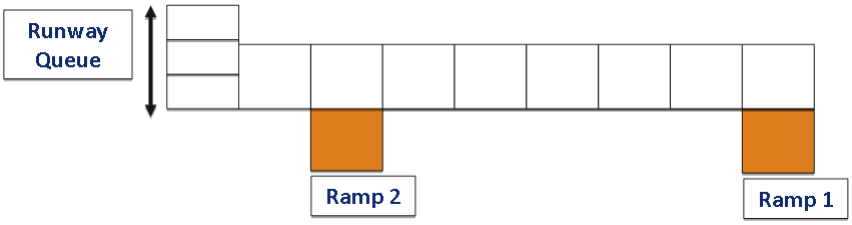

Figure 30: Partial observation level one, observations include the control points and the total number taxiing aircraft.

The observation vector corresponding to the level one of information is the succession of the number of aircraft in the three zones described above, as illustrated in Eq. (34).

$$o = \begin{bmatrix} N_{white} & N_{ramp_1} & N_{ramp_2} \end{bmatrix} \tag{34}$$

Level two, surface surveillance covers 200 meters ahead of ramp one control point: The second level of information is illustrated in Fig. 31. The agent can now observe 200 meters in front of the ramp one control point. The partial surface information provided to the agent is the following:

- the number of aircraft in the white zone,
- the availability of ramp one and two,

- the first zone after ramp 1, in red in Fig. 31.

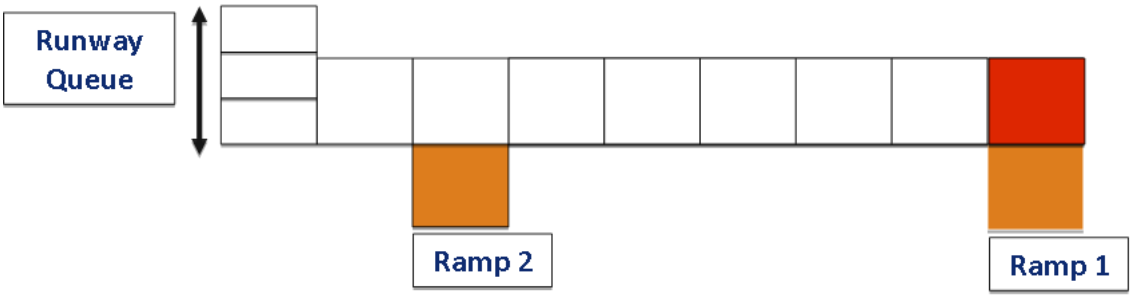

Figure 31: Partial observation level two, watching over 200 meters ahead of ramp one control point.

The observation vector corresponding to the second level of information is the succession of the number of aircraft in the four zones described above in Fig. 31 and illustrated in the following equation,

$$o = \begin{bmatrix} N_{white} & N_{red_1} & N_{ramp_1} & N_{ramp_2} \end{bmatrix}. \tag{35}$$

Level three, surface surveillance covers 400 meters ahead of ramp one control point: The third level of information is illustrated in Fig. 32. The agent can observe now 400 meters in front of the ramp one control point.The partial surface information provided to the agent is the following,

- The number of aircraft in the white zone,
- the availability of ramp one and two,
- the aircraft occupation of each of the two red zones in Fig. 32.

The observation vector corresponding to the third level of information is the succession of the number of aircraft in the five zones described above in Fig. 32 and illustrated in the following equation,

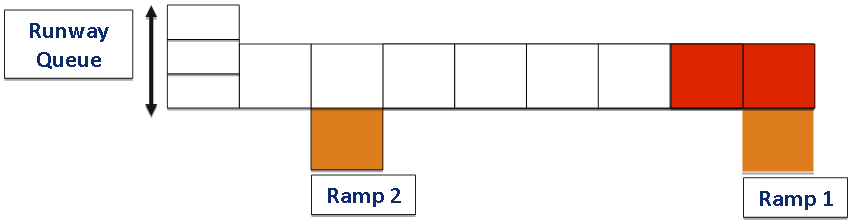

Figure 32: Partial observation level three, watching over 400 meters ahead of ramp one control point.

$$o = \begin{bmatrix} N_{white} & N_{red_1} & N_{red_2} & N_{ramp_1} & N_{ramp_2} \end{bmatrix}. \tag{36}$$

Level four, surface surveillance covers 800 meters ahead of ramp one control point: The fourth to eighth level of information are illustrated in Fig. 33. In level four, the agent can observe up to 800 meters downstream of the ramp one control point.

The partial surface information provided to the agent is the following,

- The number of aircraft in the white zone,
- the availability of ramp one and two,
- the aircraft occupation of each of the four red zones in Fig. 33.

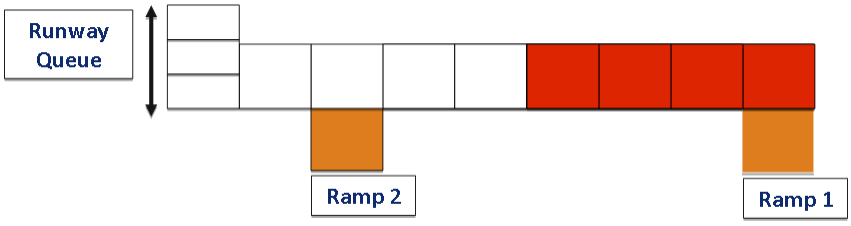

Figure 33: Partial observation level four, watching over 800 meters ahead of ramp one control point.

The observation vector corresponding to the fourth level of information is the succession of the number of aircraft in the four zones described above in Fig. 33 and illustrated in Eq. (37).

$$o = \begin{bmatrix} N_{white} & N_{ramp_1} & N_{ramp_2} & N_{red_1} & N_{red_2} & N_{red_3} & N_{red_4} \end{bmatrix} \tag{37}$$

Level five, surface surveillance covers 1400 meters ahead of ramp one control point: The fifth level of information is illustrated in Fig. 34. In level four, the agent can observe up to 1400 meters downstream of the ramp one control point.

The partial surface information provided to the agent is the following,

- The number of aircraft in the white zone,
- the availability of ramp one and two,
- the aircraft occupation of each of the seven red zones in Fig. 34.

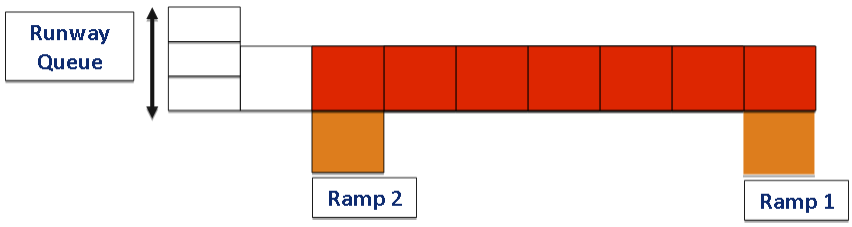

Figure 34: Partial observation level five, watching over 1400 meters ahead of ramp one control point.

The observation vector corresponding to the fifth level of information is the succession of the number of aircraft in the four zones described above in Fig. 34 and illustrated in Eq. (38).

$$o = \begin{bmatrix} N_{white} & N_{ramp_1} & N_{ramp_2} & N_{red_1} & N_{red_2} & N_{red_3} & N_{red_4} & N_{red_5} & N_{red_6} & N_{red_7} \end{bmatrix} \tag{38}$$

3.2.3 Results and Discussion

The optimization results are validated and the results are discussed. The impact of surface surveillance information on departure operations is evaluated.

3.2.3.1 Validation

Numeric approximations: The number of transitions is significantly increased in the two ramp model, and the number of decisions to chose from is multiplied by two. The fixed alternating ramp policy yields 562,956 non zero transitions and the statistically fair ramp policy yields 367,881. Therefore the computation requirements in terms of memory, time, and precision are higher than for the one ramp model. Indeed, the one ramp model yielded policies which, when simulated, generated results similar to what the optimization software predicted, thus validating the reliability of the solution. However for the two ramp model, the solution state-action probabilities y_{ik} yielded by CPLEX tended to diverge significantly from the probabilities derived from the simulation of the optimal policy when the utilization rate is approaching the maximum feasible rate. Therefore, additional attention is paid to the computation of transition probabilities and numerical approximations are made to improve the accuracy of the solution.

It was found that significant computational errors occurred in Matlab when the transition probabilities were evaluated. Since a transition from one state to another arises from the combination of up to 13 sub-transitions, as described previously, the number of significant digits required to express the transition probabilities is much larger than the 15 digits allowed by the 53 bit significand of the double precision arithmetic.

The sub-transition probabilities m, c_1, and c_2 had their number of significant digits lowered as illustrated below,

$$c_1 = 0.514 \approx 0.5,$$

$c_2 = 0.0929 \approx 0.1,$

$m = 0.9084 \approx 0.9.$

The transition probability with the largest number of significant digits is now 12 digit long, $m^{10} \cdot ((1 - c(1)) \cdot (1 - c(2)))$. Indeed, it has the same number of digits than $9^{10} \cdot ((10 - 5) \cdot (10 - 1)) = 156905298045$. The number with the most significant digits can be represented exactly using double precision floating point arithmetic, i.e. using a 53 bit significand.

Upper bound for the utilization rate: Lowering the number of significant digits of the sub-transition probabilities has allowed us to express the transition probabilities exactly. This has removed most computation errors, and improved the reliability of the optimal solutions. However, as utilization rates approach the maximum feasible rate, computation errors and approximations done by the software CPLEX still tend to degrade the solution quality. For this reason, finding a theoretical upper bound for the maximum feasible utilization rate is of particular interest. In addition, as explained previously in section 3.2.1.4, the second model fixes a runway utilization and minimizes the number of taxiing aircraft, therefore it is important to have a good idea about the theoretical limit of the runway utilization rate to validate the results.

An upper bound for the maximum utilization feasible rate can be derived by solving the equations representing the queuing model made of the spatial samples leading to the runway, and the runway queue as illustrated in Fig. 35. Indeed, it is possible to evaluate the theoretical utilization rate achieved when an aircraft is always waiting to move forward at the threshold of the second ramp area. This extreme case is reachable only if the fairness constraints are relaxed. Consequently, it provides a upper bound for the maximum feasible utilization rate when fairness is enforced.

A large majority of the queueing theory equations used in practice are those derived under the assumption of statistical equilibrium, starting with Erlang's first

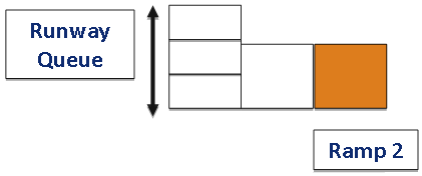

Figure 35: Reduced taxiway system used to estimate the maximum feasible utilization rate

results in 1909 on "The Theory of Probabilities and Telephone Conversations" [33]. Among these results, the birth-death process has been particularly useful to model steady-states probabilities [21]. The birth-death process is a special case of continuous-time Markov process where the states represent the current size of a population and where the transitions are limited to births and deaths. Modeling queuing systems using state equations and birth-death processes leads us to well known closed-form results to estimate the probability of each queue length. Birth-death queuing processes have been studied in the discrete case as well, using discrete Markov Processes [32], [13]. These results are of special interest to our problem since they include the probability of having an empty queue, and they help us determine the utilization rate. In particular, the model developed in this thesis is comprised of a runway queue which may, in rare instances, send two aircraft in one time-step. This implies the queue length may transition up or down by more than just one aircraft. Therefore the runway queue developed in this thesis is not exactly a birth-death process but is close to a discrete quasi-birth-death process [20]. However, there are still a few more differences between the models in this thesis and a discrete quasi birth-death process: in our case the runway queue and the intermediate taxiway spatial samples, do not have an infinite capacity. Therefore specific formulas must be derived for this model. A generic method applied to solve Discrete Markov Processes and demonstrated in the case of discrete birth-death processes in [3], was directly applied to solve this particular queuing system.

First, the runway queue alone is considered to detail the approach for a simple

case, based on a limited number of states, and to evaluate the impact of the runway queue size on the utilization rate. It is first assumed that an aircraft will enters the runway queue, if the queue is not full, with a probability of arrival α. Second, the system illustrated in Fig. 35 is considered.

The variables used in the equations below are defined as follow.

- Let t_0 be the probability that no take-off clearance is issued.
- Let t_1 be the probability that one take-off clearance is issued.
- Let t_2 be the probability that two take-off clearances are issued.
- Let d_0 be the probability of having a state transition from a runway queue with 1 aircraft to a runway queue with 0 aircraft.
- Let d_1 be the probability of having a state transition from a runway queue with 2 or 3 aircraft to a runway queue with 1 or 2 aircraft, respectively.
- Let d_2 be the probability of having a state transition from a runway queue with 3 aircraft to a runway queue 1 aircraft.
- Let u be the probability of having a state transition from a runway queue with 1 or 2 aircraft to a runway queue with 2 or 3 aircraft, respectively.

d_0, d_1, d_2 and u are the transition probabilities of the quasi death-birth process [20] that is the runway queue. The system is illustrated in Fig. 36.

The following equations express the values of the transition probabilities of the quasi death-birth as functions of α and the base probabilities which define the Markov

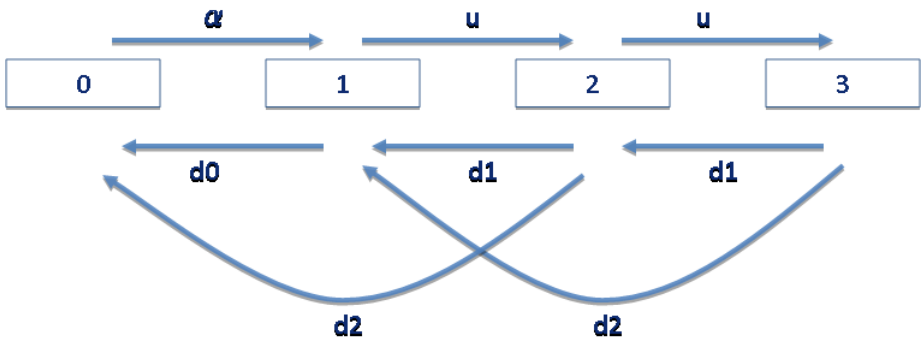

Figure 36: Runway Queue States - A Discrete Quasi-Death-Birth Process

Process (section 3.1.1.2). We have

$$t_0 = 1-(1-c_1)\cdot(1-c_2) = c_1+c_2-c_1\cdot c_2, \tag{39}$$

$$t_1 = (1-c_1)\cdot c_2+(1-c_2)\cdot c_1, \tag{40}$$

$$t_2 = c_1\cdot c_2, \tag{41}$$

$$d_0 = (1-\alpha)\cdot t_0, \tag{42}$$

$$d_1 = (1-\alpha)\cdot t_1+\alpha\cdot t_2, \tag{43}$$

$$d_2 = (1-\alpha)\cdot t_2, \tag{44}$$

$$u = \alpha\cdot(1-t_0). \tag{45}$$

The state transition flow equations illustrated in Fig. 36 are expressed in the following equations. They define the dynamic of the runway queue system. Let Π_n be the steady state probability that the runway queue contains n aircraft,

$$\Pi_0\cdot\alpha = \Pi_1\cdot d_0+\Pi_2\cdot d_2, \tag{46}$$

$$\Pi_1\cdot(u+d_0) = \Pi_0\cdot\alpha+\Pi_2\cdot d_1+\Pi_3\cdot d_2, \tag{47}$$

$$\Pi_2\cdot(u+d_1+d_2) = \Pi_1\cdot u+\Pi_3\cdot d_1, \tag{48}$$

$$\Pi_0+\Pi_1+\Pi_2+\Pi_3 = 1. \tag{49}$$

The solution describes the runway queue behavior when an aircraft has a constant

probability α of entering the queue,

$$\begin{aligned}
\Pi_0 &= \frac{(d_0+d_1+d_2)\cdot d_2\cdot u+d_0\cdot(d_1^2+2\cdot d_1\cdot d_2+d_2^2)}{\alpha\cdot u^2+(\alpha\cdot(d_1+2\cdot d_2)+(d_0+d_1+d_2)\cdot d_2)\cdot u+(\alpha+d_0)\cdot(d_1^2+2\cdot d_1\cdot d_2+d_2^2)},\\
\Pi_1 &= \frac{\alpha\cdot(d_2\cdot u+d_1^2+2\cdot d_1\cdot d_2+d_2^2)}{\alpha\cdot u^2+(\alpha\cdot(d_1+2\cdot d_2)+(d_0+d_1+d_2)\cdot d_2)\cdot u+(\alpha+d_0)\cdot(d_1^2+2\cdot d_1\cdot d_2+d_2^2)},\\
\Pi_2 &= \frac{\alpha\cdot(d_1+d_2)\cdot u}{\alpha\cdot u^2+(\alpha\cdot(d_1+2\cdot d_2)+(d_0+d_1+d_2)\cdot d_2)\cdot u+(\alpha+d_0)\cdot(d_1^2+2\cdot d_1\cdot d_2+d_2^2)},\\
\Pi_3 &= \frac{\alpha\cdot u^2}{\alpha\cdot u^2+(\alpha\cdot(d_1+2\cdot d_2)+(d_0+d_1+d_2)\cdot d_2)\cdot u+(\alpha+d_0)\cdot(d_1^2+2\cdot d_1\cdot d_2+d_2^2)}.
\end{aligned} \tag{50}$$

Assuming it is possible to always have an aircraft at the runway queue threshold, the arrival rate α would be the probability that this aircraft moves i.e. $\alpha = m$. The solution to these equations yields a 0.996 utilization rate, for $\alpha = m$. This result shows that the runway queue size does not significantly limit by itself the runway utilization rate by itself. This rate of utilization is above the upper bound for the utilization rate of the system illustrated in Fig. 35, because the probability of having an aircraft right in front of the runway queue and ready to enter is not 1, therefore $\alpha \neq m$. In addition, the system of equations (46 to 49) is not valid for the whole system because the state of the runway queue impacts the rest of the taxiway system and vice versa.

Therefore, states need to refer not only to the number of aircraft in the runway queue but also to the positions of aircraft on the taxiway portion between ramp two and the runway queue, as illustrated in Fig. 35, in order to find better upper bound on runway utilization in the case no fairness rule is enforced. This brings the total number of relevant states to 16. Similarly to the above simpler quasi birth-death process, the system behavior is determined by solving the equations of a Markov Process. These latter equations are similar to the Eq. (46 to 49) in the case of the simple runway queue studied earlier. However, the number of different transitions, and corresponding transition probabilities, is now larger than that of the quasi death-birth process describing only the runway queue. The equations describing the steady-state probabilities are as follow,

$$\Pi_j - \sum_{i=0}^{15} \Pi_i \cdot p_{j|i} = 0, \text{ for } j = 0..15, \tag{51}$$

$$\sum_{i=0}^{15} \Pi_i = 1. \tag{52}$$

To evaluate each transition probability $p_{j|i}$, it is assumed that the decision to send an aircraft on ramp two is always taken every time it is feasible. Based on this assumption, the sub-transition functions described in section 3.1.1.3 are slightly modified and applied to the reduced taxiway system illustrated in Fig. 35, forcing a clearance decision whenever feasible. Once all the transition probabilities are evaluated using the basic probabilities c_1, c_2, and m, the linear system of 16 equations (51 and 52) is solved to find the steady state probability Π_i for each one of the 16 states.

Finally, the steady probabilities Π_i of the states, for states with at least one aircraft in the runway queue, are added. This yields an upper bound for the runway utilization rate of 0.989 for the two ramp model.

Solution reliability: The optimal policies are simulated using the model developed in section 3.2. For each policy, the average number of taxiing aircraft is compared with the corresponding CPLEX output, to validate the feasibility of the optimal policy. Fig. 37 shows the difference between the average number of taxiing aircraft yielded by the CPLEX output and the average number of taxiing aircraft yielded by the simulation, as a function of the utilization rate. The differences remaining between the CPLEX output and the simulation results, is generated by CPLEX intermediate computation errors. This difference is not significant for utilization rates under 0.98. However there is a difference in performance for rates just above 0.98.

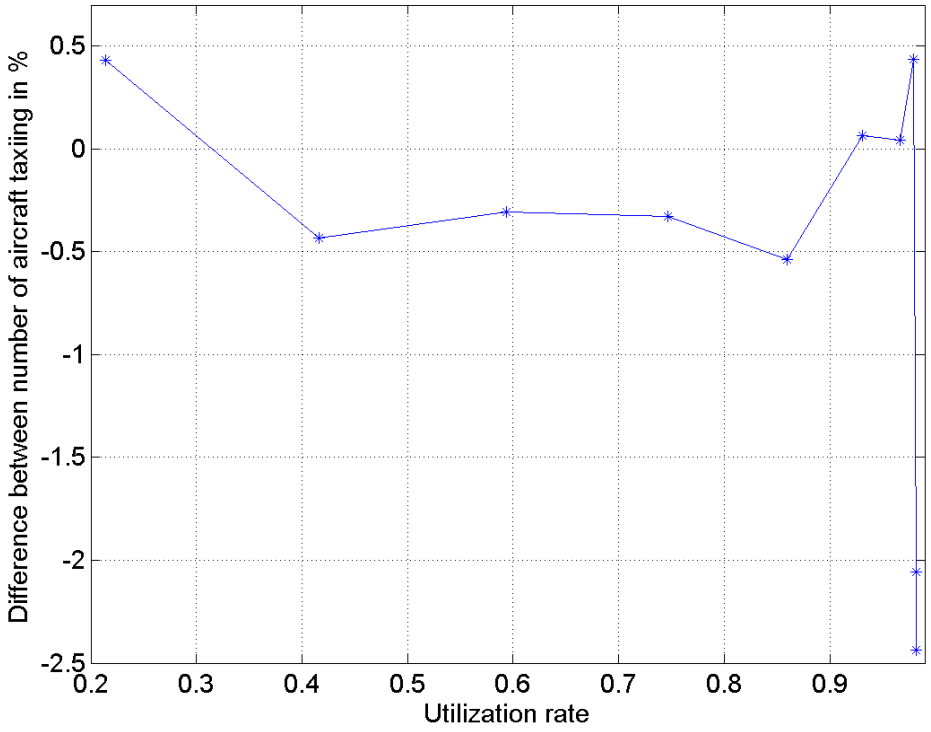

Figure 37: Difference between the average number of taxiing aircraft yielded by the CPLEX out-put and the average number of taxiing aircraft yielded by the simulation, as a function of the utilization rate

3.2.3.2 Optimal policies against benchmark policy

Fig. 38 illustrates the utilization rate of the LaGuardia Airport two ramp model as a function of the average number of taxiing aircraft. Fig. 39 shows the reduction in percent of the average number of taxiing aircraft for optimal policies, as a function of the utilization rate, when compared with a threshold policy which alternates between ramp one and ramp two.

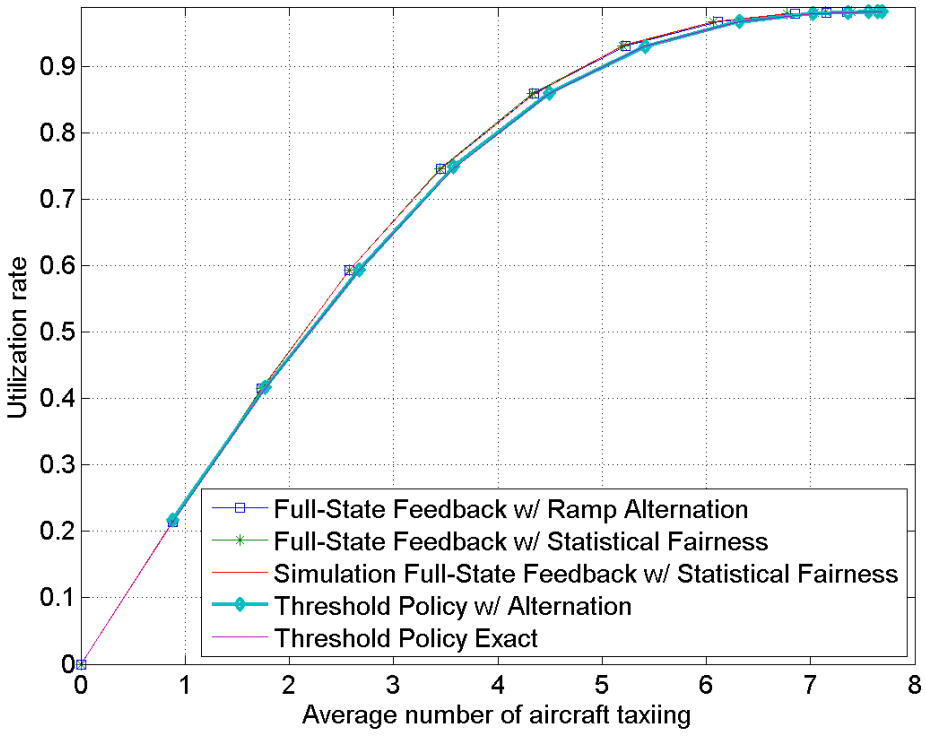

Figure 38: Runway utilization rate as a function of the average number of taxiing aircraft at LaGuardia Airport

When the number of taxiing aircraft is limited to one aircraft by the threshold policy, the difference of performance between the full-state feedback policy and the threshold policy is inexistent, as illustrated by Fig. 39. This confirms the intuition that there is no benefit in knowing the exact position of aircraft when there can be no conflict between aircraft on the taxiway.

When the threshold for the number of taxiing aircraft is increased to two and and

then three, the threshold policy starts yielding a lower utilization rate for the same number of taxiing aircraft than the full-state feedback policy, as shown in Fig. 38 and 39. Indeed, the threshold policy releases aircraft blindly, based on the number of taxiing aircraft. Consequently aircraft have a higher probability of conflicting with each other on the taxiway. The optimal full-state feedback policy performs better because it manages the release of aircraft using the exact position of the other aircraft already taxiing.

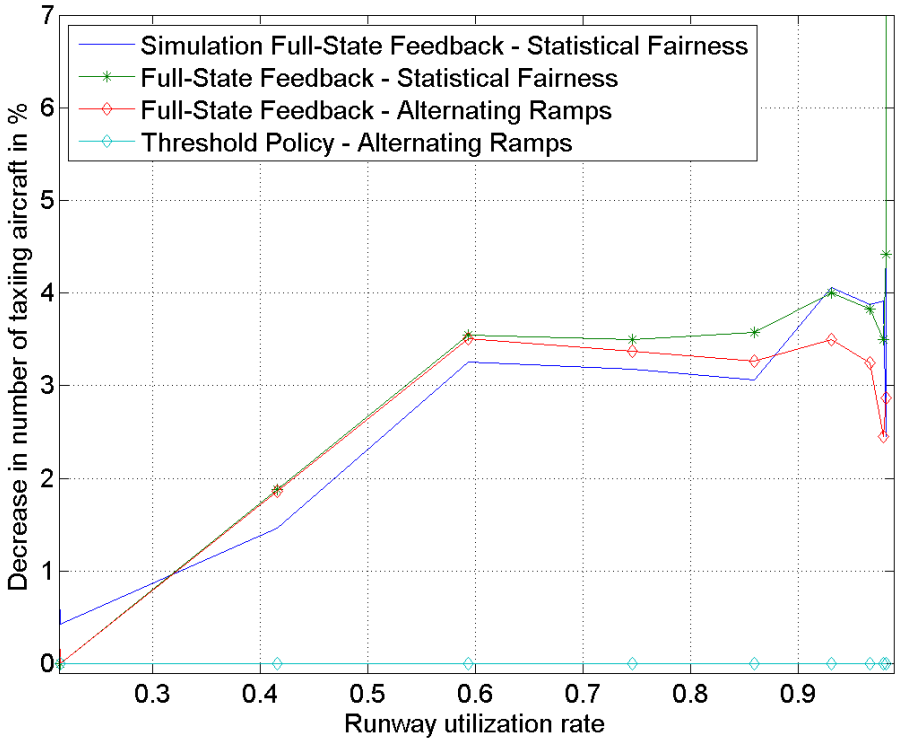

Figure 39: Reduction in percent of the average number of taxiing aircraft as a function of the utilization rate, when compared with a threshold policy which alternates between ramp one and ramp two.

Among the two full-state feedback policies studied in section 3.2.2.1, the one based on statistical fairness yields the best results, as shown in Fig. 39. However, it performs close to the policy that enforces a strict alternating policy. It is noticeable that the *simulation* of the statistical fairness optimal policy, produces performances that are

slightly worse than those directly indicated by the optimization software output. Consistent with the reliability analysis, there is a sharp divergence of reliability when the runway utilization rate exceeds 0.98.

The full state feedback policies perform consistently better, generating a smaller average number of taxiing aircraft, when compared with the threshold benchmark policy. This performance is consistently better over a wide array of runway utilization rates, which correspond not only to intermediate runway capacities, but also to situations where the runway is used at maximum capacity. For rates between 0.6 and 1, the reduction of the number of taxiing aircraft is consistently above 3.5 percent. Most interestingly, as the runway utilization rate increases from 0.92 to 0.96, the savings reach 4 percent.

3.2.3.3 Influence of different levels of observation

To better understand the influence of information on the operational efficiency of departure operations for the two ramp area model, several levels of information are studied using the Most Likely State algorithm described in section 3.1.2.3. The levels of information are described in more detail in section 3.2.2.2.

Level one, the control points: The first level of surface surveillance provides the ground controller with only the total number of aircraft and informs her/him of the possible presence of an aircraft blocking access from ramp one or two, as illustrated in Fig. 30. This information is necessary for the agent to make a feasible decision. The orange zones correspond to the areas about which this information is available. The first level of information significantly underperforms compared with the threshold policy, as shown in Fig. 40.

Investigating the behavior of the first level of information, it was observed that it containes so little information that the agent in charge of taxi-clearances using a Most Likely State control strategy generates estimates significantly far from reality

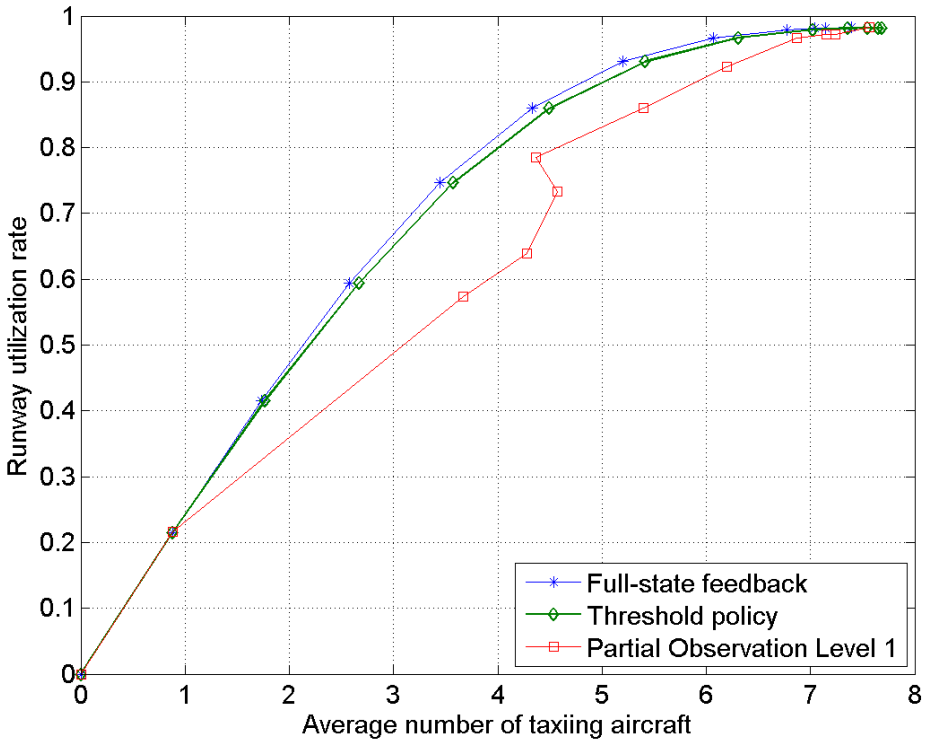

Figure 40: Utilization as a function of the average number of taxiing aircraft. Surface surveillance provided to the Most Likely State algorithm covers the control points.

when trying to guess the current state. For instance, the Most Likely State algorithm could often not determine for sure which ramp area had sent an aircraft. Fig. 41 illustrates this issue.

These poor results yield a steep decline in performance for partial observation when compared with the previous simpler model with just one ramp area. Indeed, the previous section had concluded that, compared with a threshold policy, there were some benefits to estimating the surface state using only the number of taxiing aircraft and whether or a not a taxi clearance is feasible. This difference suggests that because of the higher complexity, the agent needs a higher level of information to be able to perform at the same level as a simple alternating threshold policy.

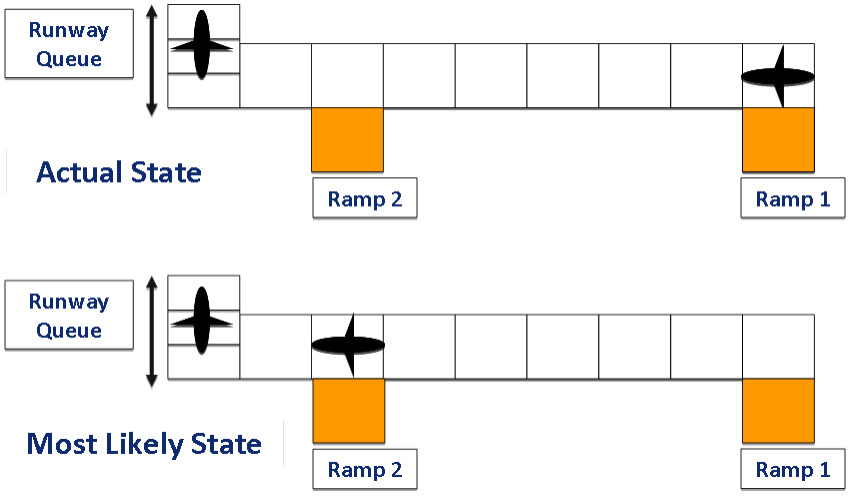

Figure 41: Most Likely State at the level one of information: example of inaccurate estimation.

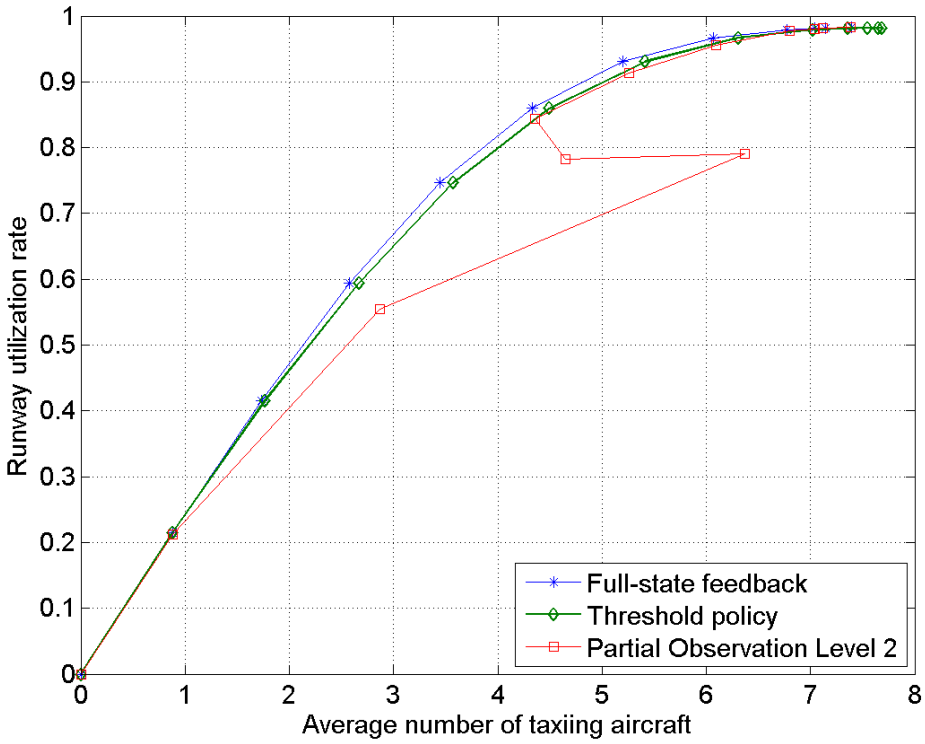

Figure 42: Utilization as a function of the average number of taxiing aircraft. Surface surveillance covers 200 meters ahead of ramp one control point.

Level two, surface surveillance covers 200 meters ahead of ramp one control point: The additional piece of surface information, shown in red in Fig. 31, allows the agent to have a better idea of which part of the taxiway system is occupied by an aircraft just after a clearance. However, aircraft still have significant room to move unpredictably and undetected. Large mistakes on the estimation of the airport surface, similar to the one in Fig. 41, still happen for intermediate runway utilization rates once aircraft drift into the blind zone (shown in white). The level two of observation performs similarly to the benchmark threshold policy for high utilization rate, as illustrated in Fig. 43. The accuracy of estimations is still too poor to generate benefits compared with the threshold policy.

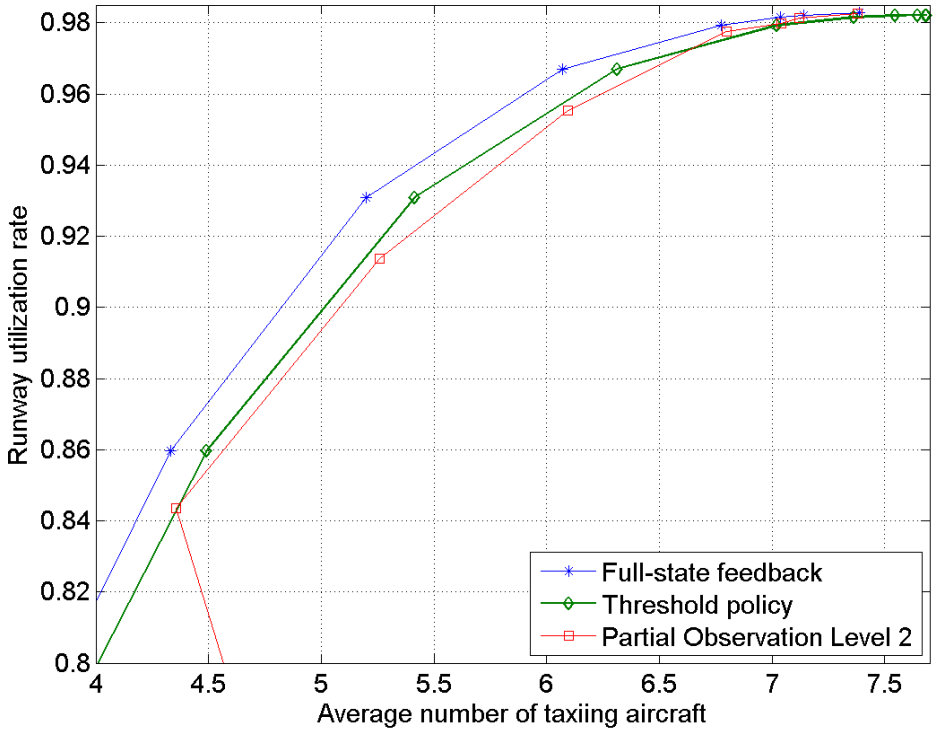

Figure 43: Utilization as a function of the average number of taxiing aircraft, for utilization rates above 85%. Surface surveillance covers 200 meters ahead of ramp one control point.

Level three, surface surveillance covers 400 meters ahead of ramp one control point: The level three of information provides the heuristic algorithm with information on aircraft positions over the 400 meters in front of the ramp one control point, as shown in red in Fig. 32. Fig. 44 and Fig. 45 display the trade-off between utilization rates and number of taxiing aircraft for level three of partial information, the benchmark threshold policy, and the optimal full-state feedback policy. Having access to surface surveillance covering 400 meters helps the heuristic control policy to perform more consistently than with fewer information sources, as shown in Fig. 45. For utilization rates above 60%, it performs approximately at the same level as the benchmark policy, as illustrated in Fig. 44. The 400 meters of surface surveillance are sufficient to avoid significant state estimation mistakes for intermediate runway

utilization rates.

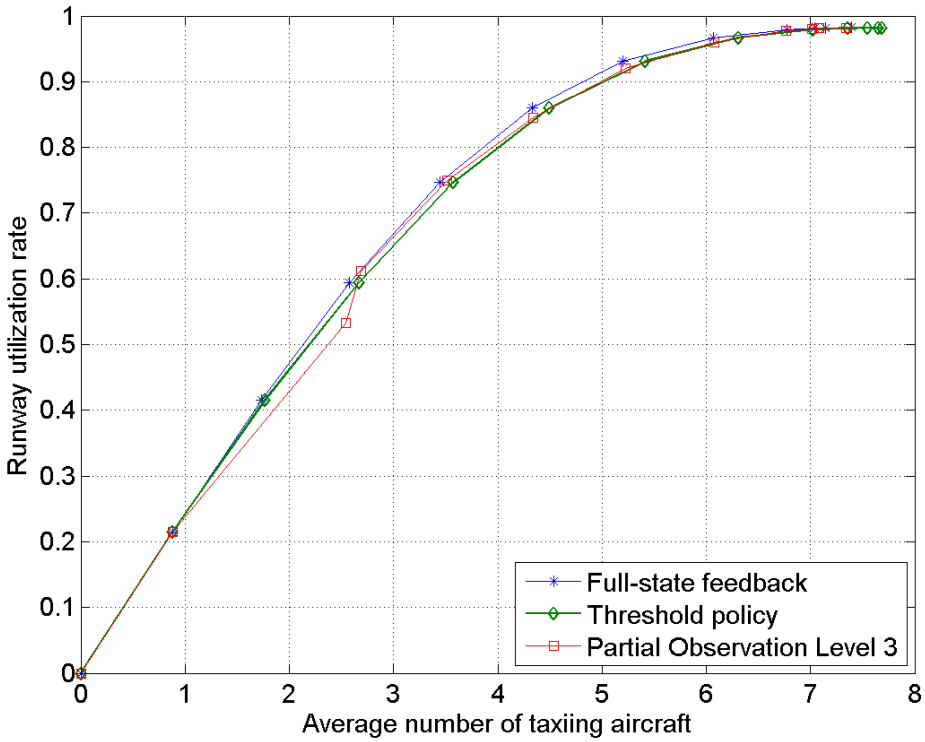

Figure 44: Utilization as a function of the average number of taxiing aircraft. Surface surveillance covers 400 meters ahead of ramp one control point.

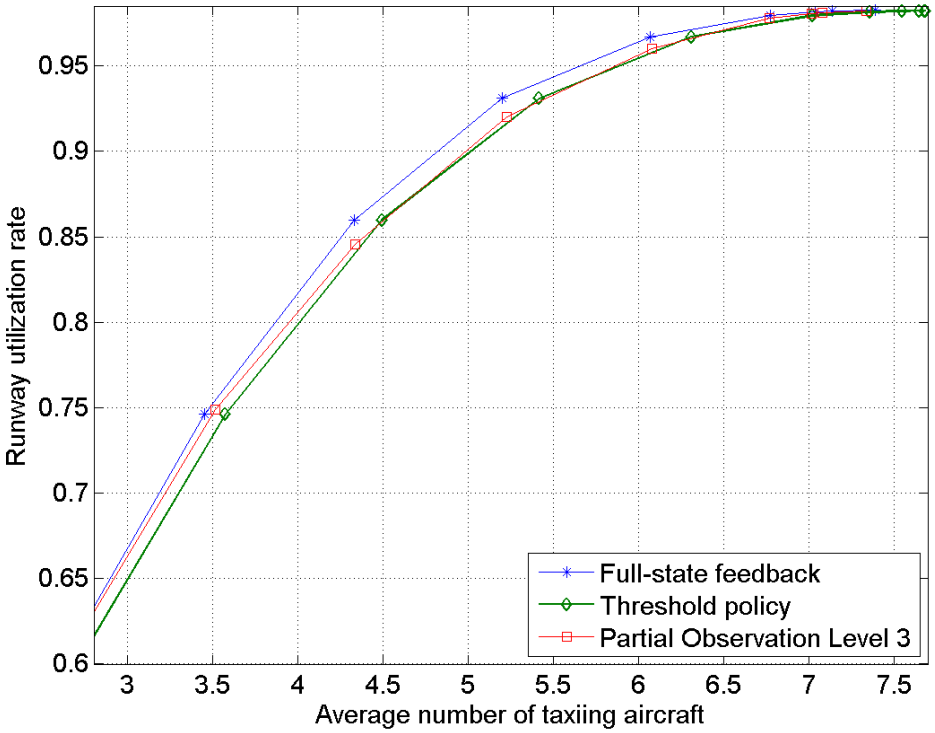

Figure 45: Utilization as a function of the average number of taxiing aircraft, for utilization rates above 60%. Surface surveillance covers 400 meters ahead of ramp one control point.

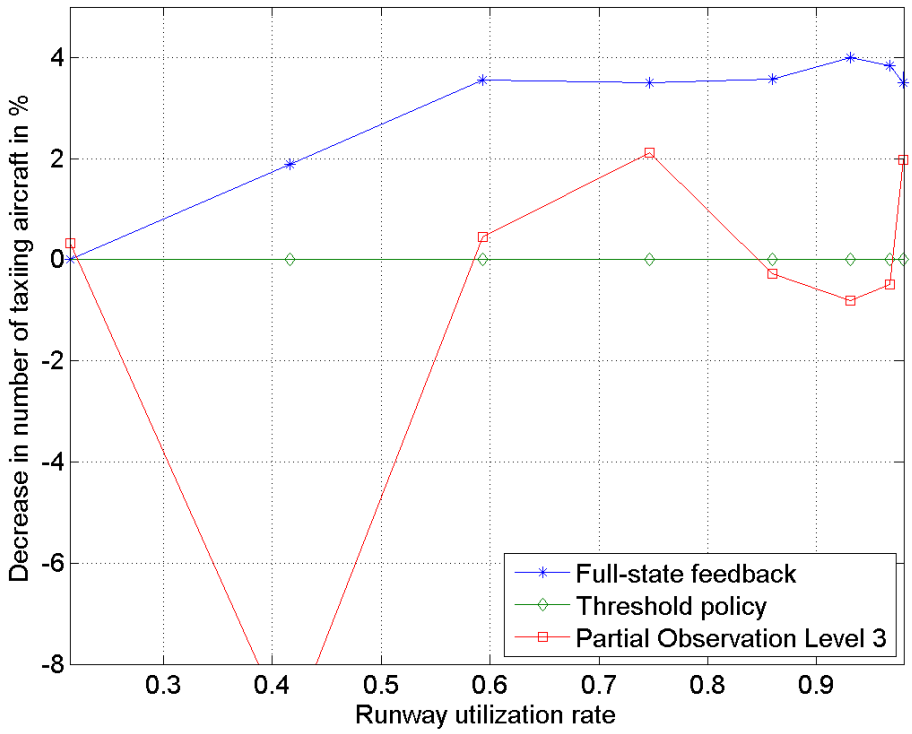

Figure 46: Reduction in percent of the number of taxiing aircraft as a function of the utilization rate, when compared with a threshold policy which respects ramp alternation. Surface surveillance covers 400 meters ahead of the control point of ramp one.

Level four, surface surveillance covers 800 meters ahead of ramp one control point: The level four of information provides the heuristic algorithm with information on aircraft positions over the 800 meters in front of the ramp one control point, as shown in red in Fig. 33. At this level of surface information, the Most Likely State algorithm starts performing similarly to the optimal full-state feedback policy for utilization rates above 60 percent, as illustrated in Fig. 47 and Fig. 48. Fig. 49 shows the difference between the tradeoff curves for given utilization rates and outlines the performance of the level four of partial observation and of the full-state feedback in comparison with the baseline threshold policy.

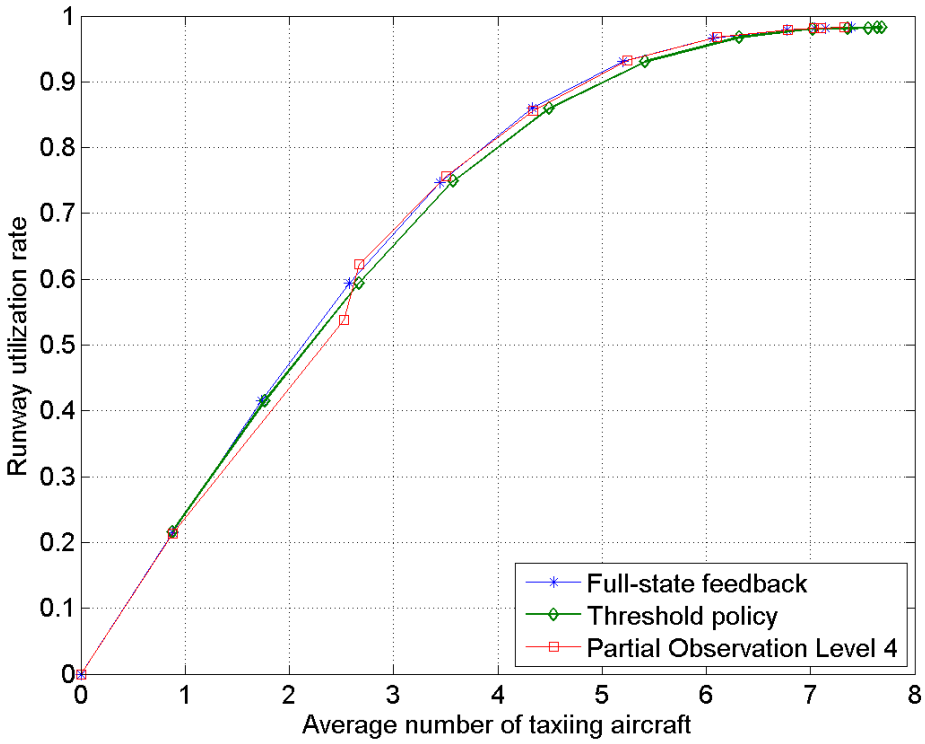

Figure 47: Utilization as a function of the average number of taxiing aircraft . Surface surveillance covers 800 meters ahead of ramp one control point.

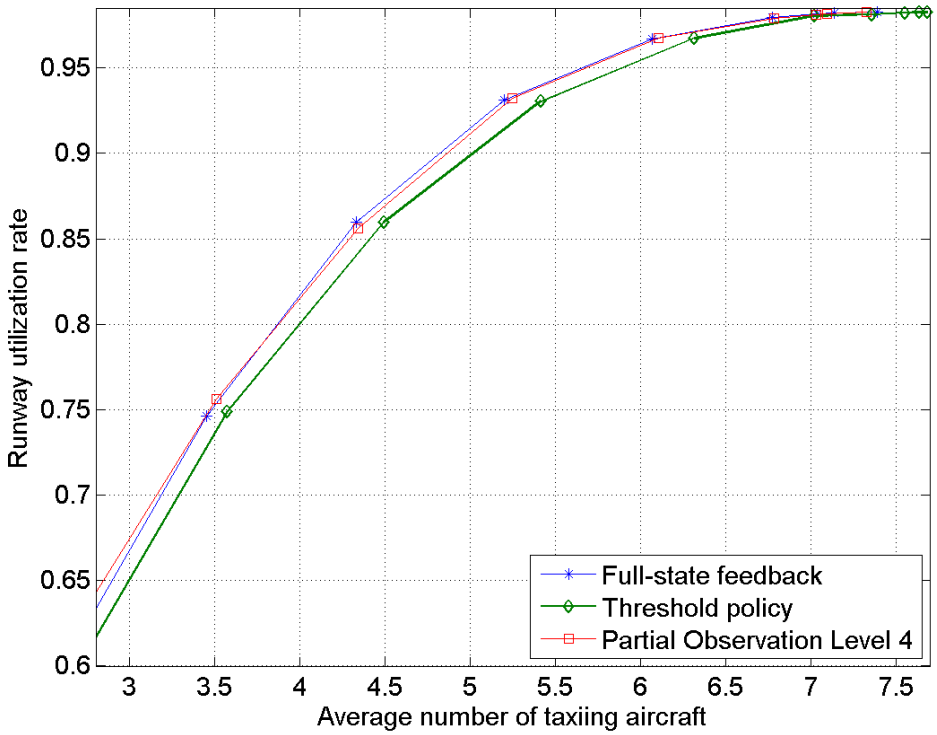

Figure 48: Utilization as a function of the average number of taxiing aircraft, for utilization rates above 60% . Surface surveillance covers 800 meters ahead of ramp one control point.

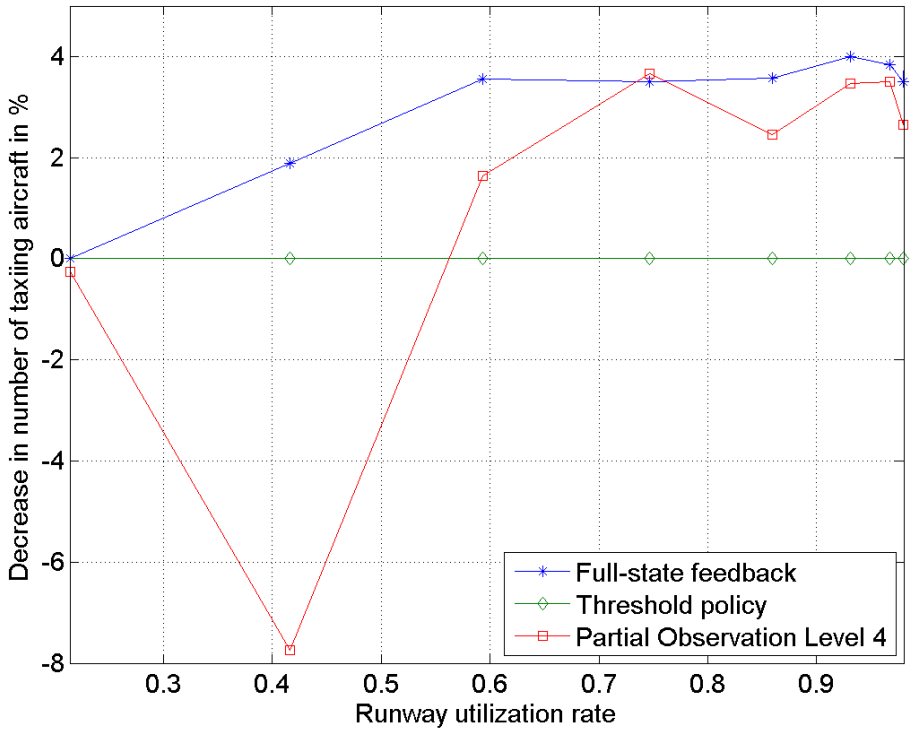

Figure 49: Reduction in percent of the number of taxiing aircraft as a function of the utilization rate, when compared with a threshold policy which respects ramp alternation. Surface surveillance covers 800 meters ahead of the control point of ramp one, at LaGuardia.

Level five, surface surveillance covers 1400 meters ahead of ramp one control point: The level of surface information now covers from ramp one to ramp two, as illustrated in Fig 34 , and allows the heuristic control policy to account exactly for states which may generate a conflict between an aircraft exiting ramp two and an aircraft arriving on the taxiway. This level of information performs almost exactly as the optimal policy, as illustrated in Fig. 52.

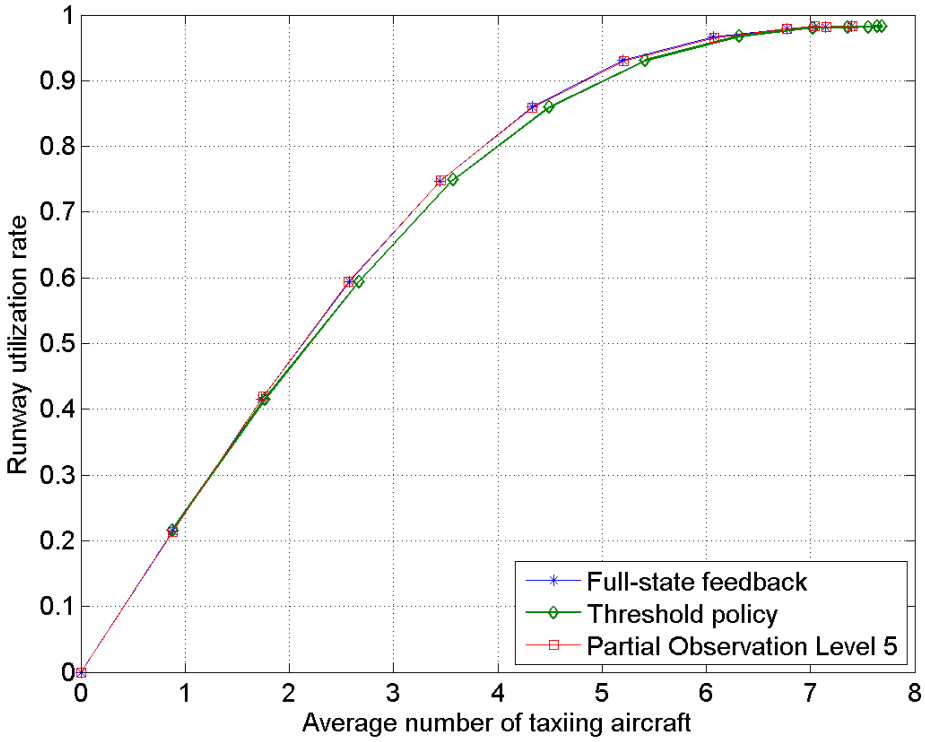

Figure 50: Utilization as a function of the average number of taxiing aircraft . Surface surveillance covers 1400 meters ahead of the control point of ramp one.

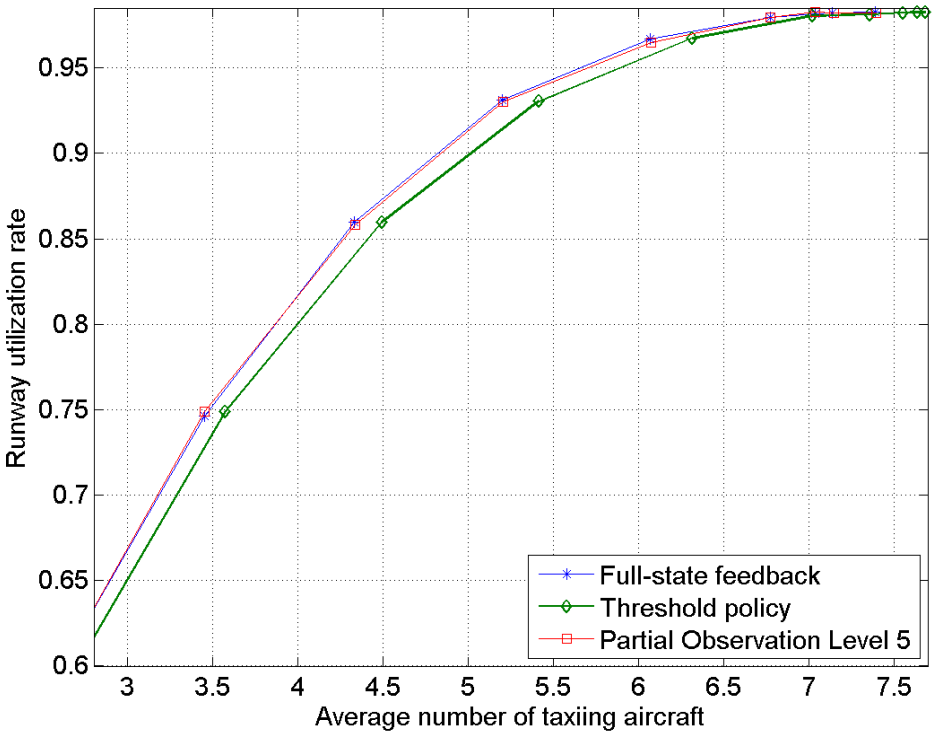

Figure 51: Utilization as a function of the average number of taxiing aircraft, for utilization rates above 60% . Surface surveillance covers 1400 meters ahead of the control point of ramp one.

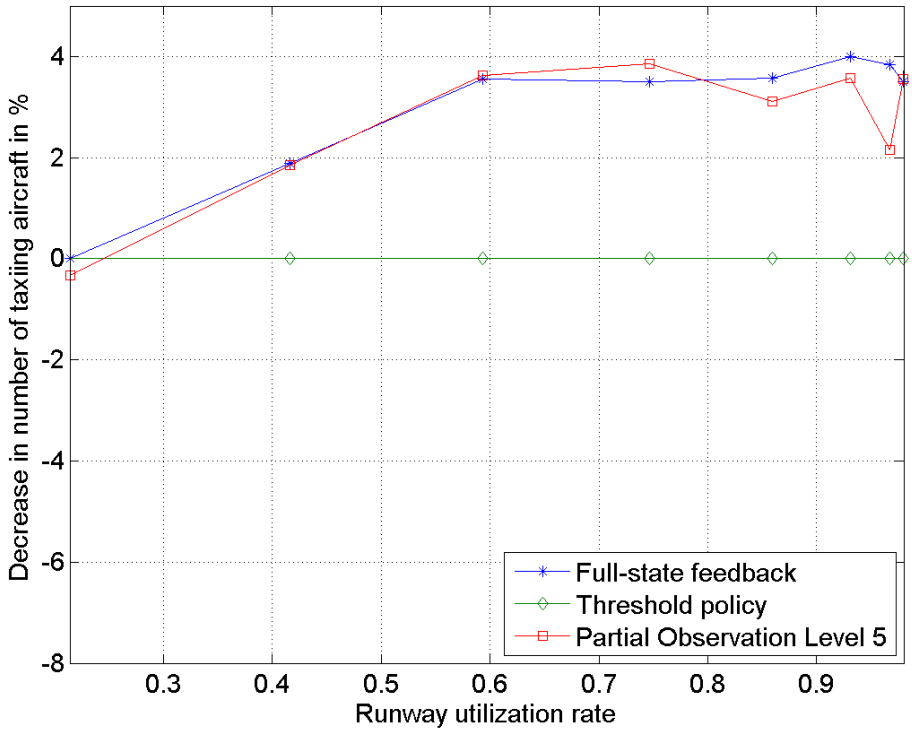

Figure 52: Reduction in percent of the number of taxiing aircraft as a function of the utilization rate, when compared with a threshold policy which respects ramp alternation. Surface surveillance covers 1400 meters ahead of the control point of ramp one, at LaGuardia.

Analysis: Partial surveillance information is fed to a heuristic control policy trying to estimate the current state and picking the corresponding optimal decision. The statistical fairness results suggest that the utility of surveillance information strongly depends on its impact on conflict mitigation for taxiway departure operations. Indeed, it has been observed that as surface information helps better locate aircraft positions before the second ramp area access, the performance of the heuristic control policy improves significantly. When the heuristic control policy receives more information about aircraft positions before ramp number two, it becomes able to better estimate states that accurately represent a risk of runway under-utilization. The optimal decision is then often to insert an aircraft from the ramp which is closest to the runway (ramp number two). Similarly, the heuristic policy can decide more accurately when not to send an aircraft if it estimates that the next most likely sate includes another aircraft that will block the intersection.

The Most Likely State heuristic policy needs a minimum level of information to perform at least as well as a threshold policy. Indeed, there is a large difference of performance between level one, two, and level three. Level one provides so little information that it is not even possible to consistently know if an aircraft is close to the runway threshold or not, as illustrated in Fig. 41. For high utilization rates, level two is comparable to a threshold policy, but level one performs far worse than a threshold policy. Level one sometimes generates estimates which give the agent the illusion that aircraft are closer to the runway than they actually are (Fig. 41). These mistakes are very costly, since the agent may not send an aircraft, thinking it is likely that one will arrive at the runway soon, when actually it is not. Level two still often generates costly mistakes when estimating the position of aircraft on the taxiway for intermediate utilization rates. The level three of information, where the heuristic has access to surface surveillance at the control point and 400 meters ahead allows the Most Likely State algorithm to avoid such mistakes.

3.2.3.4 Relaxing fairness constraints

Previous optimizations have strictly enforced fairness constraints. This section explores how departure operations react and how performance increases when fairness constraints are relaxed, in the case of an optimized full-state feedback policy using statistical fairness constraints to balance taxi clearances.

As fairness constraints are gradually removed, the second ramp area is gradually favored more and more, with results shown in Fig. 53. The curve which saturates the fastest, the one marked with stars, correspond to an agent who only clears aircraft from the second ramp area and ignores the first ramp area.

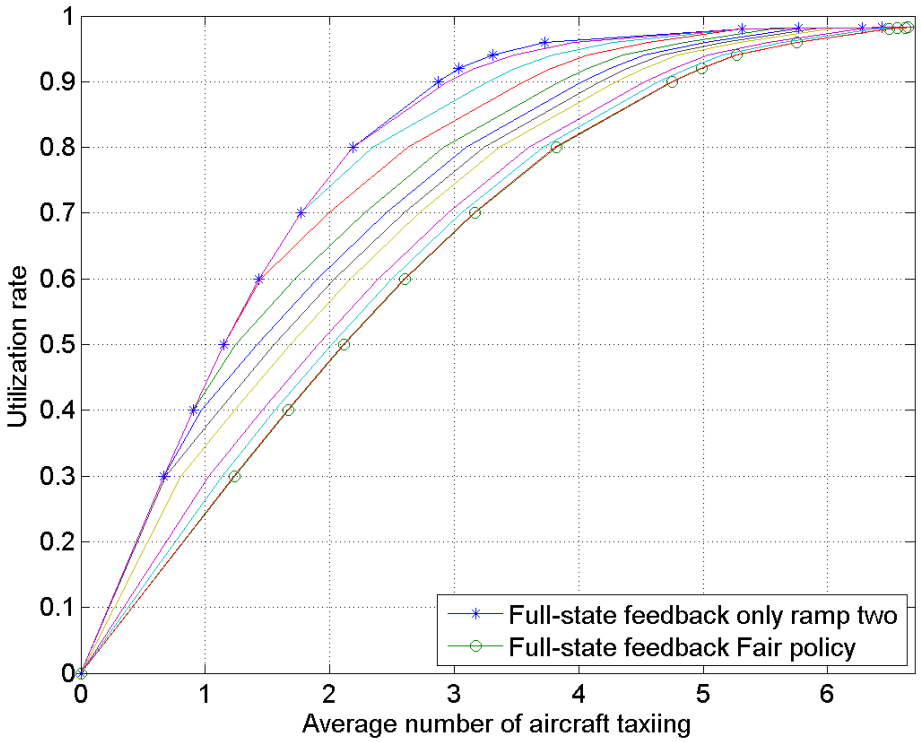

Figure 53: Utilization rate as function of the average number of taxiing aircraft.

Indeed, relaxing fairness constraints allows more aircraft to be cleared from the closest ramp, and this decreases the average number of taxiing aircraft for a given runway utilization rate. Fig. 54 measures these benefits against the benchmark

threshold policy and quantifies how much the pushback frequencies between ramp one and ramp two diverge. For each point, the ratio $\frac{\text{Ramp 2 clearance frequency}}{\text{Ramp 1 clearance frequency}}$ is displayed.

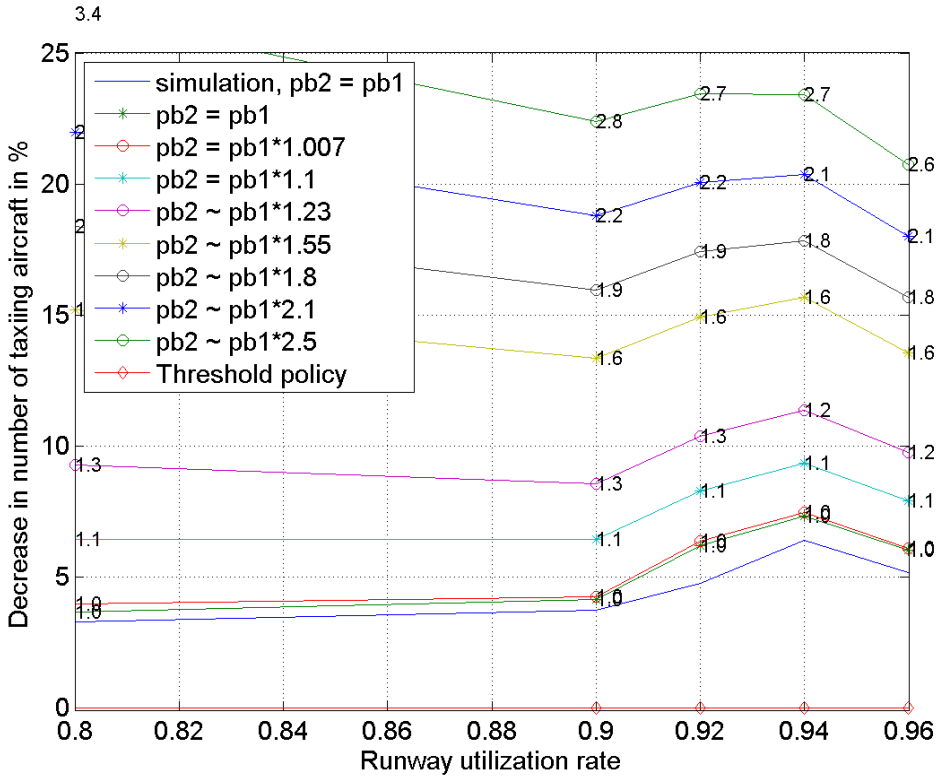

Figure 54: Reduction in percent of the number of taxiing aircraft as a function of the utilization rate, when compared with a threshold policy which respects ramp alternation.

Fig. 54 shows that performance may be significantly improved by increasing the turn-over of the ramp area which is close to the runway. For instance, an increase of 25 percent in the ramp two clearance frequency, would lead to a ratio $\frac{\text{Ramp 2 clearance frequency}}{\text{Ramp 1 clearance frequency}} = 1.67$, which corresponds to the yellow curve in Fig. 54 and yields up to 15 percent reduction in the average number of taxiing aircraft.

3.2.4 Conclusion

At LaGuardia airport, it is assumed the main ramp area and the ramp area closest to the runway threshold are used to control departure operations during periods of high activity and that both ramps have to clear aircraft at the same rate. Under these assumptions, providing surface surveillance to an agent which is entrusted with issuing taxi clearances can help improve operations and decrease the average number of taxiing aircraft by 4 percent while maintaining a runway utilization rate between 0.92 and 0.96.

The study of the different levels of observation suggests that the utility of surveillance information for airport departure operations increases significantly when it directly helps manage conflicts on the ground, thus reducing wasteful surface queues.

Finally, providing surface surveillance information to the agent can be combined with an increase in the share of taxi clearances that the closest ramp is allowed to issue to lower further the average number of taxiing aircraft. For example, optimizing operations with a 25 percent increase in the clearance frequency from the closest ramp yields a 10 percent reduction in the average number of taxiing aircraft, compared with the full-state feedback policy enforcing fairness between ramp areas.

3.3 Three conflicting ramp areas: Seattle Tacoma International Airport

The purpose of the third model is to apply the optimization-based valuation method to a different airport, Seattle-Tacoma International Airport. This airport involves a higher number of ramp area exit points. A model of the departure operations of Seattle-Tacoma International Airport has been developed. Fig. 55 shows the airport layout.

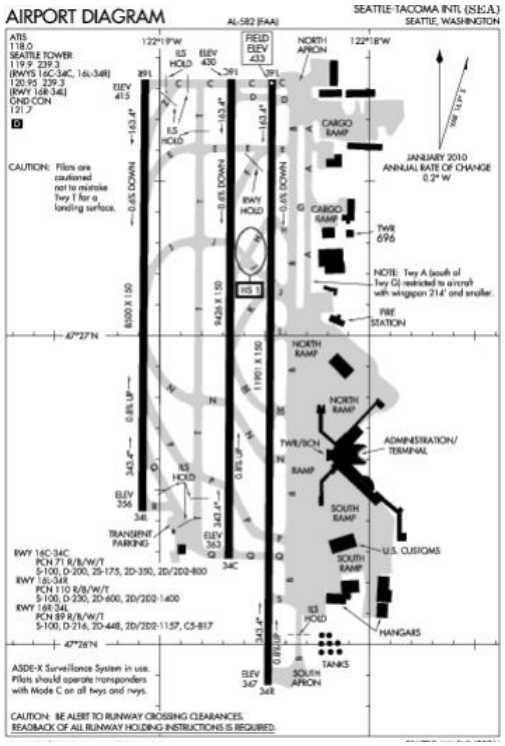

Figure 55: Diagram of Seattle-Tacoma International Airport

3.3.1 Stochastic modeling of surface departure operations

The runway configuration with departure operations on runway 16L is the most used configuration. According to the 2006 ASPM data, Seattle Airport departs aircraft under this configuration 56% of the time. The model of ground operations is developed and calibrated to simulate traffic from the control exit points of three main ramp areas, as illustrated in Fig. 56, and departing on runway 16L. The three ramp areas

are connected to the main taxiway and clearance decisions are optimized. The three ramps compete for access to the taxiway system, and at the same time cooperate to maintain an appropriate runway utilization rate. The runway utilization rate is set using the constraints defined in section 3.2.1.4 and the cost function is similarly equal to the number of taxiing aircraft.

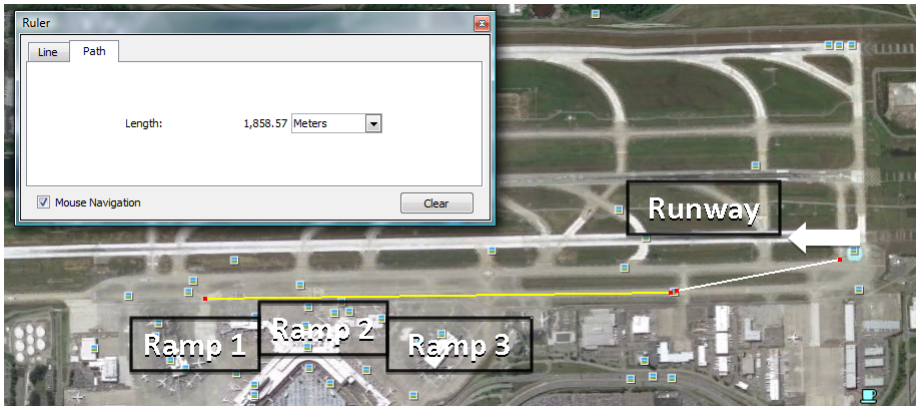

Figure 56: Satellite picture of Seattle-Tacoma International Airport, three ramp area model, departures on runway 16L.

3.3.1.1 Decisions

In this model, decisions involve three ramp control points. Therefore, the Linear Program is now optimizing a Markov Decision process relying on triplets of binary decision variables, d_1, d_2, and d_3. These decisions are respectively the decision to clear an aircraft from ramp one, two, and three. The notations remain the same, i designates the state and k the decision in the equations governing the Markov Decision Process. However to express the triplets (d_1, d_2, d_3) of decision, k takes values between 0 and 7 such that the binary value of k is a binary triplet e.g. $k = 4 = (1, 0, 0) =$ (pushback from ramp 1, no pushback from ramp 2, no pushback from ramp 3).

3.3.1.2 Calibration

The three-ramp-area model builds upon the model described in section 3.1.1.2. The ramp area access points or spots are modeled based on the topology of the Seattle-Tacoma International Airport taxiway system. Similarly to the previous models, each spatial sample represents 200 meters. The three ramp areas access points are modeled based on their distance to the runway queue, as illustrated in Fig. 56.

In this third model, the taxiway stochastic properties are chosen consistently with the previous calibrations of surface operations models. More specifically, an aircraft with no obstacle in front of it has a probability of m of moving forward and each spatial sample represents 200 meters. As for the previous model, the probability of receiving a take-off clearance for an aircraft at the runway threshold is determined by two Bernoulli variables with parameters c_1 and c_2. These variables are set to reproduce the standard deviation (0.603) and average (0.712) take-off rate that the Seattle airport reach at saturation, as described previously in Eq. (5). Solving this equation yields $c_1 = 0.58$ and $c_2 = 0.13$. The final state vector is represented by a binary vector of dimension thirteen. Two bits are used to code the runway queue, which can hold up to three aircraft. Ten bits are used to describe the taxiway system. Eight bits describe the main taxiway and three bits represent the ramp accesses. Fig. 57 illustrates the architecture of the new model, where each box in the graph may contain at most one aircraft.

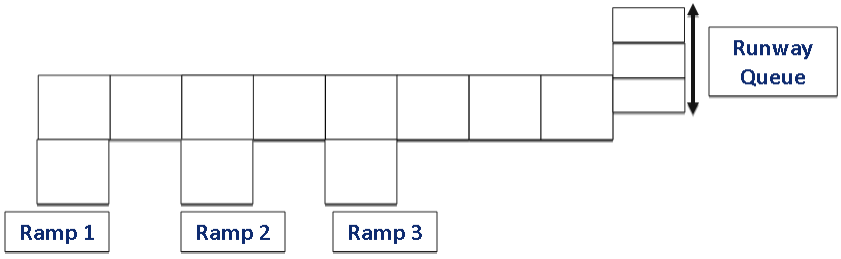

Figure 57: Satellite picture of Seattle-Tacoma International Airport, three ramp area model

3.3.1.3 Model Validation

As for the previous model developed, the Seattle-Tacoma International Airport model is validated against historical data. The Seattle airport average throughput rate is expressed as a function of the number of taxiing aircraft, using ASPM historical data from January to September 2006 when the runway configuration is set with departures on runway 16L.

The graph provided in Fig. 58 shows the throughput as a function of the number of taxiing aircraft, and yields the average take-off rate. Fig. 59 also shows the throughput as a function of the number of taxiing aircraft for the stochastic model. The model behaves similarly to the airport, and reproduces the stochastic nature of departure operations. When the number of taxiing aircraft reaches 12, the model saturates, and yields a maximum take-off rate distribution averaging 0.726 aircraft per minute, with a standard deviation of 0.583 aircraft per minute. These are similar to the average (0.712) and the standard deviation (0.603) of the take-off rate at Seattle airport, when the taxiway is saturated by departing aircraft. For the model, the saturation level of the take-off rate is reached at a slightly lower number of taxiing aircraft than for the ASPM data because the model accounts for operations on the taxiway only from ramp control points. In contrast the ASPM data includes all aircraft on the ground starting at pushback. As in section 3.2.1.3, we compare both throughput curves once the ASPM curve has been shifted to match the saturation level of both curves. For runway utilization rates above 30%, the shift efficiently isolates taxiway operations starting at the control points in the ASPM data, as illustrated in Fig. 59 .

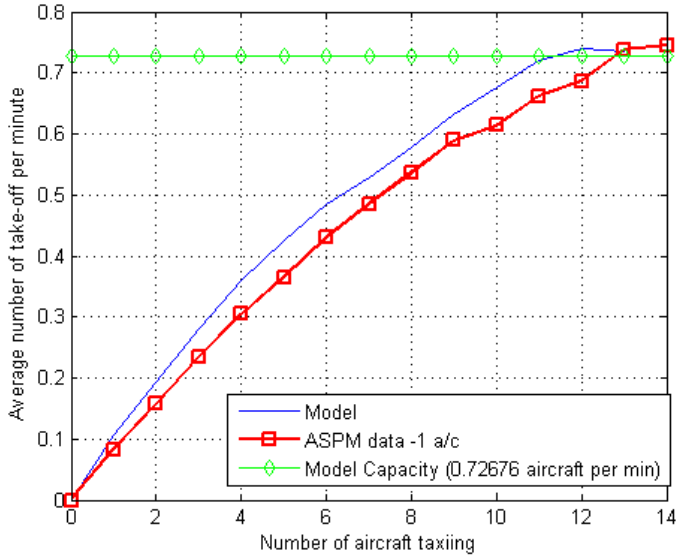

Figure 58: Seattle-Tacoma International Airport throughput as a function of the number of taxiing aircraft. The ASPM data reflects all departure operations on the ground starting at pushback.

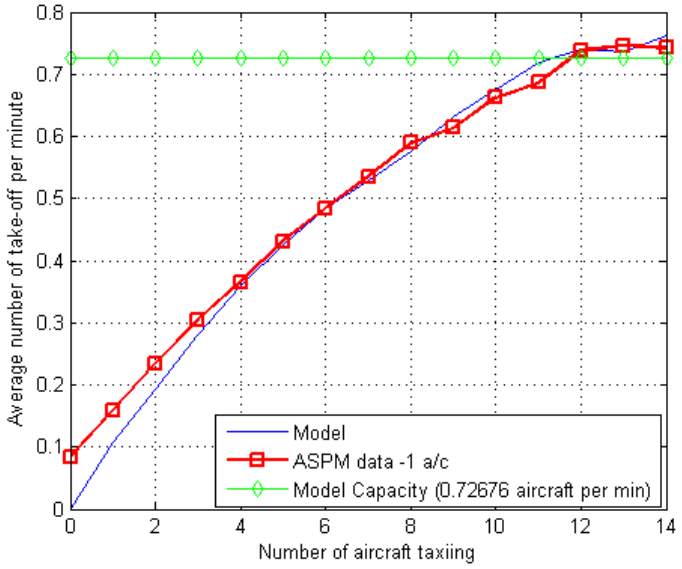

Figure 59: Seattle Airport throughput as a function of the number of taxiing aircraft. The ASPM curve is shifted by 1 aircraft to isolate taxiway operations starting at ramp exit control points, for utilization rates above 30%.

3.3.2 Impact of Aircraft Position Information

The fundamental approach to understand and valuate the impact of aircraft position information is the same, as described in section 3.1.2.1. It is based on optimization of Markov Decision Processes (MDP) and Partially Observable Markov Decision Processes (POMDP).

However, the optimization of the three ramp model yields a significantly more complex optimal policies. These policies must solve conflicts between ramps, cooperate to ensure fairness, and anticipate and react to last-minute events. Therefore, to better capture the higher complexity, the methodology presents a few differences when compared with the single ramp area model. The notion of fairness between ramp areas is defined and implemented within the control strategies using a statistically fair taxi clearance policy as described in section 3.2.2.1.

Second, several levels of partial information are studied to better capture the performance differences for intermediate levels. This approach therefore includes the study of:

- a high level of surface information, named "full state feedback",
- three lower levels of aircraft surface position information, named "estimated state feedback", level one being the lowest information level and level three the highest level, before "full state feedback",
- a basic benchmark policy relying solely on the number of aircraft, named "threshold policy".

Fair benchmark threshold policy: As in section 3.3.2, the benchmark threshold policy alternates between the ramp areas one, two, and three to enforce fairness between the ramp areas. The exact values of the utilization rates for the threshold

policy are derived similarly, by solving the Markov Process equations, which represent the threshold policy as specified by Eqs. (29) and (30). Once the steady-state probabilities are obtained, the utilization rates and average number of taxiing aircraft are given by Eqs. (31) and (32).

3.3.2.1 Levels of information

This section details the different levels of surface information that are made available to the agent controlling the clearances. The agent uses a heuristic control policy called the Most Likely State algorithm and developed in section 3.1.2.3. Equations (22) and (21) in section 3.1.2.3 explain how different observation vectors may be integrated into the observation probability matrix. Eq. (19) describes how this matrix is used within the heuristic algorithm to update the belief state. As more information is provided to the agent, the accuracy and efficiency of the Most Likely State algorithm increases. The progression between the levels of information can be clearly observed. Their performance converges toward the "full-state feedback" level. These levels are described in this section, along with their respective observation vectors.

Level one, the control points: The first level of information includes the total number of taxiing aircraft. It also indicates if taxi clearances from ramp area one and two are feasible, which is specified by how many aircraft are in each of the spatial samples represented in orange in Fig. 60.

The observation vector corresponding to the level one of information is the succession of the number of aircraft in the four zones described above, as illustrated in Eq. (53).

$$o = \begin{bmatrix} N_{white} & N_{ramp_1} & N_{ramp_2} & N_{ramp_3} \end{bmatrix} \tag{53}$$

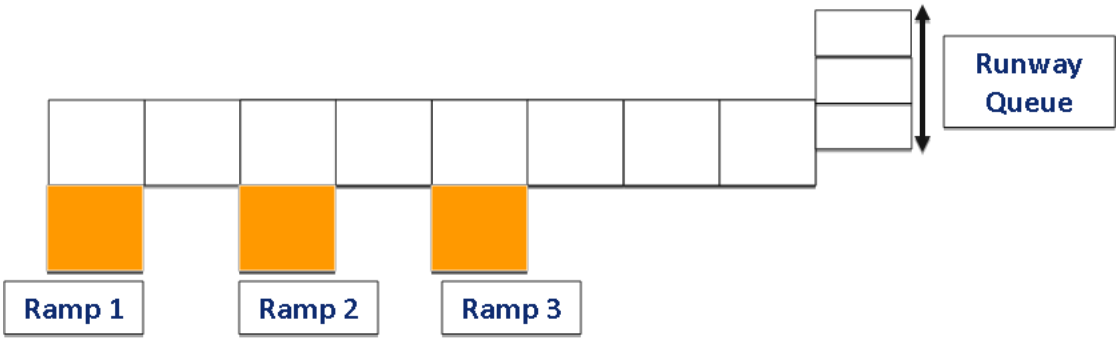

Figure 60: Partial observation level one, at Seattle airport, observations include the control points and the total number taxiing aircraft.

Level two, surface surveillance covers the taxiway system in front of the ramps: The second level of information is illustrated in Fig. 61. The agent can observe the taxiway system in front of the ramps.

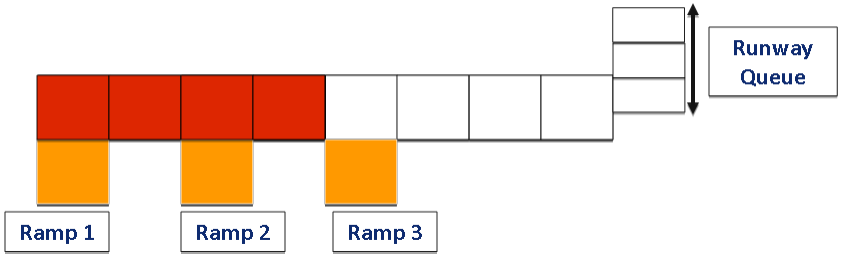

Figure 61: Partial observation level two, at Seattle airport, surface surveillance covers the taxiway system in front of the ramps.

The observation vector corresponding to the second level of information is the succession of the number of aircraft in the four zones described above in Fig. 61 and illustrated in Eq. (54).

$$o = \begin{bmatrix} N_{white} & N_{red_1} & N_{red_2} & N_{red_3} & N_{red_4} & N_{ramp_1} & N_{ramp_2} & N_{ramp_3} \end{bmatrix} \tag{54}$$

Level three, surface surveillance covers most of the taxiway system: The third level of information is illustrated in Fig. 62. The agent can now observe the taxiway system in front of the ramp areas and up to 200 meters prior to the runway queue.

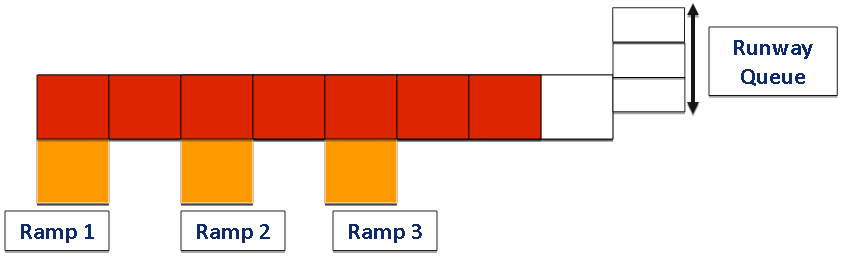

Figure 62: Partial observation level three, watching over 400 meters ahead of ramp one control point.

The observation vector corresponding to the third level of information is the succession of the number of aircraft in the five zones described above in Fig. 62 and illustrated in Eq. (55).

$$o = \begin{bmatrix} N_{white} & N_{red_1} & N_{red_2} & N_{red_3} & N_{red_4} & N_{red_{5..7}} & N_{ramp_1} & N_{ramp_2} & N_{ramp_3} \end{bmatrix} \quad (55)$$

3.3.3 Results and Discussion

The optimization results are validated and the results are discussed. The impact of surface surveillance information on departure operations is evaluated.

3.3.3.1 Validation

Numeric approximations: The potential numerical problems are described in more detail in section 3.2.3.1 have also been addressed for Seattle-Tacoma. For the three ramp model, the number of digits needed to express the transition probabilities is similar to the two ramp model. As in section 3.2.3.1, the maximum number significant digits required is evaluated. The transition probability with the largest number of significant digits is now 14 digit long, $m^{10} \cdot ((1-c(1)) \cdot (1-c(2))) = 0.12594265256412$. This number is 14 digit long, which remains below the 15 digits allowed by the 53 bit significand of the double precision arithmetic.

Solution reliability: Fig. 63 shows the difference between the average number of taxiing aircraft yielded by the CPLEX output and the average number of taxiing aircraft yielded by the simulation, as a function of the utilization rate. The difference between the results of the simulation of the optimal policy and the optimization results from the CPLEX optimization output is not significant. The difference remains below 2.5%, this verifies the validity of the CPLEX optimal solution.

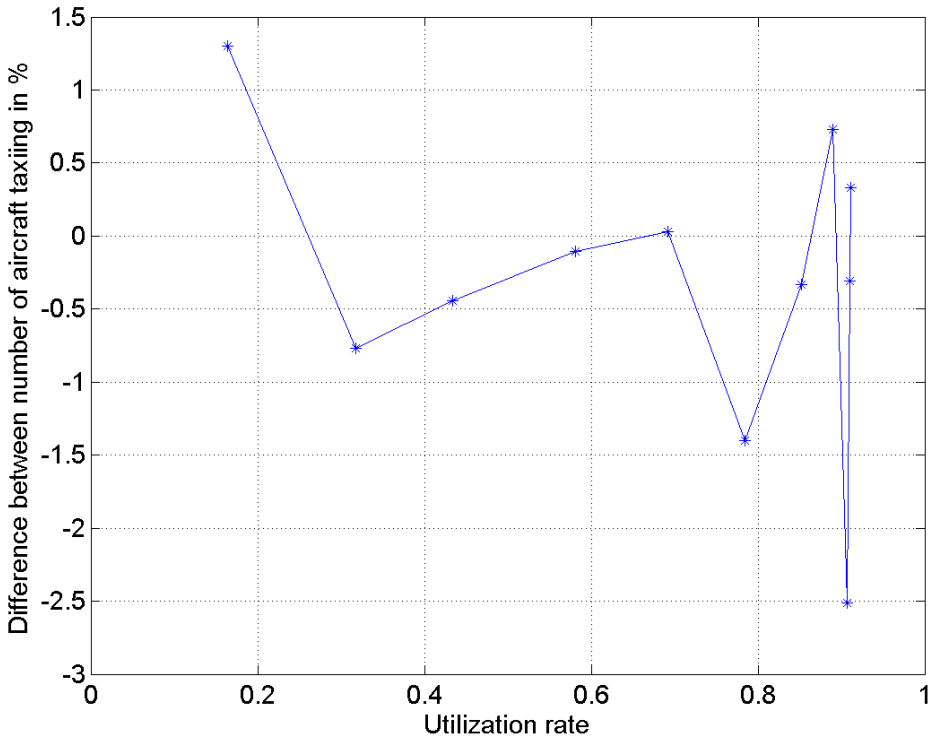

Figure 63: Difference between the average number of taxiing aircraft yielded by the CPLEX out-put and the average number of taxiing aircraft yielded by the simulation, as a function of the utilization rate, for the three ramp Seattle airport model.

3.3.3.2 Optimal policies against benchmark policy

Fig. 64 illustrates the utilization rate as a function of the average number of taxiing aircraft. Fig. 65 shows the reduction in percent of the average number of taxiing aircraft for optimal policies, as a function of the utilization rate, when compared with a threshold policy which alternates between ramps.

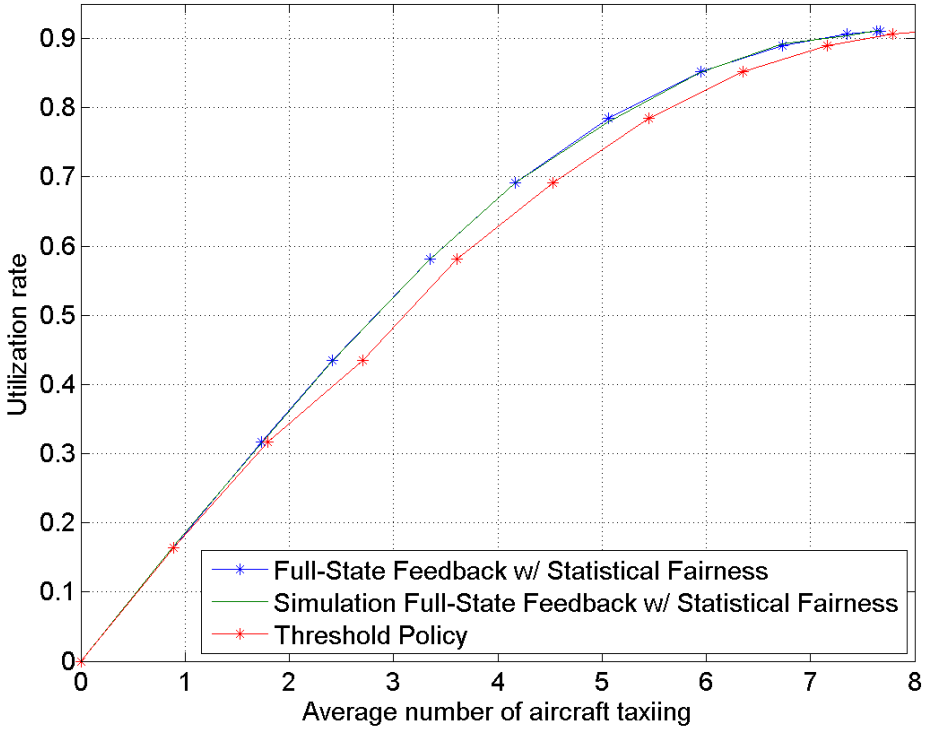

Figure 64: Runway utilization rate as a function of the average number of taxiing aircraft at Seattle airport

When the number of taxiing aircraft is limited by the threshold policy to one aircraft, the difference of performance between the full-state feedback policy and the threshold policy is inexistent as illustrated by Fig. 65.

When the threshold for the number of taxiing aircraft is increased to two and and then three, the threshold policy starts yielding a lower utilization rate for the same number of taxiing aircraft than the full-state feedback policy, as shown in Fig. 64 and 65. Indeed, the threshold policy releases aircraft blindly based on the number of

taxiing aircraft. Consequently aircraft have a higher chance of conflicting with each other on the taxiway. The optimal full-state feedback policy performs better because it manages the release of aircraft using the exact position of the other aircraft already taxiing.

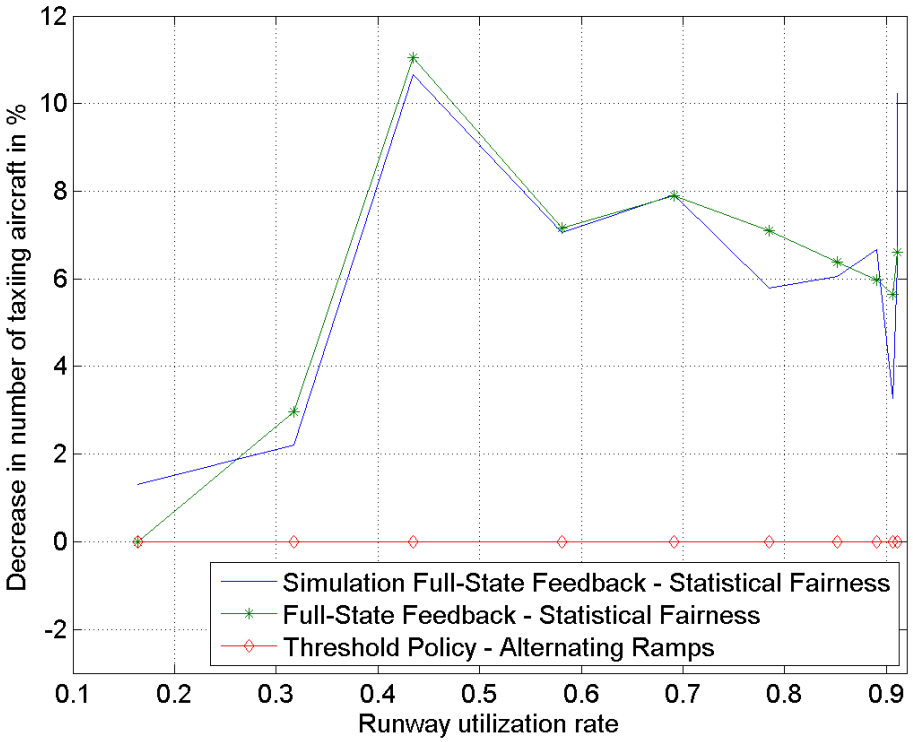

Figure 65: Reduction in percent of the average number of taxiing aircraft as a function of the utilization rate, when compared with a threshold policy, for Seattle airport.

The full state feedback policy performs consistently better, generating a smaller average number of taxiing aircraft, when compared with the threshold benchmark policy. This performance is consistently better over a wide array of utilization rates, which correspond not only to intermediate runway capacities but also to situations where the runway is used at maximum capacity. For intermediate utilization rates, the number of taxiing aircraft can be reduced between 11 and 7 percent. More important, for rates between 0.45 and 1, the reduction of the number of taxiing

aircraft is consistently above 6 percent.

3.3.3.3 Influence of different levels of observation

To better understand the influence of information on the operational efficiency of departure operations for the Seattle airport three ramp area model, several levels of information are studied using the Most Likely State algorithm described in section 3.1.2.3. The levels of information are described in more detail in section 3.3.2.1.

Level one, the control points: The first level of surface surveillance provides the ground controller with only the total number of aircraft and informs her/him of the possible presence of an aircraft blocking access from ramp one or two, as illustrated in Fig. 60. This information is necessary for the agent to make a feasible decision. The orange zones correspond to the areas about which this information is available. The first level information performs slightly under the threshold policy, as shown in Fig. 66.

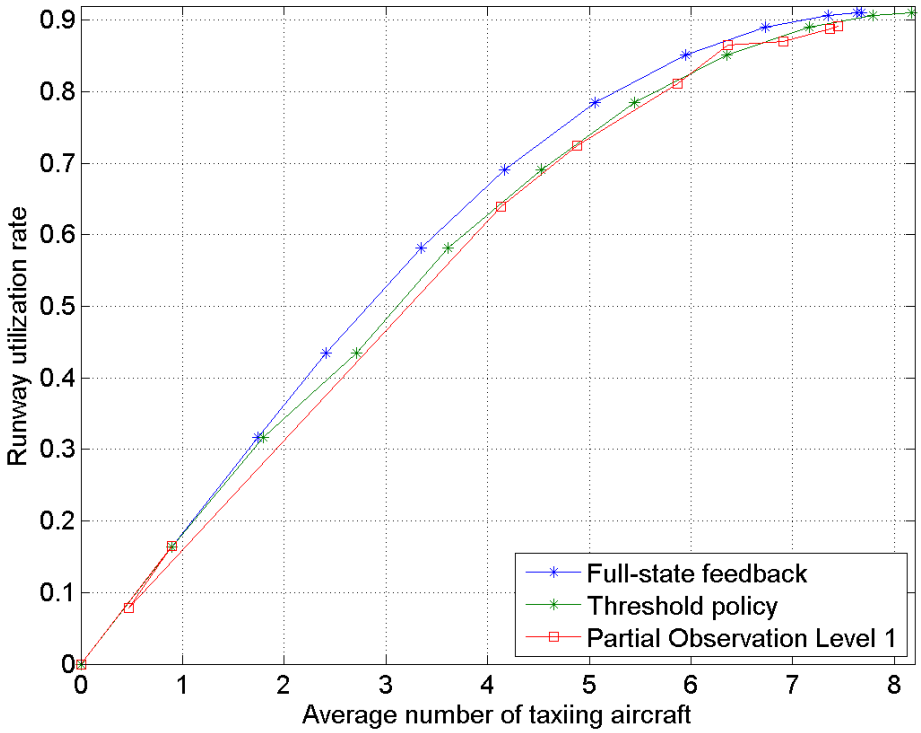

Figure 66: Utilization as a function of the average number of taxiing aircraft for Seattle airport. Surface surveillance provided to the Most Likely State algorithm covers the control points.

Level two, surface surveillance covers the taxiway system in front of the ramps: The second level of information is illustrated in Fig. 61. Once the Most Likely State algorithm has access to surface surveillance information for the zone covering the taxiway system in front of the ramps, it is able to efficiently solve conflicts and it performs as well as the optimal policy as illustrated in Fig. 67.

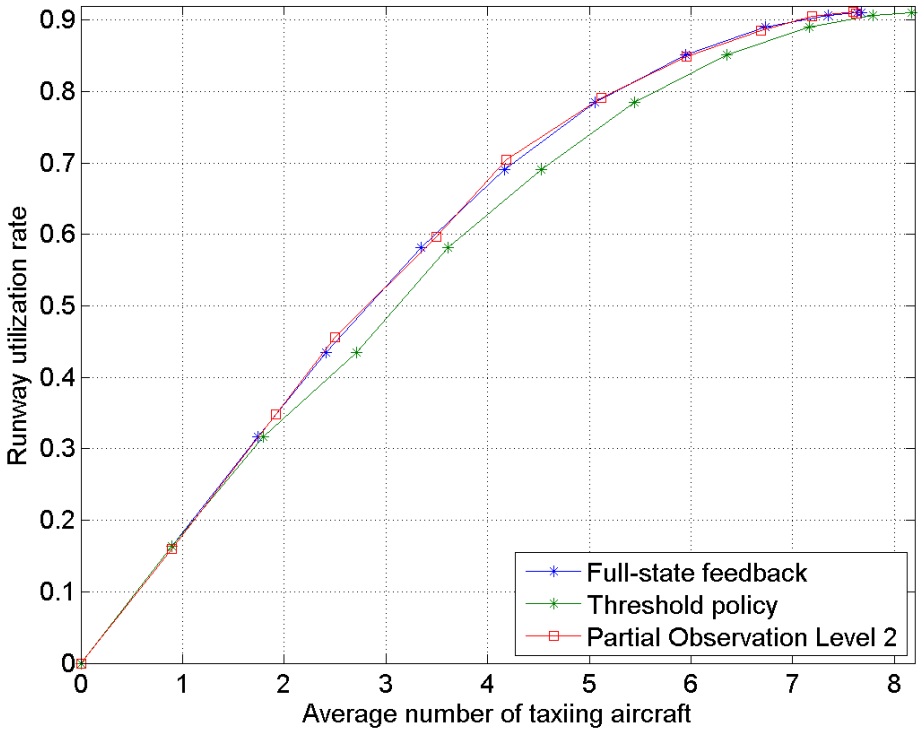

Figure 67: Utilization as a function of the average number of taxiing aircraft for Seattle airport. Surface surveillance covers the taxiway system in front of the ramps.

Level three, surface surveillance covers most of the taxiway system: The level of surface information now covers all the ramps and and most of the taxiway as illustrated in Fig. 62. This heuristic Most Likely State algorithm performs exactly as the optimal policy, as illustrated in Fig. 68.

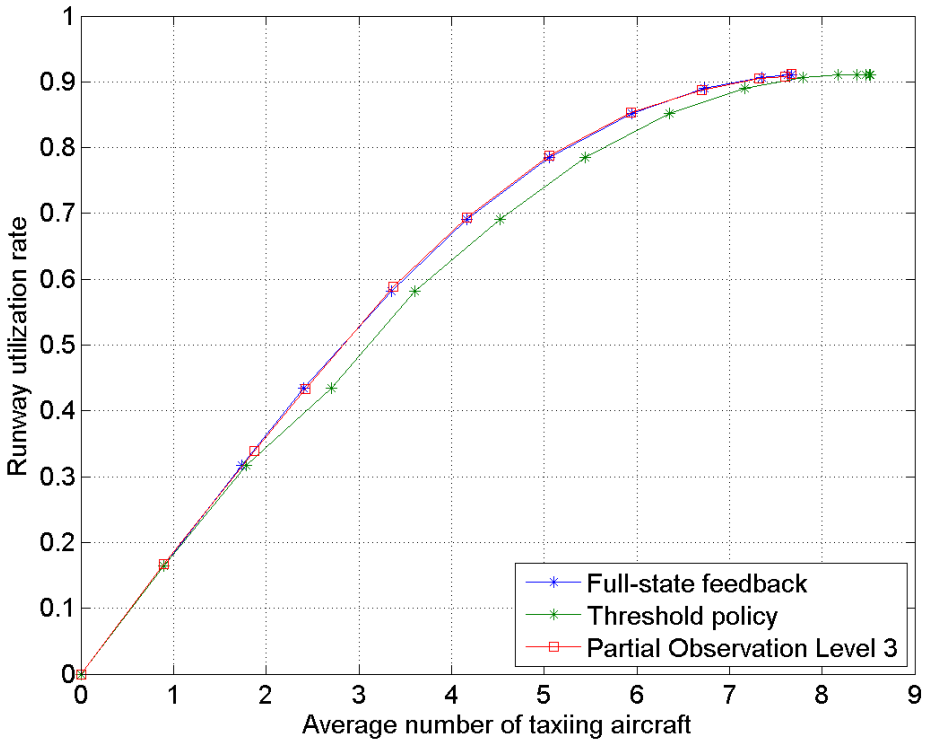

Figure 68: Utilization as a function of the average number of taxiing aircraft, for Seattle airport. Surface surveillance covers most of the taxiway system.

3.3.4 Conclusion

At Seattle airport, three main ramp areas are considered, as shown in Fig. 57. We assume they are used are used to control departure operations during periods of high activity and that these ramps have to clear aircraft for taxi at the same rate. Under these assumptions, providing surface surveillance to an agent, who optimally controls taxi clearances, can help improve operations and decrease the average number of taxiing aircraft by 6 percent while maintaining a runway utilization rate above 0.9, compared with a threshold policy which limits the number of taxiing aircraft.

The study of different levels of observation for Seattle airport suggests that the utility of surveillance information for airport departure operations increases significantly when it directly helps manage conflicts on the airport surface.

CHAPTER IV

CONCLUSION

This thesis assesses the benefits of last minute flight-swapping capabilities provided by collaborative control of departure operations through the Collaborative Virtual Queue, and estimates the benefits of providing surface surveillance information to the ramp clearance control process, within a collaborative framework.

A collaborative concept of operations, the Collaborative Virtual Queue, is developed and evaluated. In congested situations, the CVQ changes the nature of departure operations from a push system, where airlines send aircraft as soon as ready, to a pull system, where controllers decide when an aircraft can and should be cleared to taxi toward the runway queue. The CVQ can shorten the average departure taxi time, inducing a decrease in departure operating costs, and it can benefit the local environment by reducing emissions. At Boston Logan airport, when departure operations are dominated by ten airlines in competition, the CVQ can provide flight swapping capabilities that can decrease the overall passenger waiting time by 3 percent while not affecting airport departure capacity.

This research then quantifies analytically the potential benefits yielded by providing surveillance information to the agent or to an advisory system, which is entrusted with issuing push-back or taxi clearances. Our results have shown that, within the collaborative framework discussed in chapter two, surface surveillance information can significantly improve the control of stochastic departure operations on the ground. More specifically, at LaGuardia airport, controlling taxi clearances optimally using surface surveillance reduces the number of taxiing aircraft by 4% when the airport functions near capacity, compared with a threshold policy which limits the number of

taxiing aircraft. At Seattle airport, controlling taxi clearances optimally using surface surveillance reduces the number of taxiing aircraft by 6% when the airport functions near capacity, compared with a threshold policy which limits the number of taxiing aircraft. It has been observed that, in order to minimize wasteful surface conflicts and queues, the optimal full-state feedback policy relies on aircraft position information to avoid conflicts, maximize runway utilization, and balance and coordinate ramp taxi clearances.

The study of departure operations from a single ramp area and from a two ramp area, suggests that the utility of surveillance information increases when it helps minimize conflicts on the surface to better manage airport resources. Indeed, for departure operations from a single ramp area, operational improvements are larger at intermediate utilization rates. At these rates, the careful timing of clearances, based on the position of previously cleared aircraft, contributes to significantly decreasing the average number of taxiing aircraft, compared with a threshold policy or an estimated state feedback policy. For instance, the agent will not clear an aircraft if she/he can see there is a temporary queue of aircraft that formed on the surface close to the ramp area. These comparative benefits disappear when the runway utilization rate increases and even the optimal full-state feedback policy converges toward a threshold policy. For airports working close to their maximum throughput capacity, more complex departure operations, comprised of two ramp or three ramp areas, benefit more from increased surface surveillance information than operations and airports where aircraft are released from a single ramp area. Indeed, in the two and three ramp case, the agent controlling clearances can leverage surveillance information to mitigate conflicts between the two ramp areas. The position information also makes it easier to achieve fair balance clearances between ramps, while benefiting from the proximity of the closest ramp area to reduce the risk of runway under-utilization. As a result, surveillance information significantly improves departure operations of a two

and three ramp area taxiway system, even as the runway is used close to its maximum capacity.

REFERENCES

[1] "Airport noise regulations." http://www.boeing.com/commercial/noise/ laguardia.html. Accessed on Auguts 2009.

[2] "Surface management system." http://www.metronaviation.com/solutions/traffic-flow-management/systems/sms.html. Accessed on August 2009.

[3] "Discrete time markov chains." http://www.stanford.edu/class/ ee384x/Handouts/rev3_v4.pdf, 2006. Accessed on June 2010.

[4] "Cdm@cdg." http://www.euro-cdm.org/library/ airports/cdg/cdm_cdg_presentation_to _eurocontrol_2007_11_21.pdf, 2007. Accessed on November 2010.

[5] "Advanced surface movement guidance and control systems." http://www.eurocontrol.int/airports/public/standard_page/ APR2_Projects_ASMGCS_2.html, 2008. Accessed on October 2009.

[6] "Airport collaborative decision making." http://www.eurocontrol.int/airports/ public/standard_page/APR2_ACDM_2.html, 2008. Accessed on November 2009.

[7] "Ilog CPLEX user's manual: Continuous optimization." http://yalma.fime.uanl.mx/cplex11-manual/Content/Optimization/ Documentation/CPLEX/_pubskel/XPlatform/User_man496.html, 2008. Accessed on February 2010.

[8] "Apm taxi times: Definition of variables." http://aspmhelp.faa.gov/index.php/APM_Taxi_Times:_Definition_of_Variables, 2010. Accessed on October 2010.

[9] "Collaborative decision making." http://cdm.fly.faa.gov/, 2010. Accessed on November 2009.

[10] "Faa awards final set of major NextGen engineering contracts." http://www.faa.gov/news/press_releases/news_story.cfm?newsId=11561, June 2010. Accessed on June 2010.

[11] "Faa's NextGen implementation plan," tech. rep., Federal Aviation Administration, 2010.

[12] "Matlab documentation." http://www.mathworks.com/access/helpdesk/help/ techdoc/matlab_prog/, 2010. Accessed on March 2009.

[13] Alfa, A. S., "Discrete time queues and matrix-analytic methods," *Sociedad de Estadistica e Investigacidn Operativa*, vol. 10, no. 2, pp. 147–210, 2002.

[14] Anagnostakis, I., Clarke, J., Bohme, D., and Volckers, U., "Runway operations planning and control: Sequencing and scheduling," *Journal of Aircraft*, vol. 38, no. 6, pp. 988–996, 2001.

[15] Andersson, K., Hall, W., Atkins, S., and Feron, E., "Optimization-based analysis of collaborative airport arrival planning," *Transportation Science*, vol. 37, no. 4, 2003.

[16] Arbuckle, D., Rhodes, C. D., Andrews, M., Roberts, D., Hallowell, S., Baker, D., Burleson, C., Howell, J., and Anderegg, A., "U.S. vision for 2025 air transportation," *ATCA Journal of Air Traffic Control*, January-March 2006.

[17] Balakrishnan, H. and Jung., Y., "A framework for coordinated surface operations planning at Dallas-Fort-Worth international airport.," in *AIAA Guidance, Navigation, and Control Conference and Exhibit*, no. AIAA-2007-6553, (Hilton Head, South Carolina), American Institute of Aeronautics and Astronautics, 2007.

[18] Balakrishnan, H. personnal communication, Massachusetts Institute of Technology Cambridge, MA 02139, 2010.

[19] Besada, J., Molina, J., Garcia, J., Berlanga, A., and Portillo, J., "Aircraft identification integrated into an airport surface surveillance video system," *Machine Vision and Applications*, vol. 15, pp. 164–117, 2004.

[20] Bini, D., Latouche, G., and Meini, B., *Numerical methods for structured Markov chains*. Oxford University Press, 2005.

[21] Bose, S. K., *Chapter 1 - An Introduction to Queueing Systems*. Kluwer/Plenum Publishers, 2002.

[22] Burgain, P., Feron, E., and Clarke, J.-P., "Collaborative virtual queue: Benefit analysis of a collaborative decision making concept applied to congested airport departure operations," *Air Traffic Control Quaterly*, vol. 17(2), pp. 195–222, 2009.

[23] Capozzi., B., "Automated airport surface traffic control.," in *AIAA Guidance, Navigation, and Control Conference and Exhibit*, (Metron Aviation, Inc., Herndon, VA 20170), American Institute of Aeronautics and Astronautics, August 2003.

[24] Capozzi, B. J., DiFelici, J., and Jakobovits, R., "Towards automated airport surface traffic control: Potential benefits and feasibility," in *AIAA Guidance, Navigation, and Control Conference and Exhibit*, pp. 1–16, August 2004.

[25] Carr, F., Evans, A., Clarke, J., and Feron, E., "Modeling and control of airport queuing dynamics under severe flow restrictions," in *Proceedings of the*

American Control Conference, (Anchorage, AK), International Center for Air Transportation, 2002.

[26] Carr, F., Theis, G., Clarke, J., and Feron., E., *Evaluation of Improved Pushback Forecasts Derived from Airline Ground Operations Data.* Journal of Aerospace computing, information, and communication, Vol. 2, January, 2005.

[27] Cassandra, A., Littman, M. L., and Zhang, N. L., "Incremental pruning: A simple, fast, exact method for partially observable markov decision processes.," in *Proceedings of Uncertainty in Artificial Intelligence*, pp. 54–61, 1997.

[28] Cassandra, A. R., Kaelbling, L. P., and Kurien, J. A., "Acting under uncertainty: Discrete Bayesian models for mobile-robot navigation," in *In Proceedings of IEEE/RSJ International Conference on Intelligent Robots and Systems*, pp. 963–972, 1996.

[29] Cheng, V. H. L., Sharma, V., and Foyle, D. C., "A study of aircraft taxi performance for enhancing airport surface traffic control," *IEEE Transactions on Intelligent Transportation Systems*, vol. 2, pp. 39–54, June 2001.

[30] Delcaire, B. and Feron, E., "Development of an on-site ground operations model for Logan international airport," Tech. Rep. Research Report RR-9709, FAA Air Transportation Center of Excellence in Operations Research, Massachusetts Institute of Technology, Cambridge, MA 02139, December 1997.

[31] Dimitropoulos, K., Grammalidis, N., Simitopoulos, D., Pavlidou, N., and Strintzis, M., "Video system for surface movement surveillance at airports," *Journal of Intelligent Transportation Systems*, vol. 11, pp. 169–180, October 2007.

[32] Doorn, E. A. V. and Schrijner, P., "Geometric ergodicity and quasy-stationarity in discrete-time birth-death processes," *The Journal of the Australian Mathematical Society. Series B. Applied Mathematics*, vol. 37, pp. 121–144, 1993.

[33] Erlang, A. K., "The theory of probabilities and telephone conversations," *Nyt tidsskrift for Matematik*, vol. 20, p. 33, 1909.

[34] Feron, E., Hansman, R. J., Odoni, A., Cots, R. B., Delcaire, B., Feng, X., Hall, W., Idris, H., Muharremoglu, A., and Pujet, N., "The departure planner: A conceptual discussion," tech. rep., White paper, MIT, International Center for Air Transportation, 1997.

[35] FlightAware, "Laguardia airport map and diagram." http://flightaware.com/resources/airport/KLGA/map, 2009. Accessed online on March 2009.

[36] Foyle, D., Andre, A.D .and McCann, R., Wenzel, E., Begault, D., and Battiste, V., "Taxiway navigation and situation awareness (T-NASA) system: Problem, design philosophy, and description of an integrated display suite for low-visibility airport surface operations," *Journal of Aerospace*, vol. 105, pp. 1411–1418, 1996.

[37] Gorman, P., Hofmann, J., and Wambsgauss, M., "Collaborative decision making between the federal aviation administration and the air transport industry," in *16th Digital Avionics Systems Conference*, vol. 2, pp. 9.2–23–9.2–28, Institute of Electrical and Electronics Engineers, 0-7803-41 50-3/97, October 1997.

[38] GreenAir Communications, "Commercial air traffic annual growth to continue at 4.7 percent over next 20 years, forecasts airbus.." http://www.greenaironline.com/news.php?viewStory=596. Accessed on October 2010.

[39] Hicok, D. and Lee, D., "Application of ADS-B for airport surface surveillance," in *Digital Avionics Systems Conference. Proceedings, 17th DASC.*, 1998.

[40] Hiller, F. and Liberman, G., *Introduction to Operations Research.* 1221 Avenue of the Americas, New York, NY, 10020: McGraw-Hill, 7th edition ed., 2001.

[41] Howell, D., Fontaine, P., and Ritchey, S., "Measuring the impact of surveillance data sharing on day-to-day surface operations.," in *AIAA 4th Aviation Technology, Integration, and Operations (ATIO) Forum*, no. AIAA-2004-6239, (Chicago, IL), American Institute of Aeronautics and Astronautics, September 2004.

[42] Howell, D. and Ritchey, S., "Airline operational benefits of surface surveillance," in *USA-Europe ATM 6th Seminar*, (Baltimore, MD, USA), June 2005.

[43] Hughes, D., "ACSS readies ADS-B software.," *Aviation Week & Space Technology*, vol. 165, no. 18, p. 108, 2006.

[44] Idris, H., Clarke, J., Bhuva, R., and Kang, L., "Queuing model for taxi-out time estimation," *Air Traffic Control Quaterly*, vol. 10(1), pp. 1–22, 2002.

[45] Idris, H., Clarke, J., Bhuva, R., and Kang., L., *Queuing Model for Taxi-Out Time Estimation.* Air Traffic Control Quarterly, 2002.

[46] Intergovernmental Panel on Climate Change (IPCC), *Aviation and the Global Atmosphere.* Cambridge University Press, 1999.

[47] International Civil Aviation Organization (ICAO), "Engine emissions databank," tech. rep., International Civil Aviation Organization (ICAO), July 2007.

[48] Joint Planning and Development Office (JPDO), "Next generation air transportation system - integrated plan," tech. rep., Washington, DC, 2004.

[49] JPDO, *Concept of Operations for the Next Generation Air Transportation System.* Joint Planning and Development Office, 2007.

[50] Jung, Y. C. and Monroe, G. A., "Development of surface management system integrated with CTAS arrival tool," in *AIAA 5th Aviation, Technology, Integration, and Operations Conference*, (Arlington, Virginia), September 2005.

[51] Kaelbling, L. P., Littman, M. L., and Cassandra, "Planning and acting in partially observable stochastic domains.," *Artificial Intelligence*, vol. 101, pp. 99–134, 1998.

[52] Karp, A., "Size matters atLaGuardia," *Air Transport World*, p. 65, 2006.

[53] Kim, S. H., Feron, E., and Clarke, J.-P., "Assigning gates by resolving physical conflicts," in *AIAA Guidance, Navigation, and Control Conference*, no. AIIAA-2009-5648, (Chicago, Illinois), August 2009.

[54] Ky, P. and Miaillier, B., "SESAR: towards the new generation of air traffic management systems in europe," *ATCA Journal of Air Traffic Control*, January-March 2006.

[55] Littman, M. L., "The witness algorithm: Solving partially observable Markov decision processes," tech. rep., 1994.

[56] Mohleji and Tene., *Minimizing Departure Prediction Uncertainties for Efficient RNP Aircraft Operations at Major Airports.* McLean, VA 22102: The MITRE Corporation Center for Advanced Aviation System Development, 2006.

[57] O, M., S, H., and A, C., "On the undecidability of probabilistic planning and infinite-horizon partially observable markov decision problems.," in *Proceedings of the Sixteenth National Conference on Artificial Intelligence.*, 1999.

[58] Papadimitriou, C. and Tsitsiklis, J., "The complexity of Markov decision processes.," *Mathematics of Operations Research.*, vol. 12(3), pp. 441–450, 1987.

[59] Pujet, N., Delcaire, B., and Feron., E., *Input-output modeling and control of the departure process of congested airports.* Massachusetts Institute of Technology, Cambridge, MA 02140: American Institute of Aeronautics and Astronautics, AIAA 99-4299, 1999.

[60] Rathinam, S., Montoya, J., and Jung, Y., "An optimization model for reducing aircraft taxi times at the Dallas-Fort-Worth international airport," in *26th International Congress of The Aeronautical Sciences*, 2008.

[61] Schofield, A., "Runway risks.," *Aviation Week & Space Technology*, vol. 169, no. 14, p. 54, 2008.

[62] Simaiakis, I. and Balakrishnan, H., "Queuing models of airport departure processes for emissions reduction," in *AIAA Guidance, Navigation, and Control Conference,*, no. AIAA-2009-5650, (Chicago, IL), American Institute of Aeronautics and Astronautics, August 2009.

[63] Singh, G. and Meier, C., "Preventing runway incursions and conflicts," *Science Direct*, vol. 8, pp. 653–670, 2004.

[64] Sondik, E. J., *The Optimal Control of Partially Observable Markov Processes over the Infinite Horizon: Discounted Costs.* PhD thesis, Stanford University, Stanford, California, 1971.

[65] Thanh Le, L., *Demand Management at Congested Airports: How Far Are We From Utopia?* PhD thesis, George Mason University, Fairfax, VA, 2006.

[66] United States General Accountability Office (GAO), "Aviation and the environment strategic framework needed to address challenges posed by aircraft emissions," report to the chairman, subcommittee on aviation, committee on transportation and infrastructure, house of representatives, February 2003.

[67] U.S. Environmental Protection Agency (EPA), "Evaluation of air pollutant emissions from subsonic commercial jet aircraft," Tech. Rep. EPA-420-R-99-013, Engine Programs and Compliance Division, Office of Mobile Sources, Ann Arbor, MI, April 1999.

[68] Visser, H. and Roling, P., "Optimal airport surface traffic planning using mixed integer linear programming," in *AIAA 3rd Annual Aviation Technology, Integration, and Operations (ATIO) Forum*, vol. AIAA-2003-6797, (Denver, CO), American Institute of Aeronautics and Astronautics, November 2003.

[69] Waitz, I., Townsend, J., Cutcher-Gershenfeld, J., Greitzer, E., and Kerrebrock, J., "Report to the United States congress: Aviation and the environment: A national vision statement, framework for goals and recommended actions," tech. rep., Partner of AiR Tranportation Noise and Emissions Reduction, Cambridge, MA, December 2004.

[70] Winther, M. and Rypdal, K., "EMEP EEA emission inventory guidebook - civil and military aviation," tech. rep., European Environment Agency, 2009.

[71] Young, S. D. and Jones, D. R., "Runway incursion prevention using an advanced surface movement guidance and control system," in *19th Digital Avionics Systems Conference*, October 2000.